Interstellar shocks:
The contribution of SOFIA/GREAT

Antoine Gusdorf, LERMA, Paris, France

Claudio Codella, INAF Firenze, Italy
Rolf Güsten, MPIfR, Bonn, Germany
Sibylle Anderl, IPAG, Grenoble, France
Maryvonne Gerin, LERMA, Paris, France
Bertrand Lefloch, IPAG, Grenoble, France
Pierre Lesaffre, LERMA, Paris, France
Silvia Leurini, MPIfR, Bonn, Germany
Alexandre Marcowith, LUPM, Montpellier, France
Frédérique Motte, IPAG, Grenoble, France

Outline

- The importance of shocks in the interstellar medium of galaxies
- From low-mass star formation…
- …To higher-mass star formation
- Filaments and ridges
- Supernova remnants

The importance of shocks in the ISM of galaxies

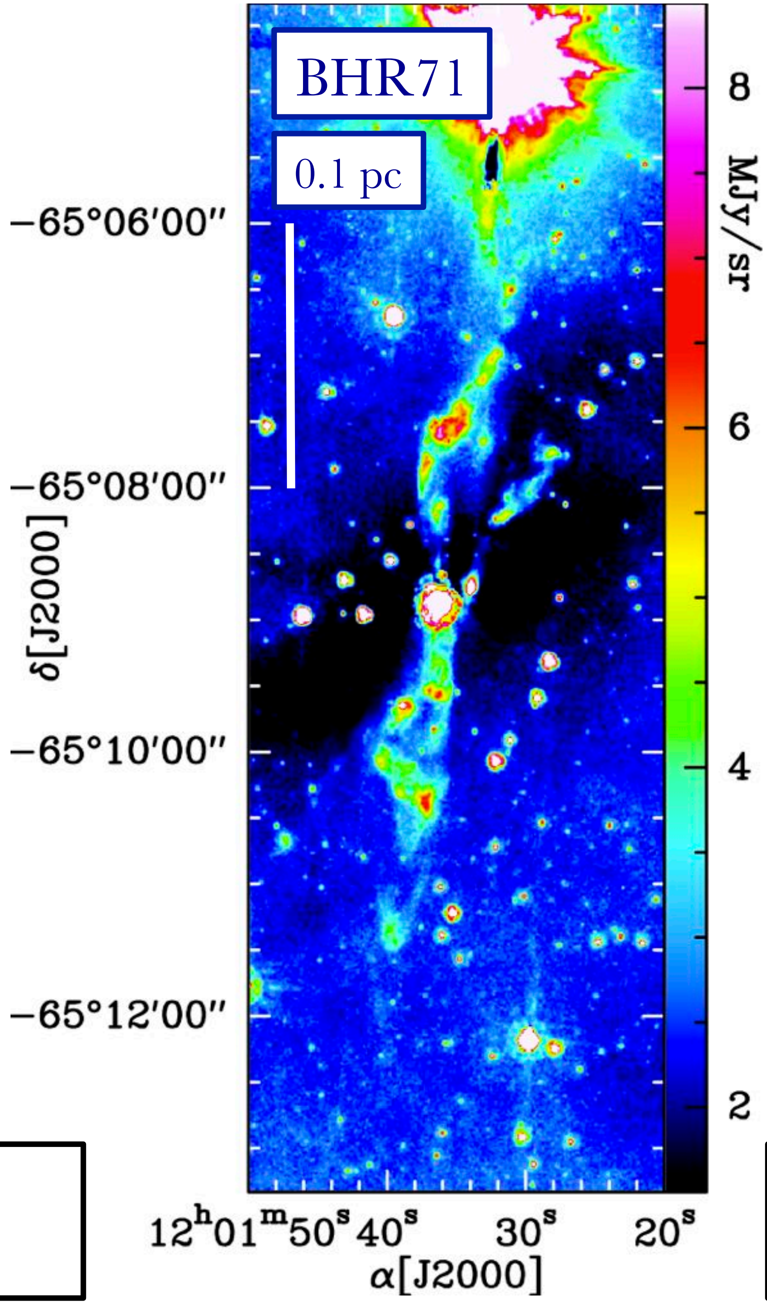

archive image
Spitzer/IRAC 8 μm

adapted from
Gusdorf et al. 2015

The importance of shocks in the ISM of galaxies

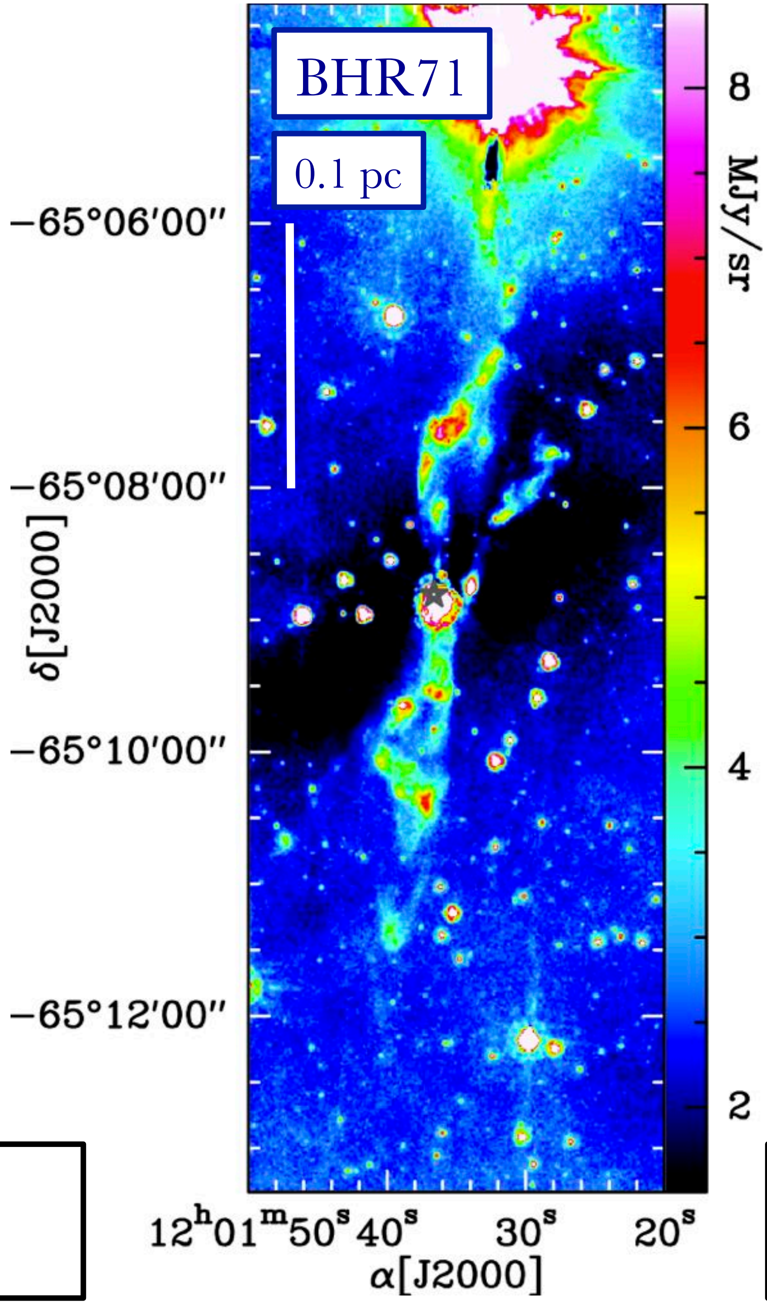

archive image
Spitzer/IRAC 8 μm

adapted from
Gusdorf et al. 2015

The importance of shocks in the ISM of galaxies

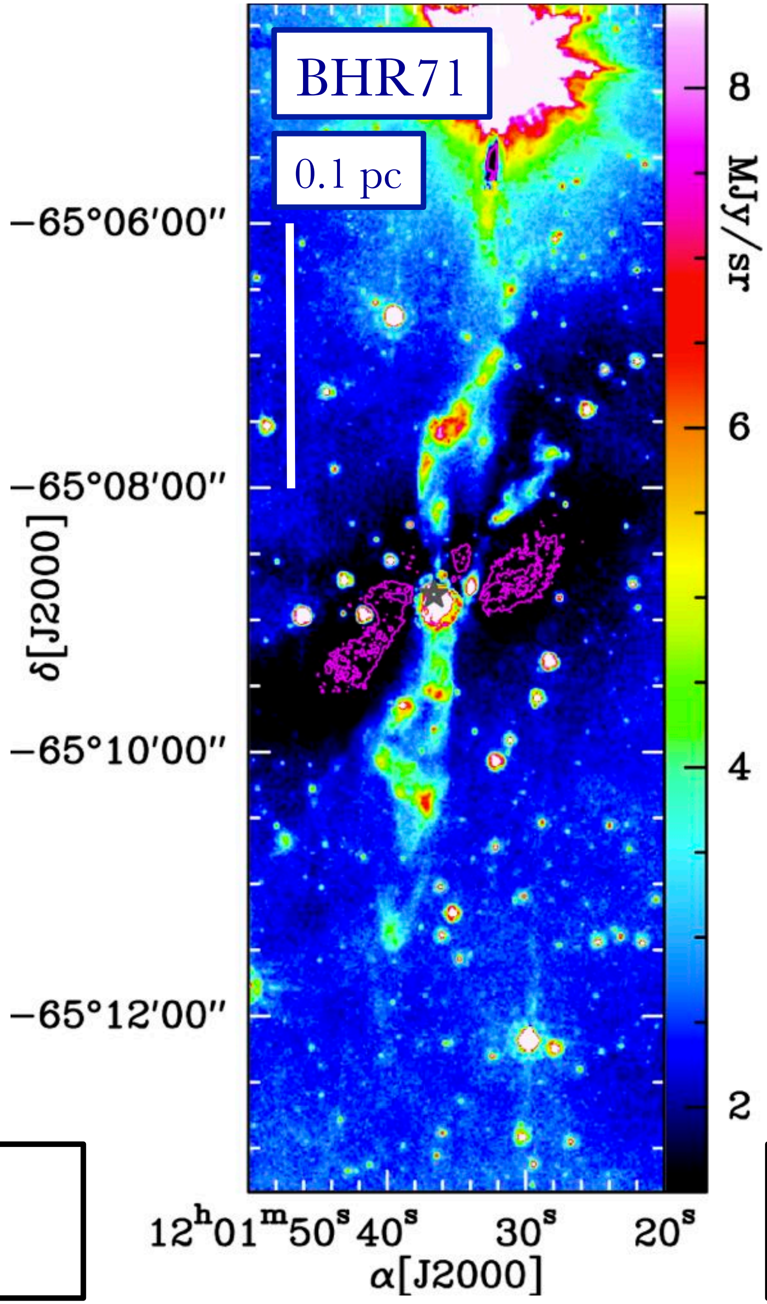

archive image
Spitzer/IRAC 8 μm

adapted from
Gusdorf et al. 2015

The importance of shocks in the ISM of galaxies

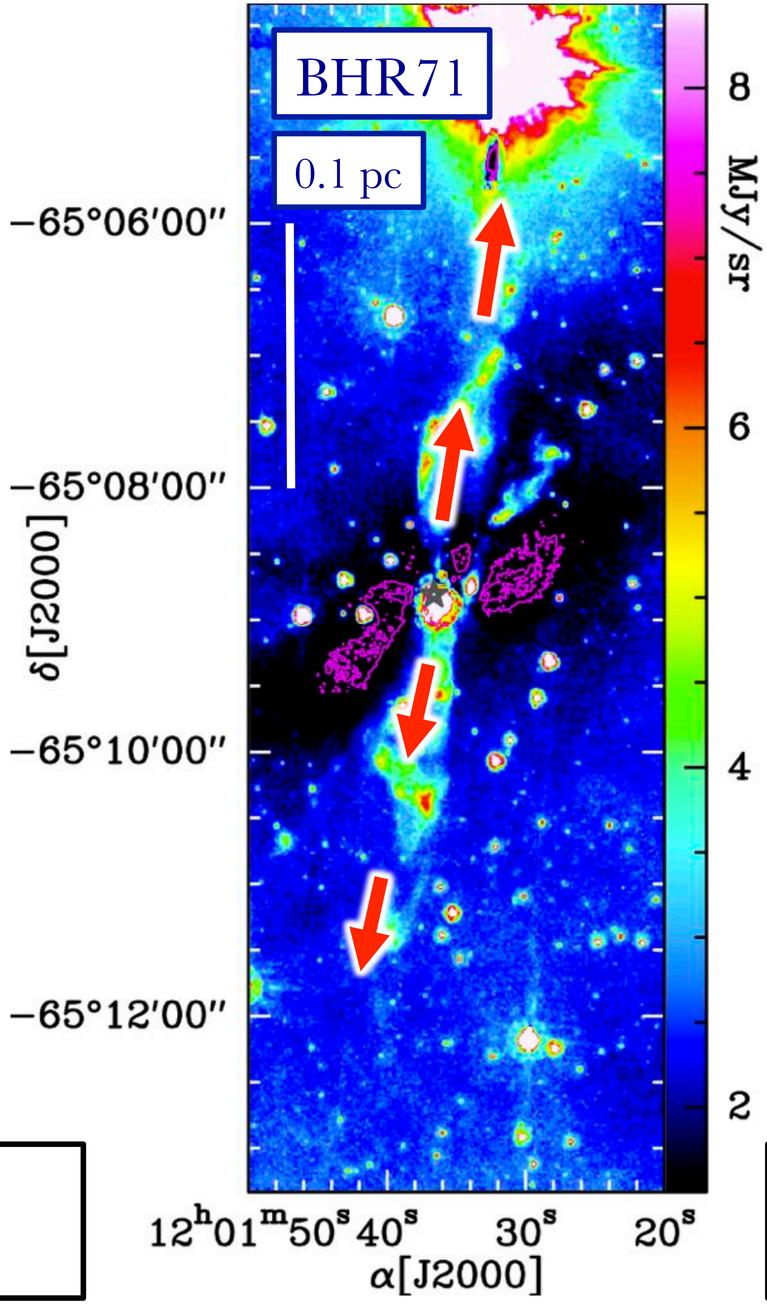

archive image
Spitzer/IRAC 8 μm

adapted from
Gusdorf et al. 2015

The importance of shocks in the ISM of galaxies

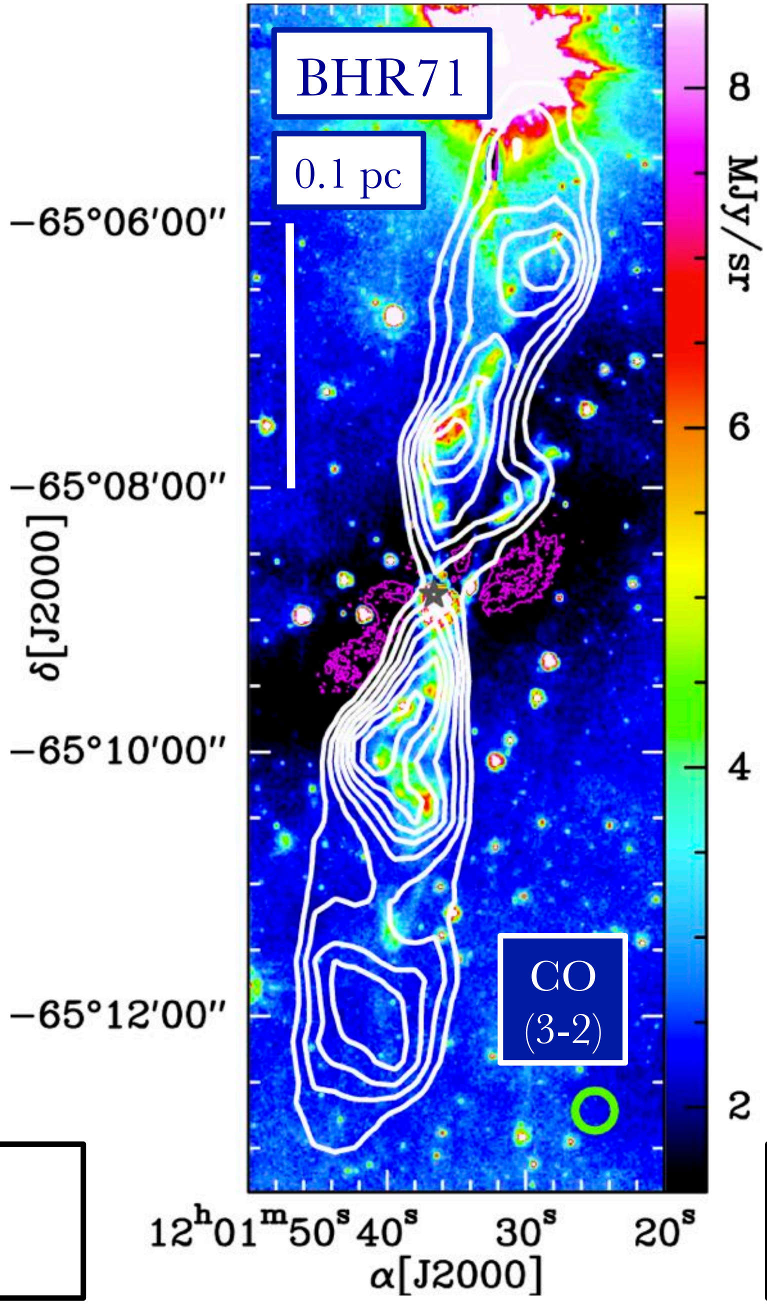

archive image
Spitzer/IRAC 8 μm

adapted from
Gusdorf et al. 2015

The importance of shocks in the ISM of galaxies

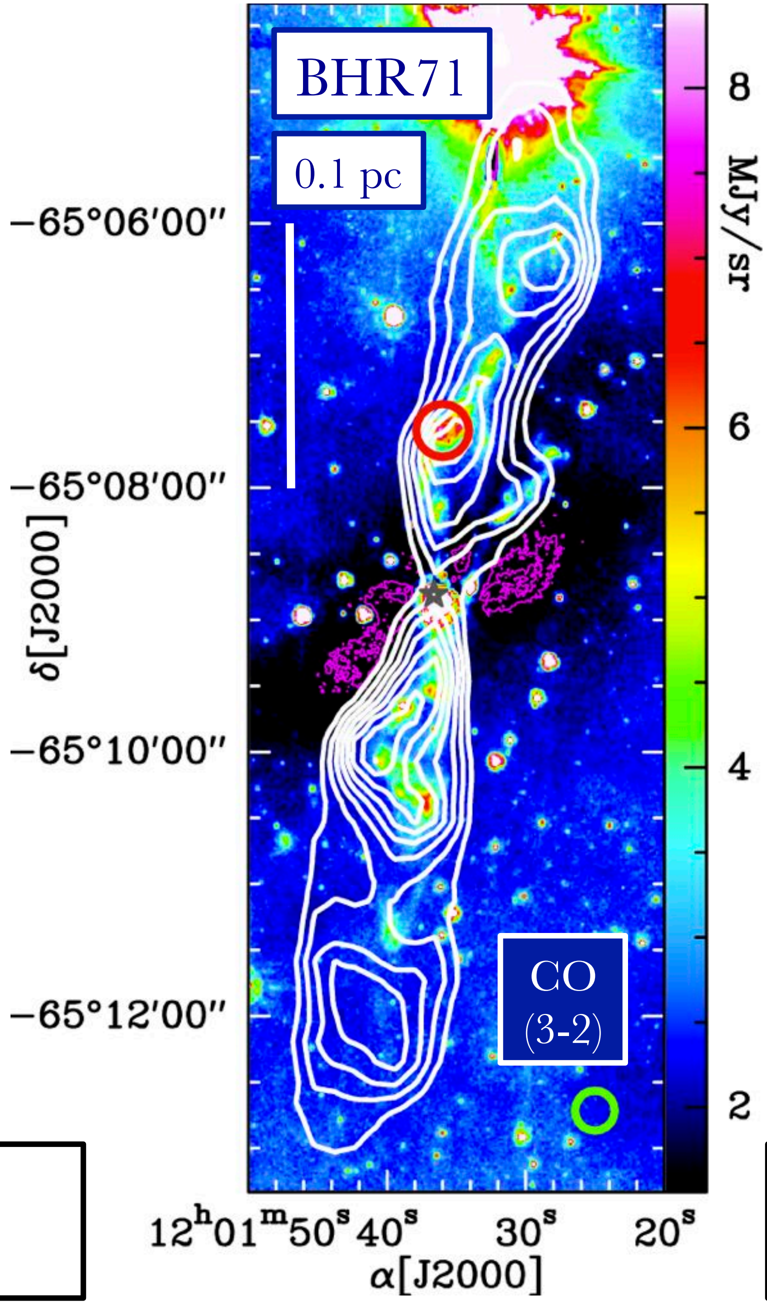

archive image
Spitzer/IRAC 8 μm

adapted from
Gusdorf et al. 2015

The importance of shocks in the ISM of galaxies

- physical processes
- chemical enrichment

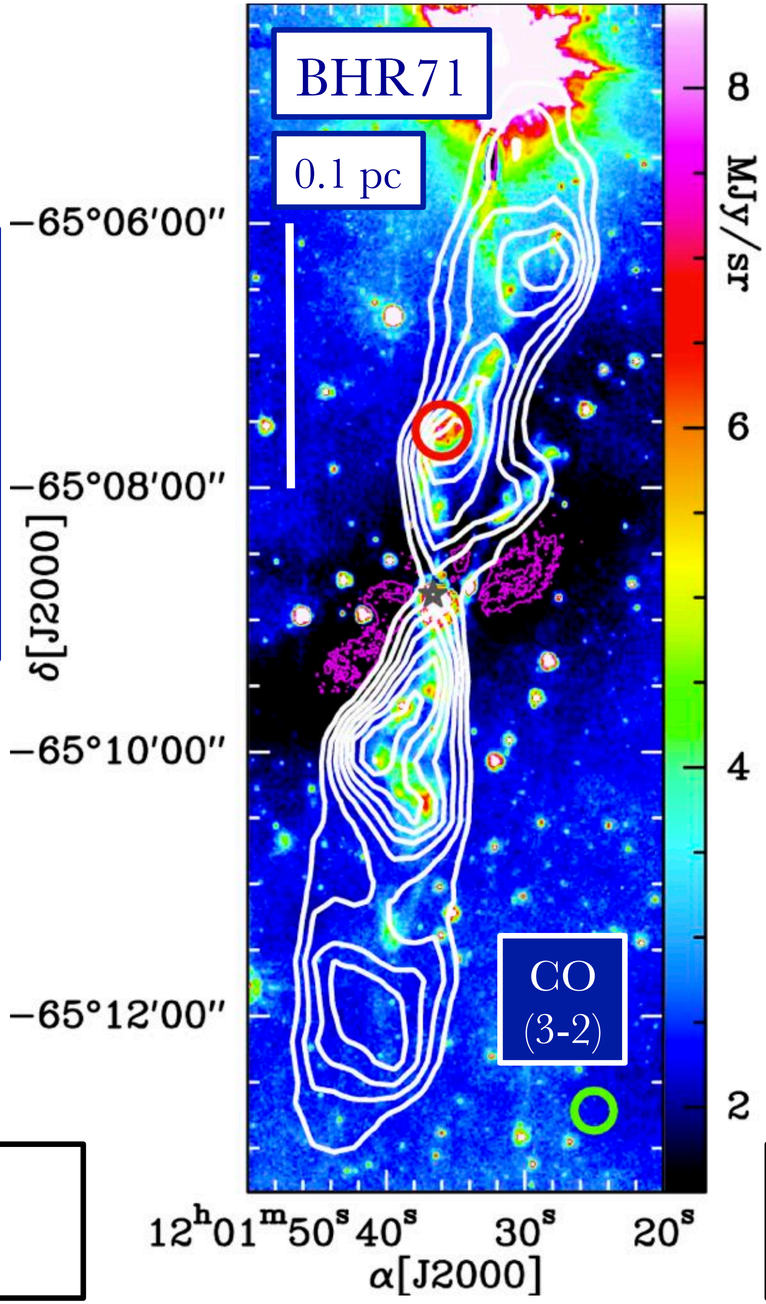

archive image
Spitzer/IRAC 8 μm

adapted from
Gusdorf et al. 2015

The importance of shocks in the ISM of galaxies

- physical processes
- chemical enrichment

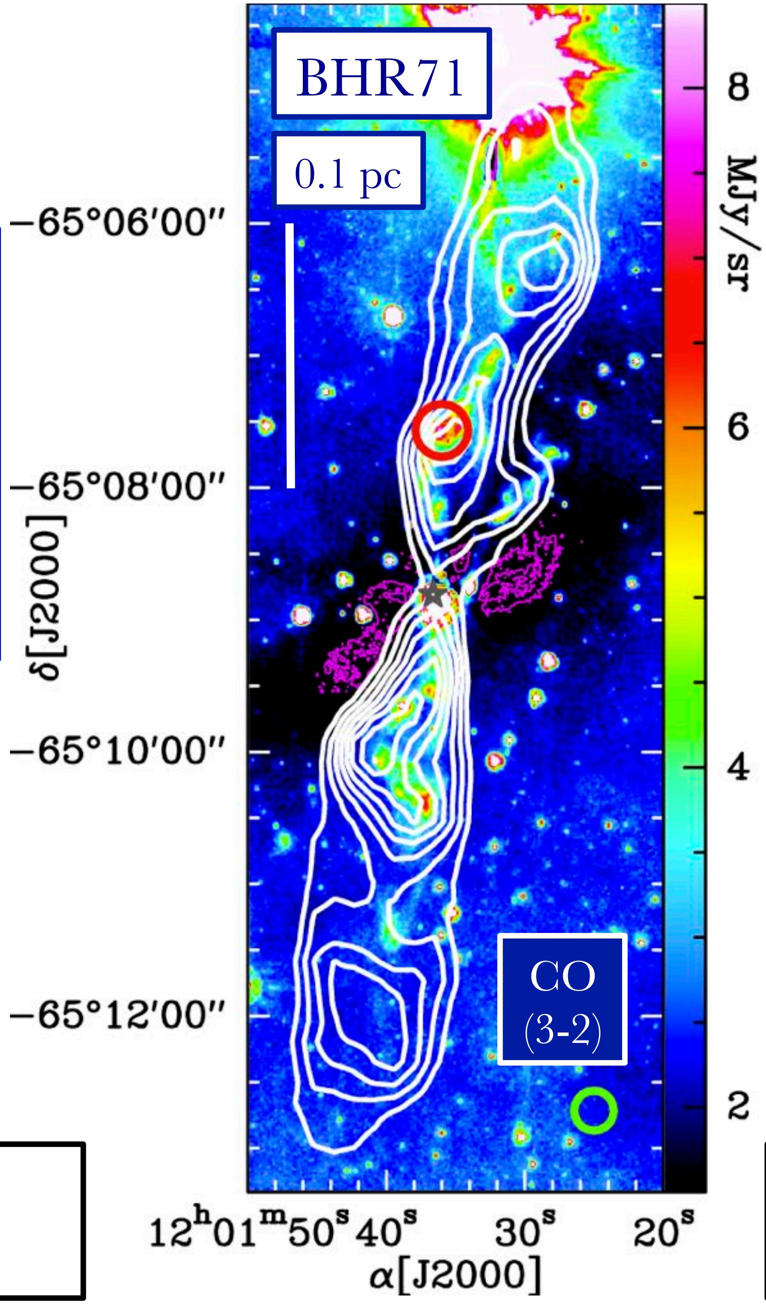

- energetic impacts
- star formation:
  - scenarios
  - triggered
- cosmic rays

archive image
Spitzer/IRAC 8 μm

adapted from
Gusdorf et al. 2015

From low-mass star formation…

Low-mass star formation: the BHR71 example

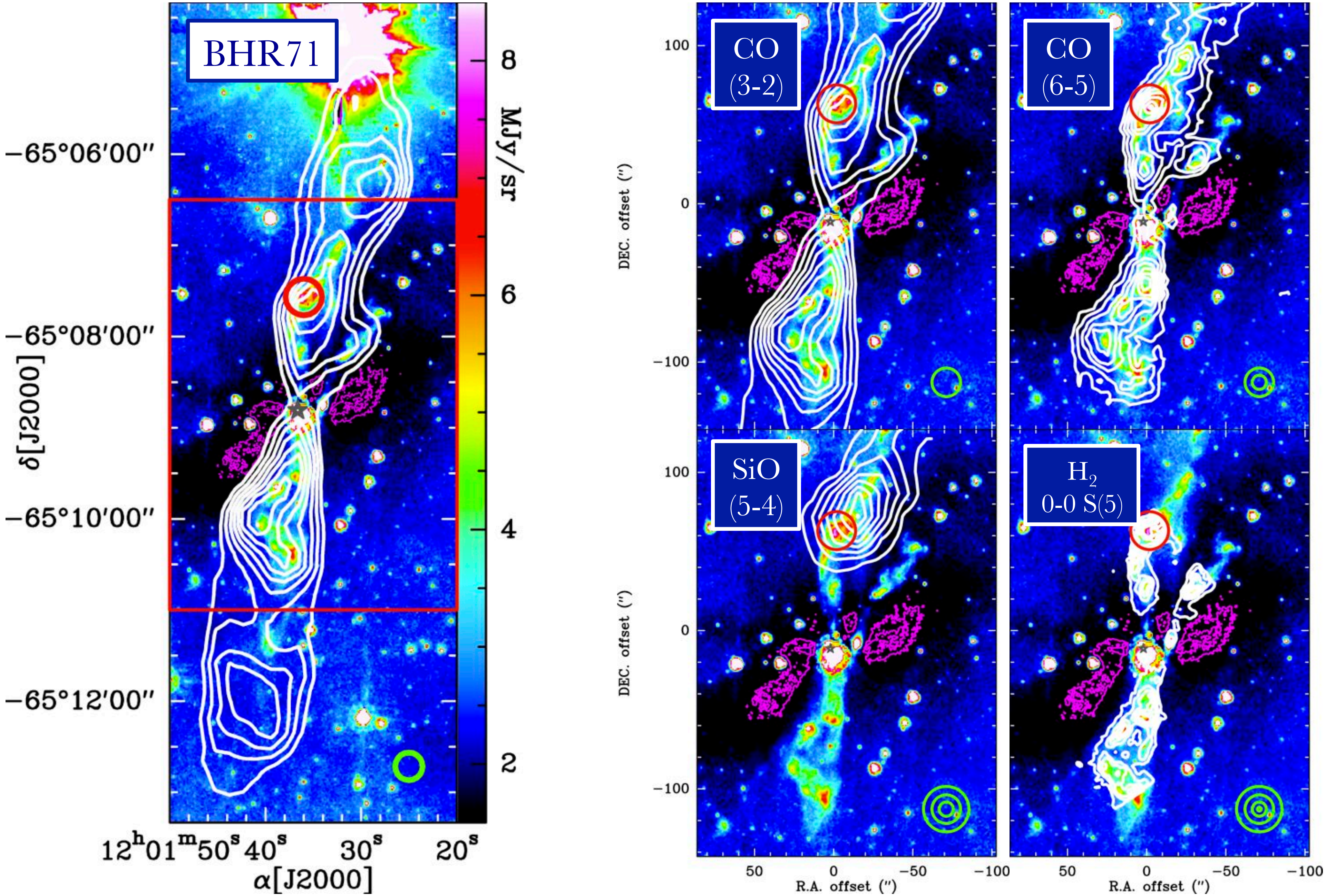

Low-mass star formation: the BHR71 example

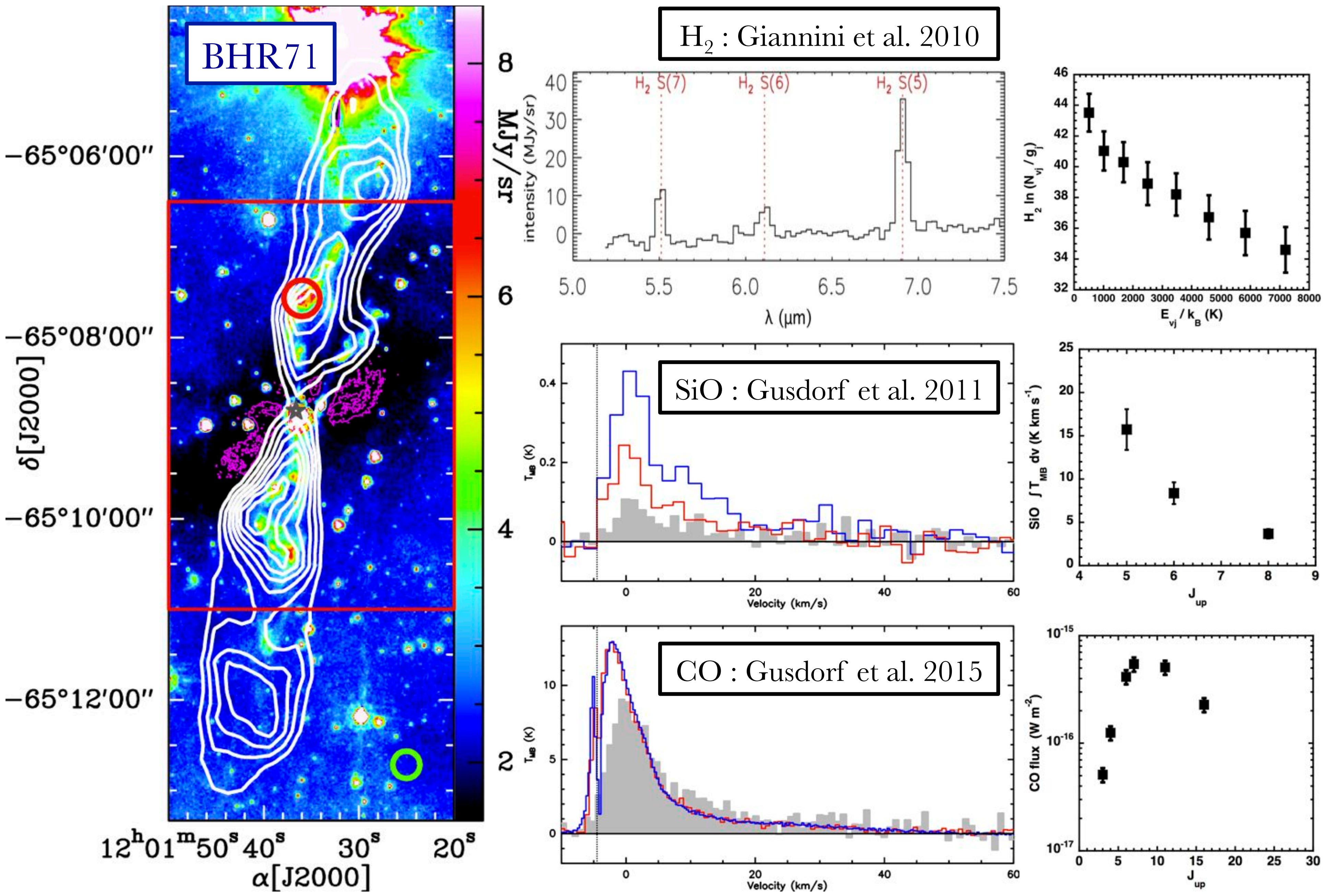

1D shock models

$n_H = 10^4\ cm^{-3}$; $v_s = 30$ km/s

- J shock (Jump) ;

B = 10 μG

$v_s > v_{critical}$

impulse heating ;

single fluid

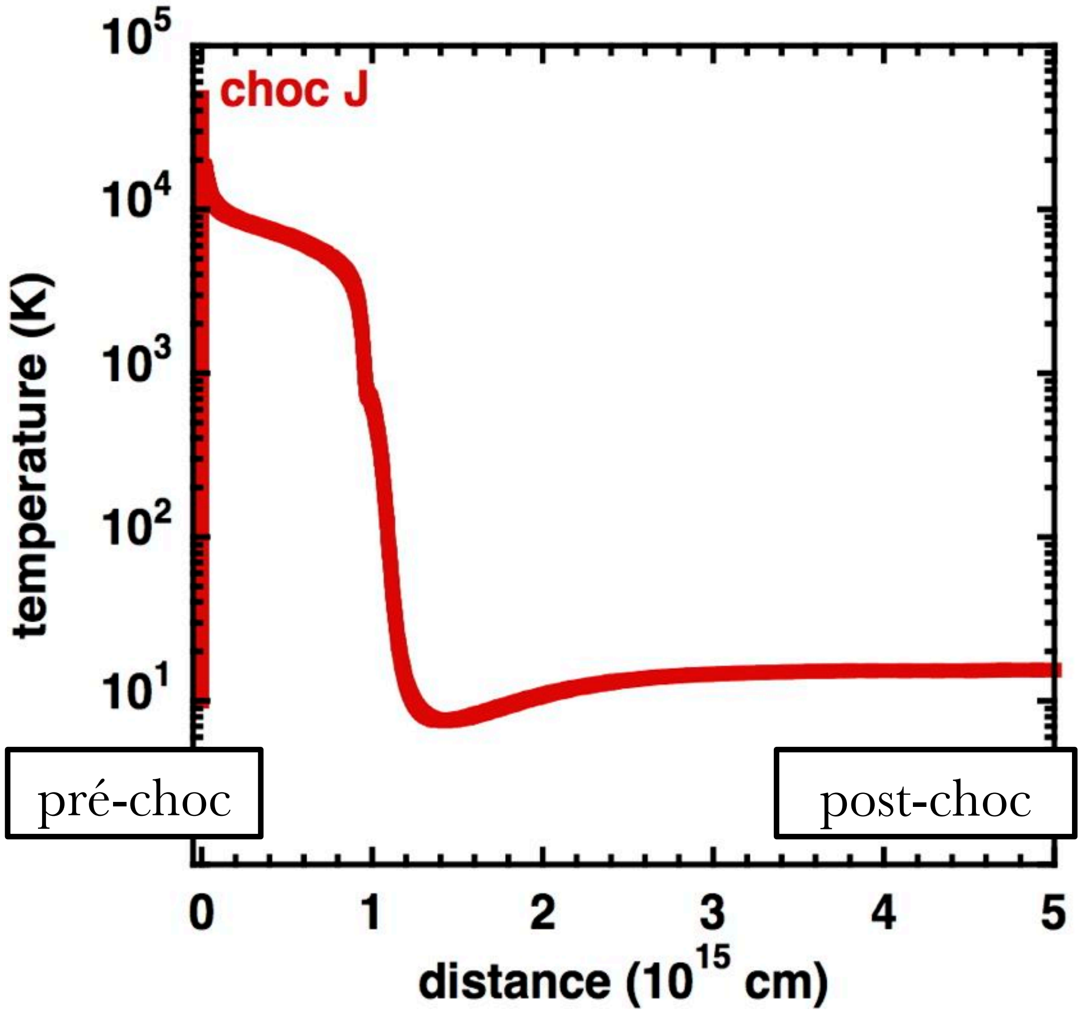

1D shock models

$n_H = 10^4$ cm^{-3} ; $v_s = 30$ km/s

- J shock (Jump) ;

B = 10 μG

$v_s > v_{critical}$

impulse heating ;

single fluid

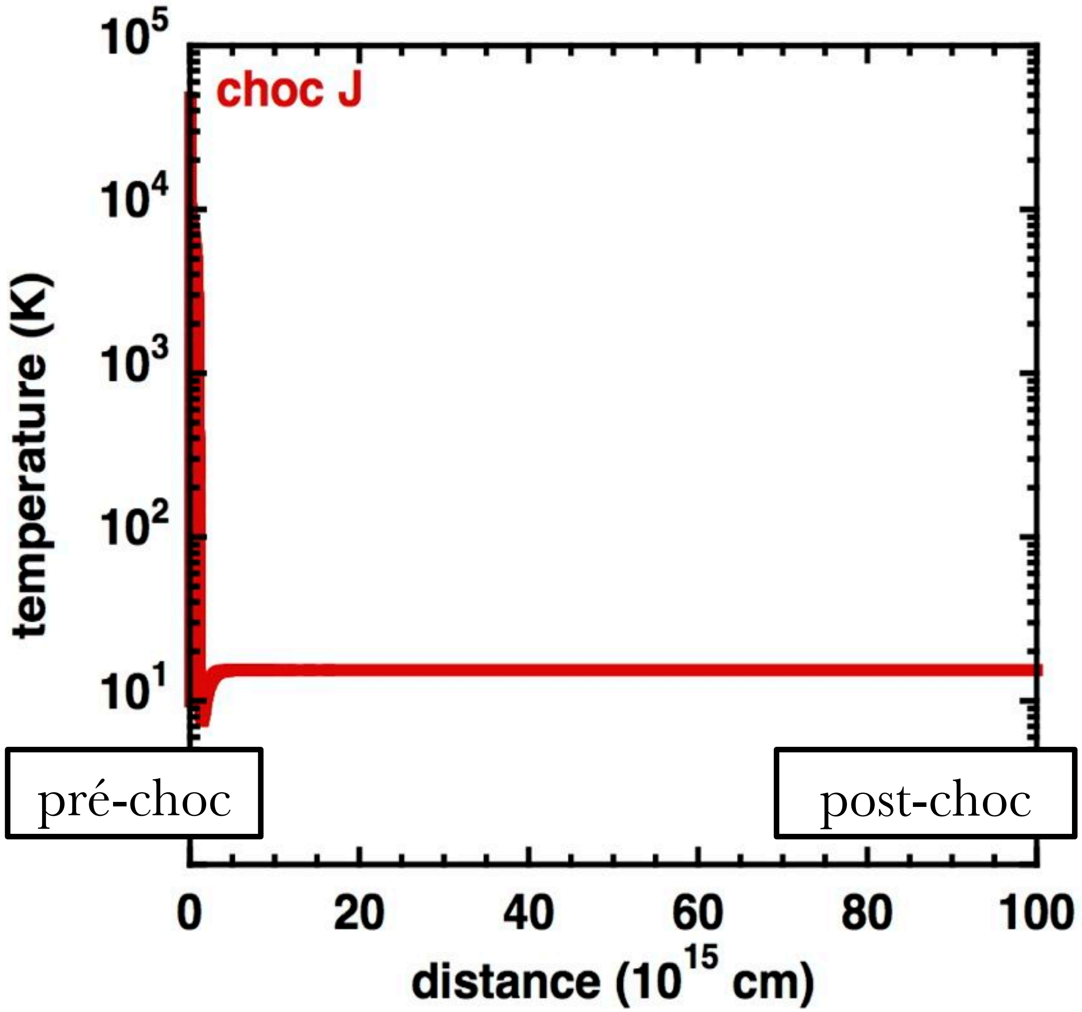

1D shock models

$n_H = 10^4\ cm^{-3}$; $v_s = 30$ km/s

- J shock (Jump) ;

B = 10 μG

$v_s > v_{critical}$

impulse heating ;

single fluid

- C shock (Continuous) ;

B = 100 μG

$v_s < v_{critical}$

ion-neutral friction ;

multi-fluid

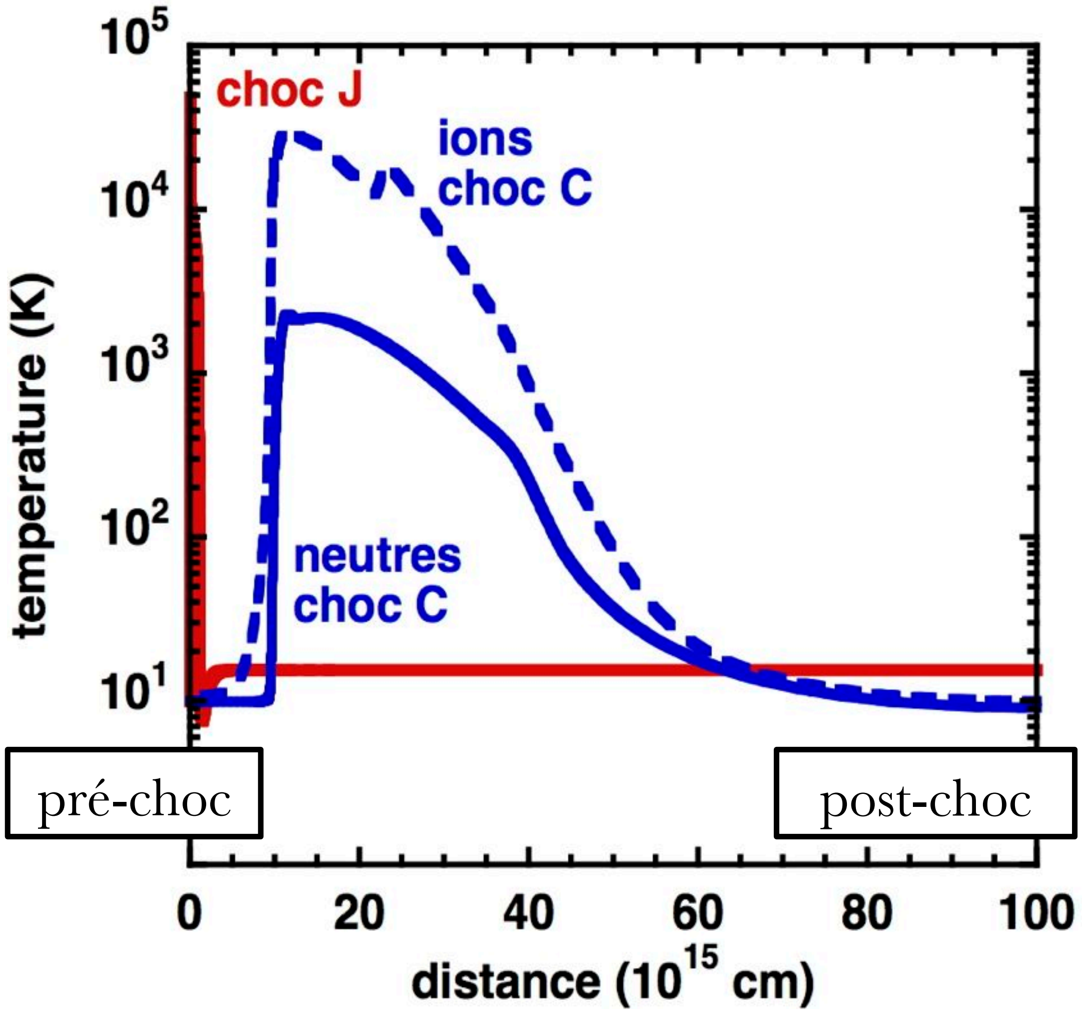

1D shock models

$n_H = 10^4\ cm^{-3}$; $v_s = 30\ km/s$

- J shock (Jump) ;

B = 10 μG

$v_s > v_{critical}$

impulse heating ;

single fluid

- C shock (Continuous) ;

B = 100 μG

$v_s < v_{critical}$

ion-neutral friction ;

multi-fluid

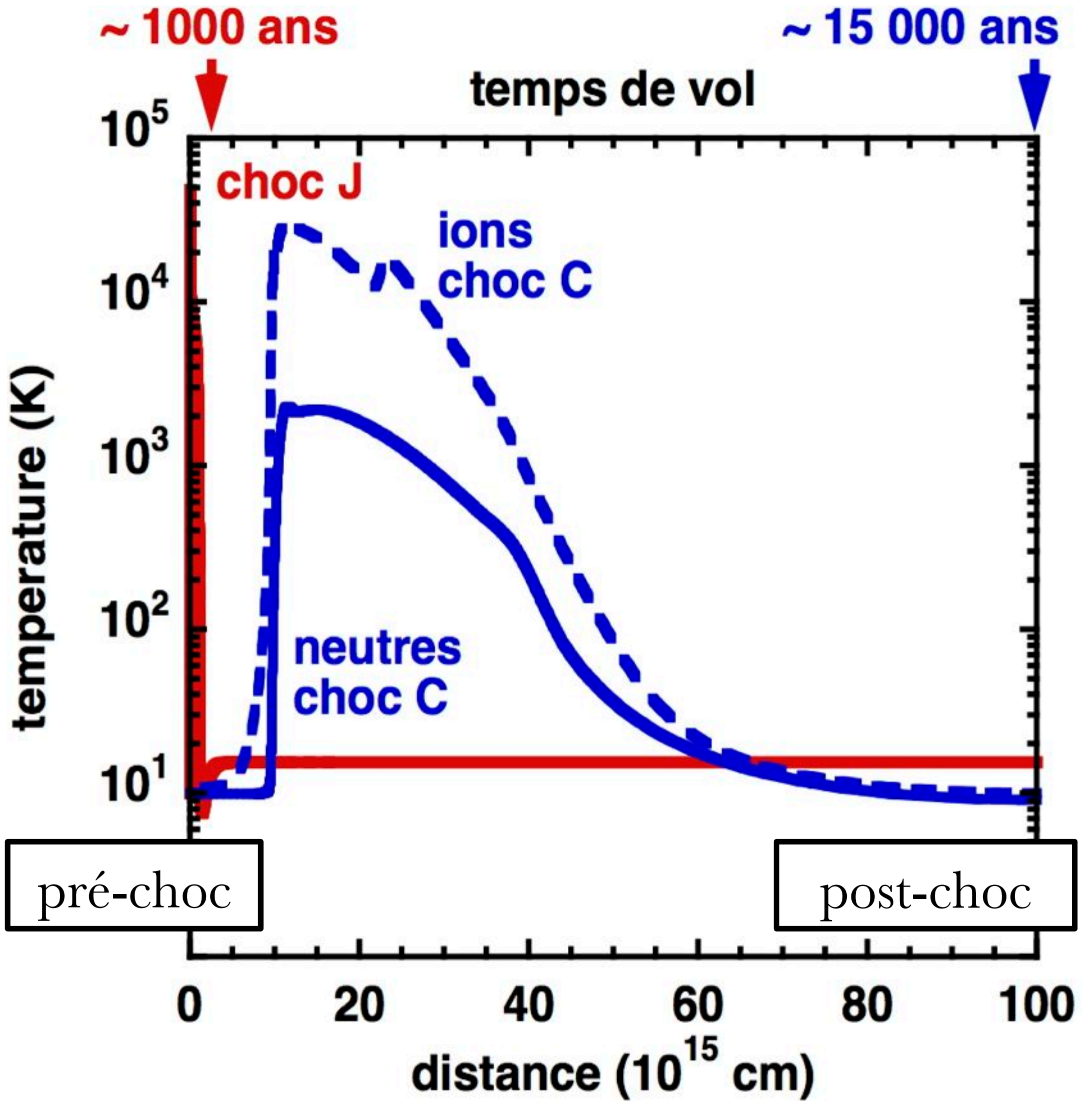

1D shock models

$n_H = 10^4$ cm^{-3}

$v_s = 30$ km/s

âge 2000 ans

CJ shock

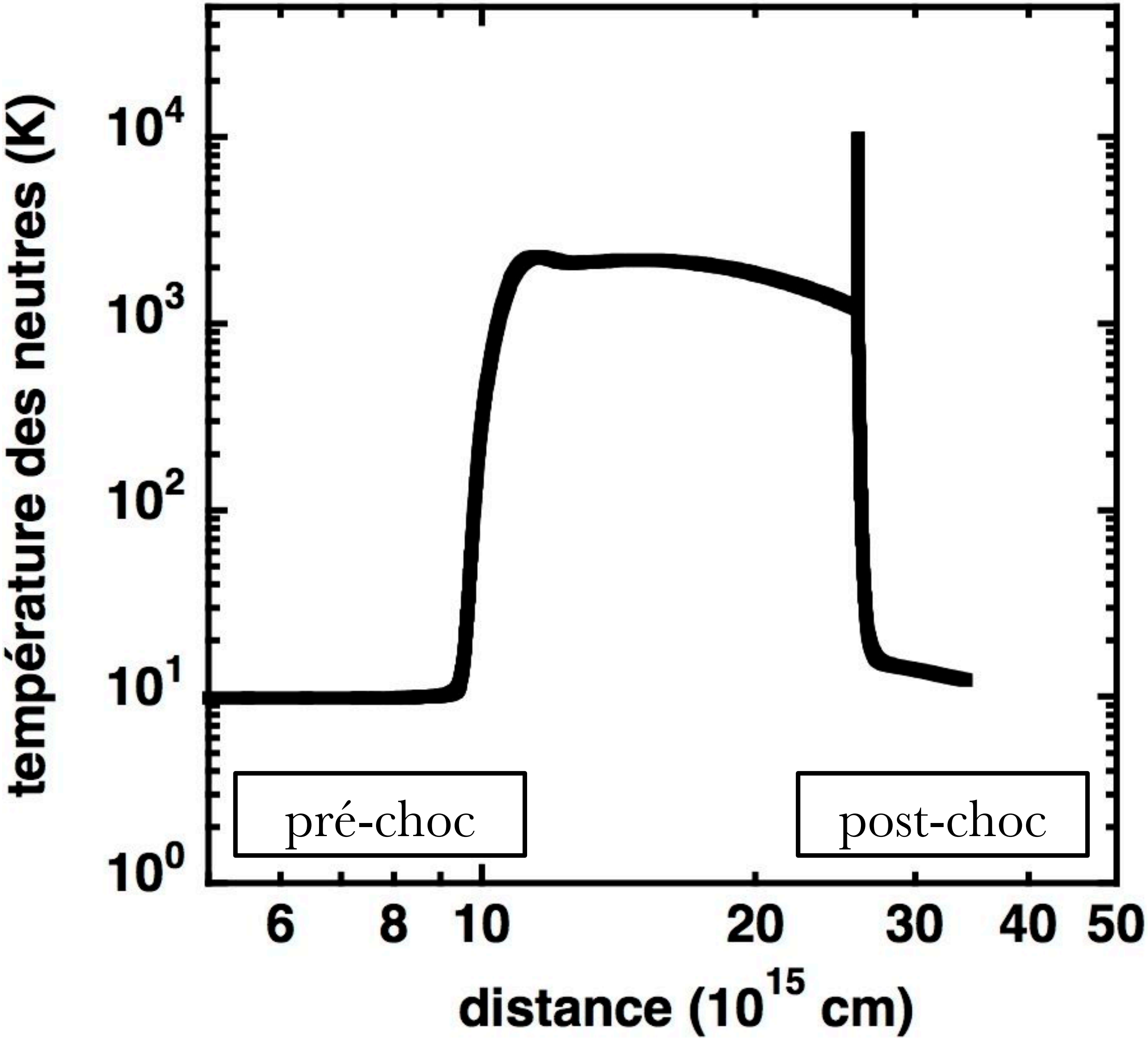

Tracing the propagation of shocks: SiO emission

pre-shock medium:

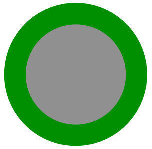

$Si^{**} \in$ cores

$SiO^{*} \in$ mantles

Tracing the propagation of shocks: SiO emission

pre-shock medium:

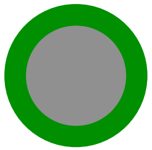

Si** ∈ cores
SiO* ∈ mantles

Grain charge

(Flower & Pineau des Forêts 2003)

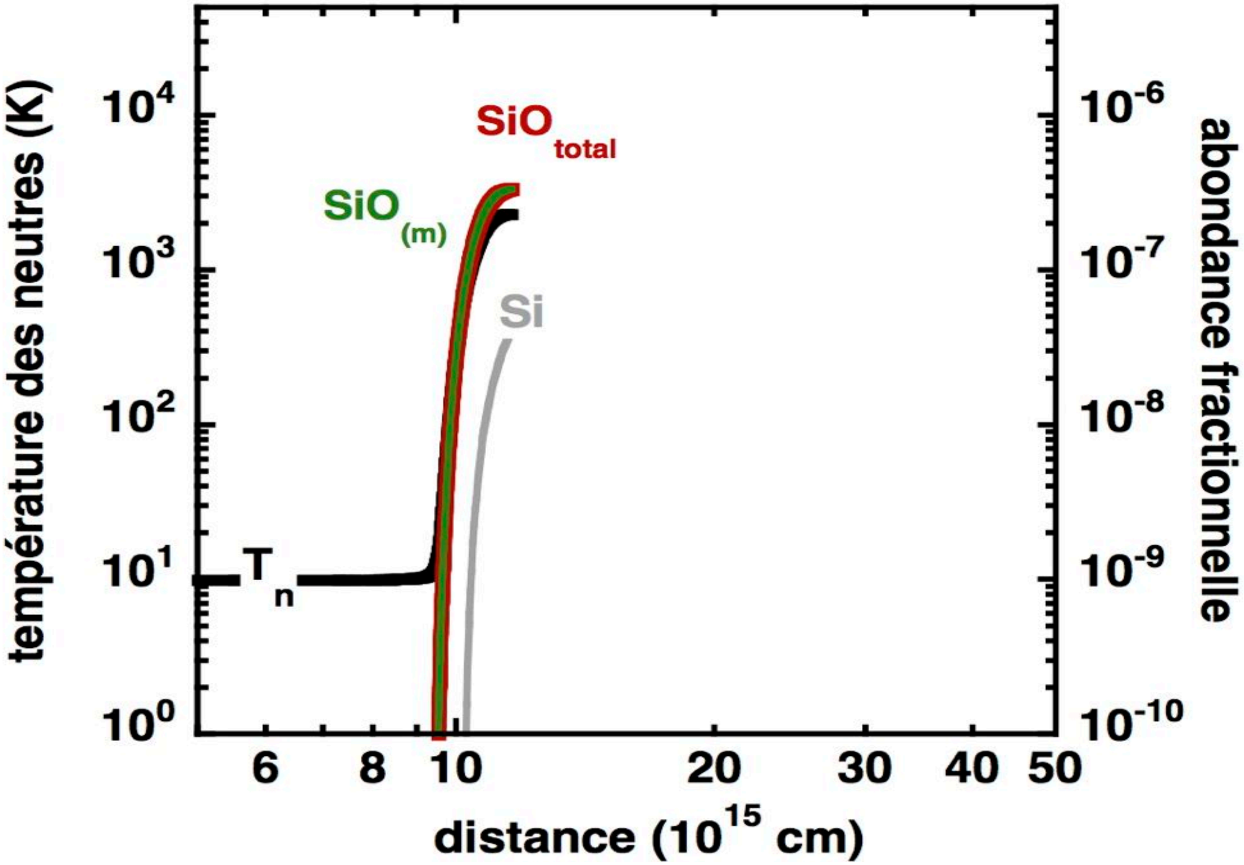

Tracing the propagation of shocks: SiO emission

pre-shock medium:

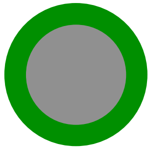

Si^{**} ∈ cores

SiO^* ∈ mantles

Grain charge

(Flower & Pineau des Forêts 2003)

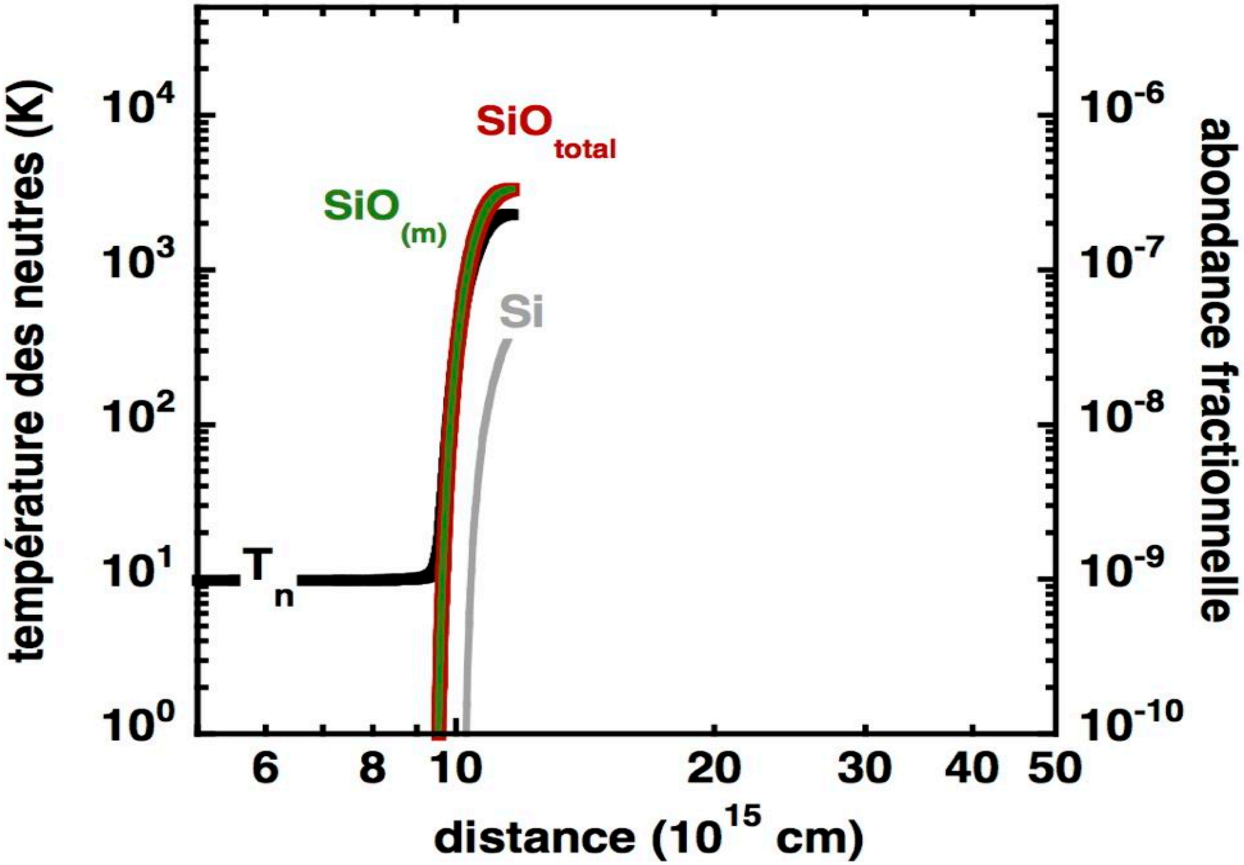

mantle sputtering (Flower & Pineau des Forêts 1994, semi-classical prescriptions) :

$SiO^* + (H, He, H_2) \rightarrow SiO + (H, He, H_2)$

core erosion (May et al. 2000, Monte-Carlo simulations) :

$Si^{**} + (He, C, N, O, H_2O, N_2, CO, O_2) \rightarrow Si + (He, C, N, O, H_2O, N_2, CO, O_2)$

Tracing the propagation of shocks: SiO emission

pre-shock medium:

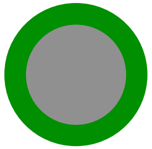

Si^{**} ∈ cores

SiO^{*} ∈ mantles

grain charge

core erosion

mantles sputtering

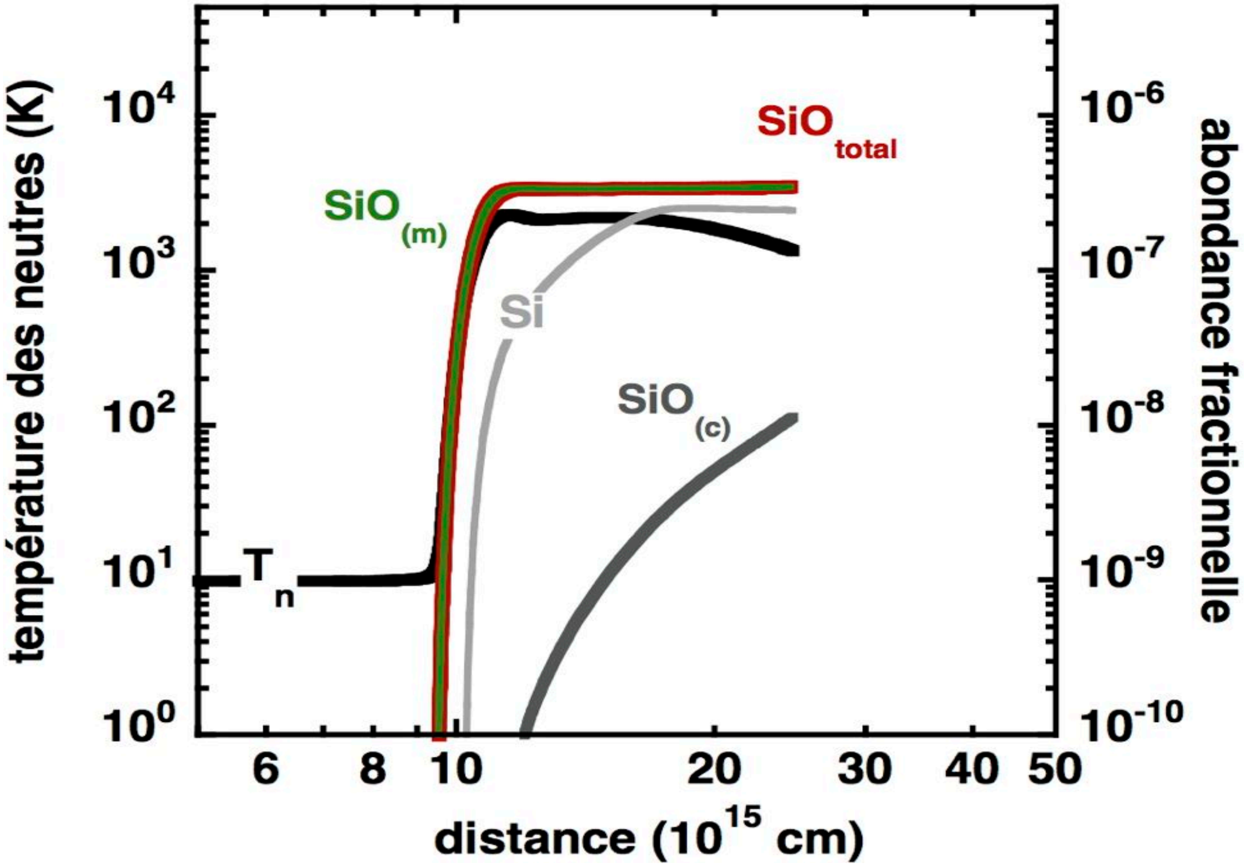

SiO formation in the gas phase, from grain-core silicium:

$Si + O_2 \rightarrow SiO + O$

(Le Picard et al. 2001, CRESU experiment)

$Si + OH \rightarrow SiO + H$

(Rivero-Santamaria, Dayou et al. 2014, quantum calculations)

Tracing the propagation of shocks: SiO emission

pre-shock medium:

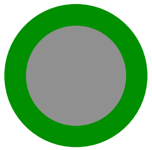

Si** ∈ cores

SiO* ∈ mantles

grain charge

core erosion

mantles sputtering

gas phase formation

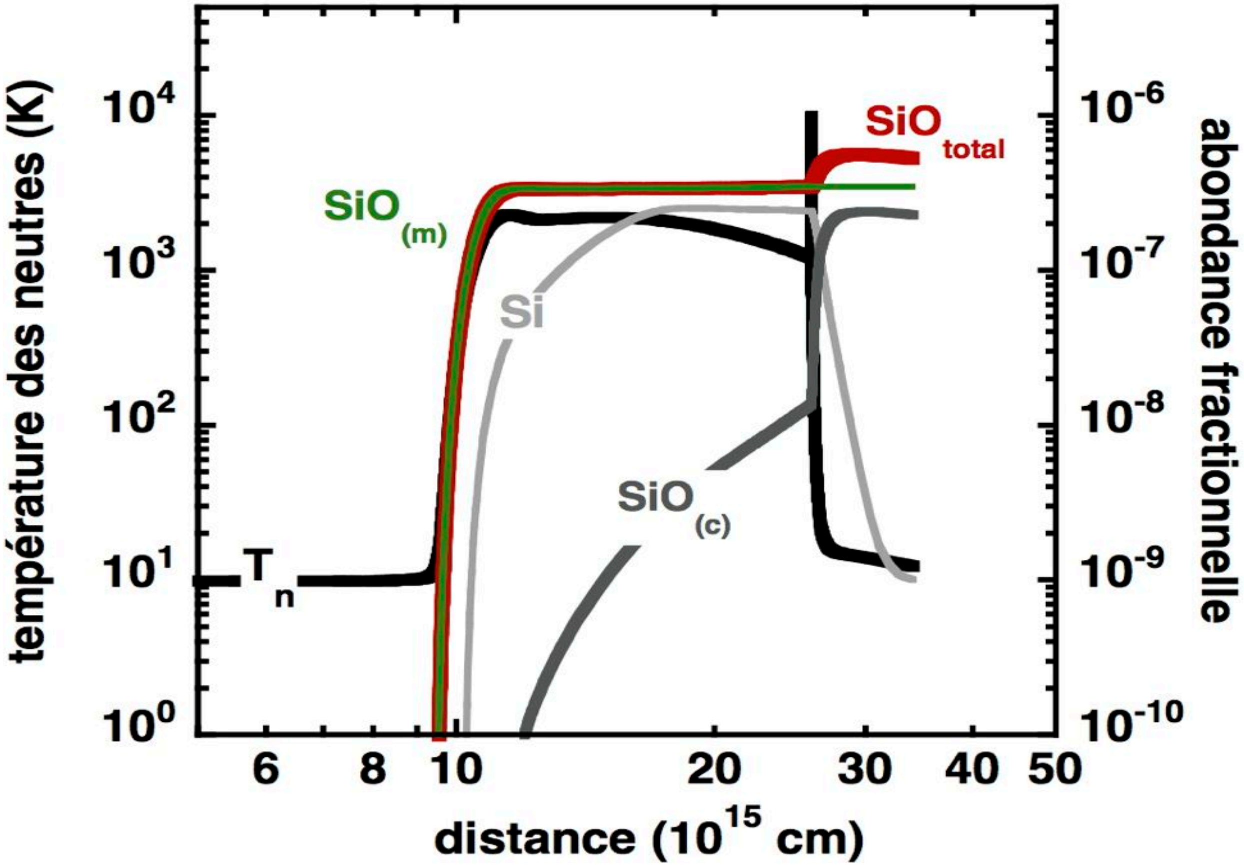

gas phase, chemical destruction of SiO:

SiO + OH → SiO_2 + H

(prescription E. Herbst)

adsorption (freeze-out) on to grains :

SiO + grain → SiO* + grain

Tracing the propagation of shocks: SiO emission

pre-shock medium:

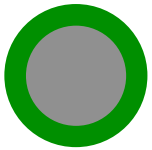

Si^{**} ∈ cores

SiO^{*} ∈ mantles

grain charge

core erosion

mantles sputtering

gas phase formation

gas phase destruction

adsorption

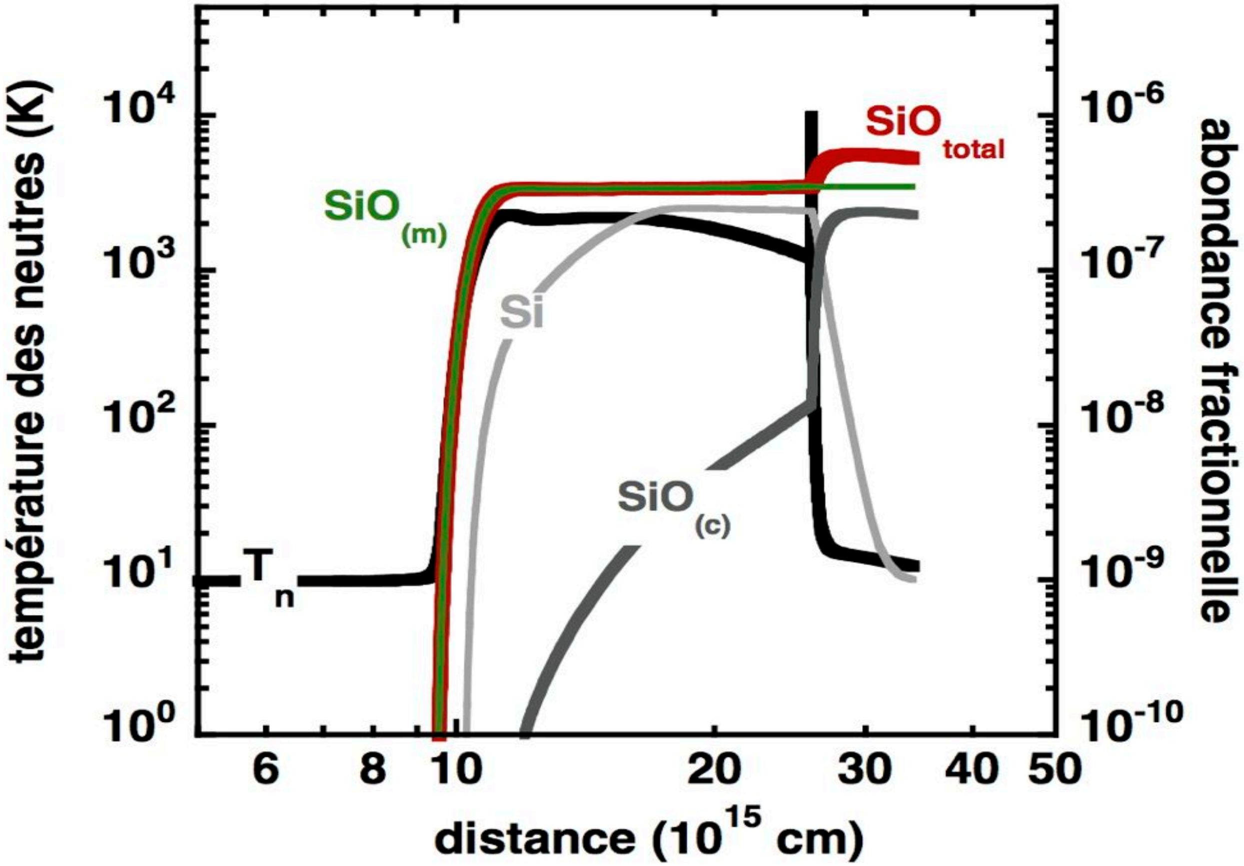

- level populations and transition emissivities calculations:
    - statistical equilibrium equations
    - 'Large Velocity Gradient' (LVG) assumption
    - collisional excitation rate coefficients of SiO by H_2, H, He

(calculated by Dayou & Balança 2006)

Comparing observations with models

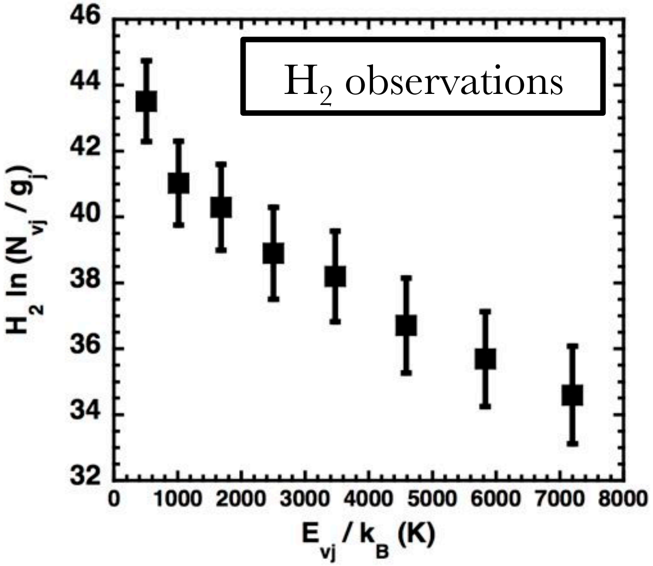

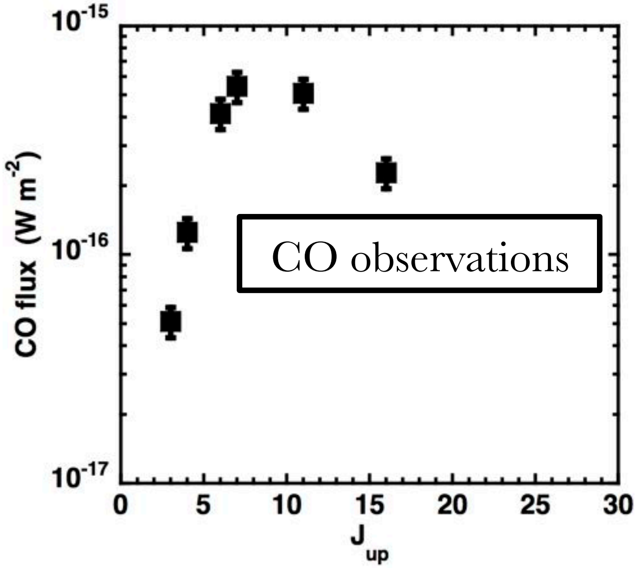

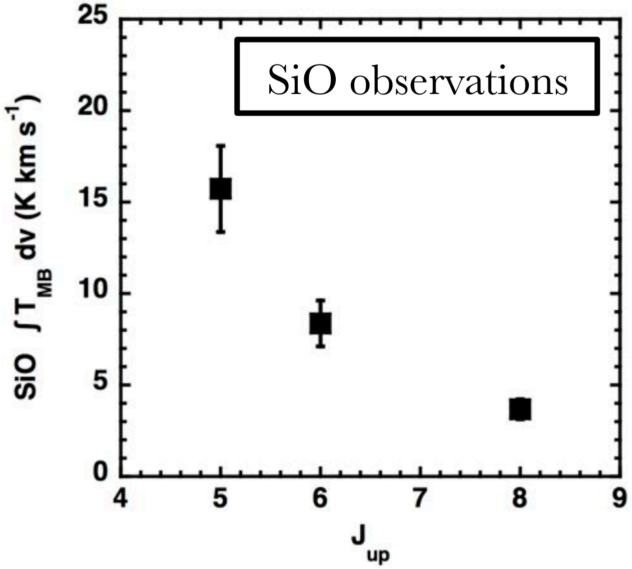

Comparing observations with models

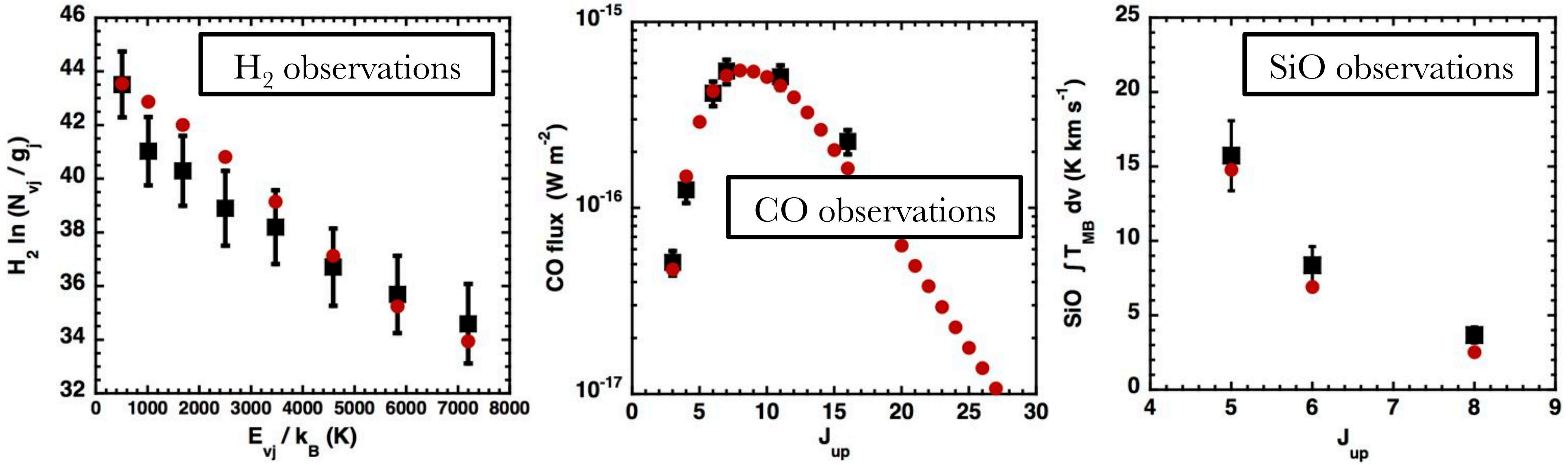

- CJ model, $n_H = 10^4$ cm^{-3}, $v_s = 22$ km/s, B = 150 μG ; 1% of Si ∈ SiO^* (pre-shock)

  - physical conditions are constrained (shock age, magnetic field strength)
  - silicon chemistry constrained (initial distribution, processes)
  - ejection rate (precise) measure: $7 \cdot 10^{-6}$ $M_\odot$/an
  - pure shock diagnosis

Gusdorf et al. 2015a

Comparing observations with models

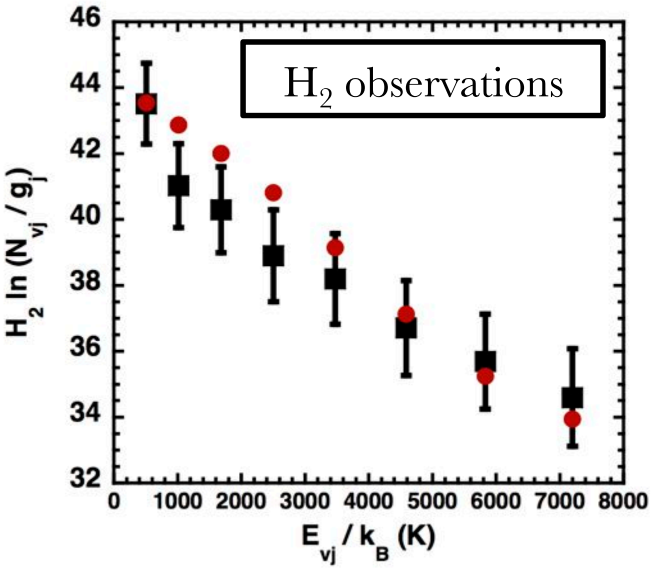

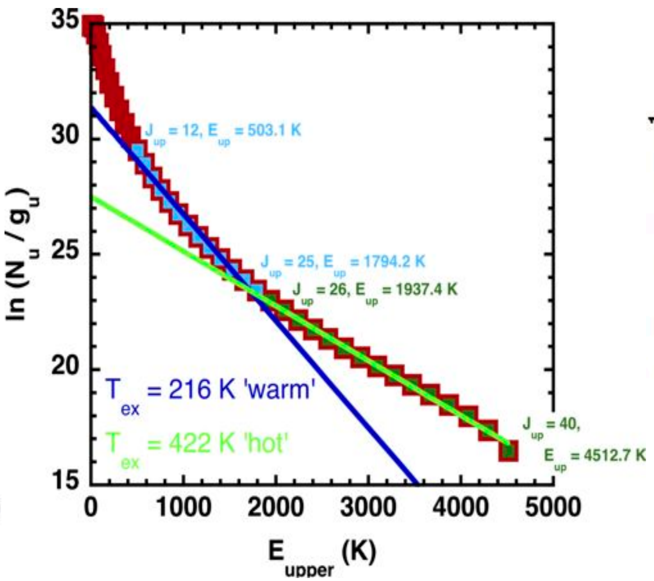

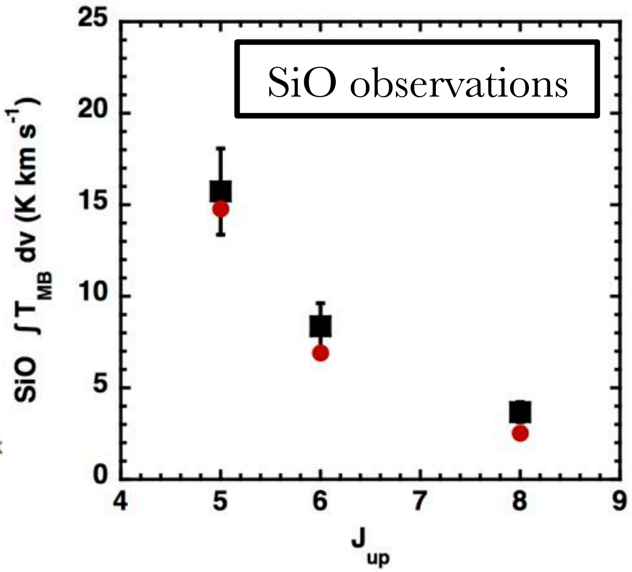

- CJ model, $n_H = 10^4$ cm^{-3}, v_s = 22 km/s, B = 150 μG ; 1% of Si ∈ SiO* (pre-shock)

  - physical conditions are constrained

  (shock age, magnetic field strength)

  - silicon chemistry constrained (initial distribution, processes)
  - ejection rate (precise) measure: $7{\cdot}10^{-6}$ $M_\odot$/an
  - pure shock diagnosis

Gusdorf et al. 2015a

BHR71: the latest news

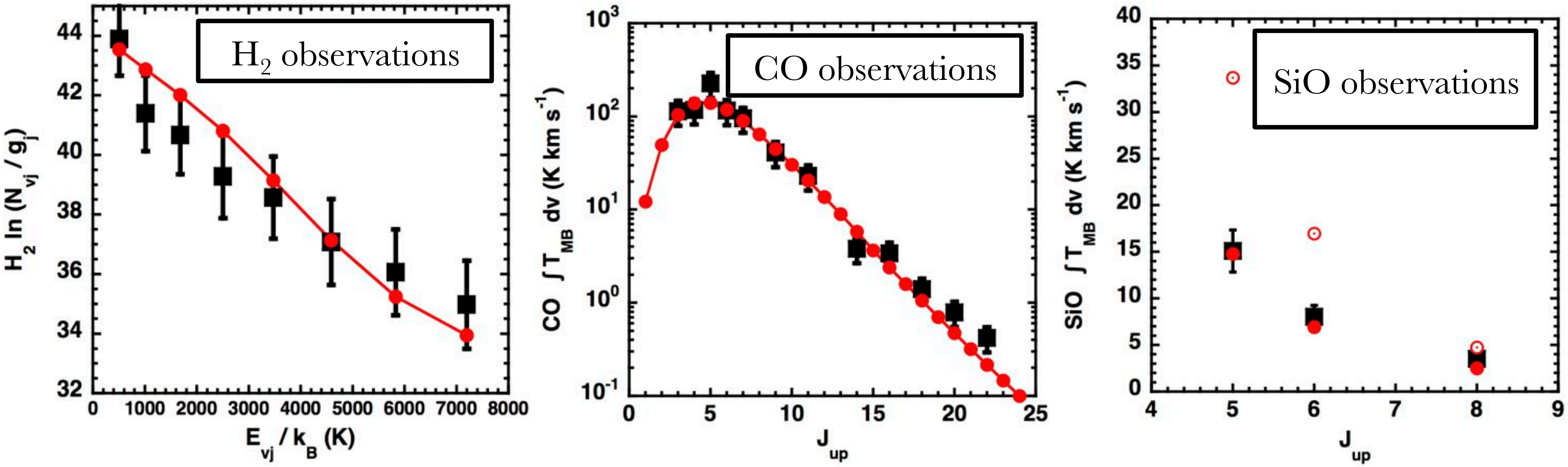

- New PACS & HIFI observations of CO, OH and OI lines

CJ model, $n_H = 10^4$ cm^{-3}, v_s = 22 km/s, B = 150 μG ; 1% of Si ∈ SiO* (pre-shock)

BHR71: the latest news

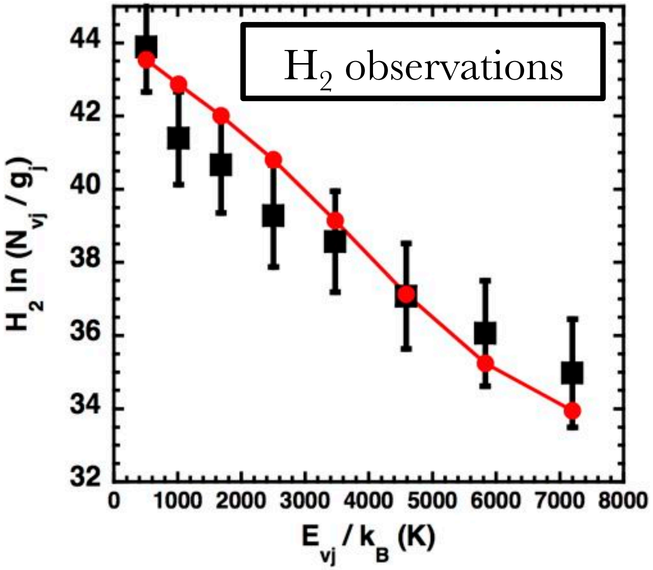

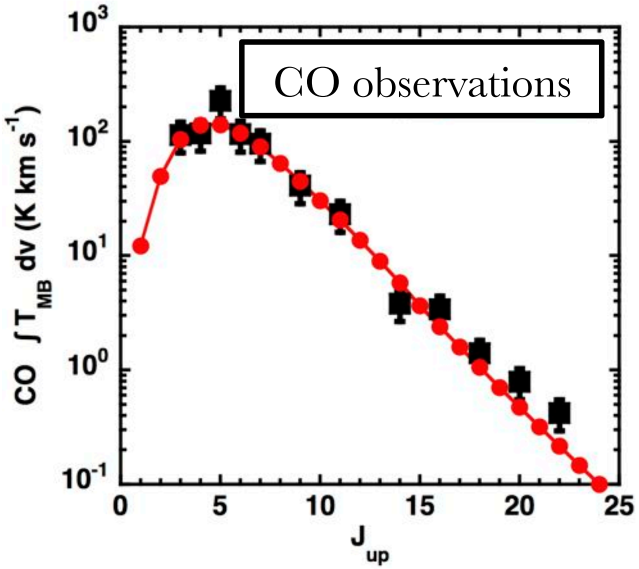

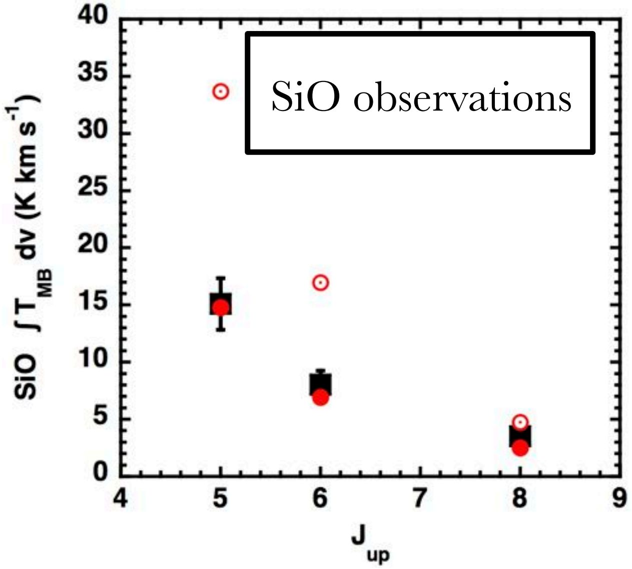

- New PACS & HIFI observations of CO, OH and OI lines

CJ model, $n_H = 10^4$ cm^{-3}, v_s = 22 km/s, B = 150 μG ; 1% of Si ∈ SiO* (pre-shock)

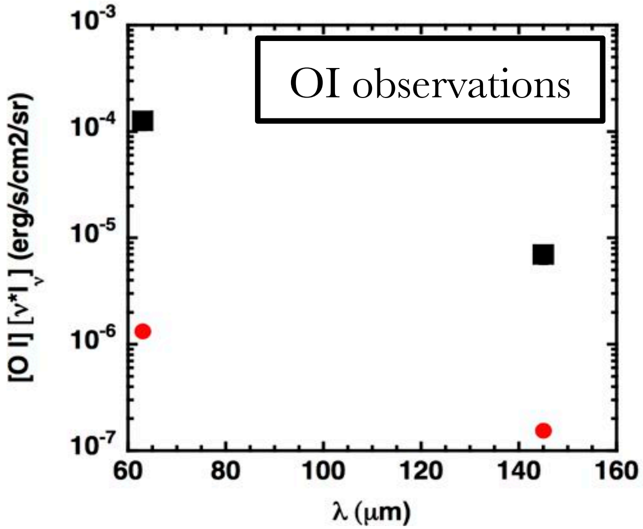

- OI: models ~1% of observations

⇒ we are missing something

⇒ irradiated shocks

⇒ some kind of jet component ?

Benedettini et al., in prep.

BHR71: the latest news

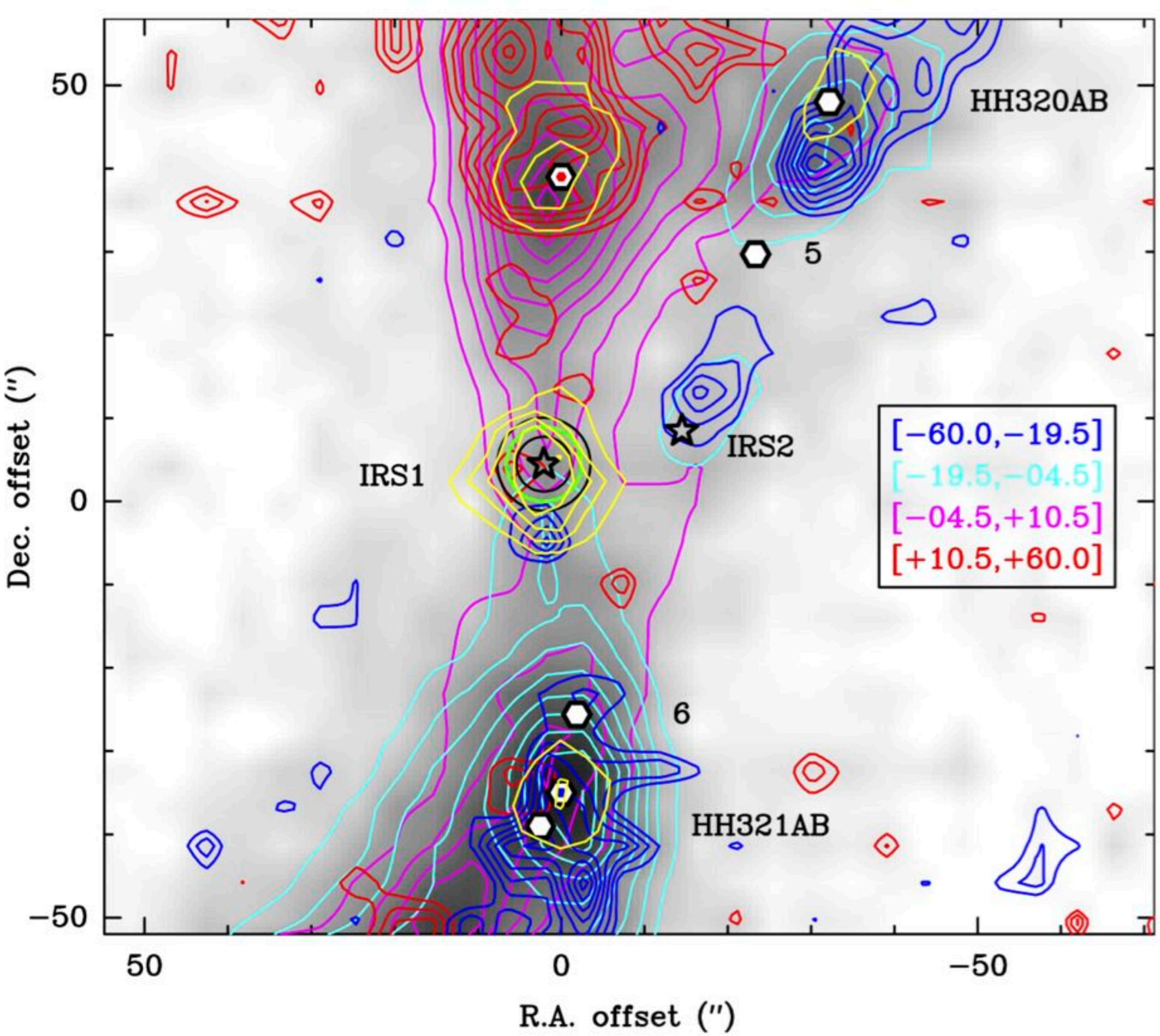

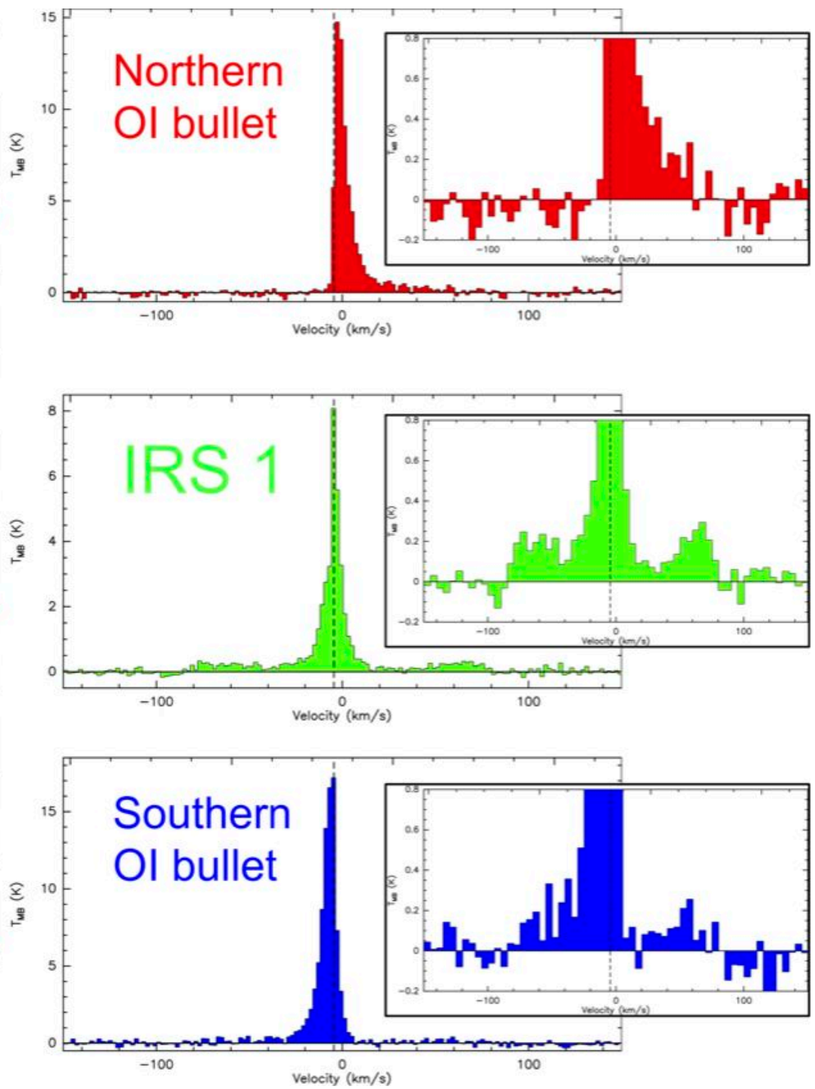

Gusdorf et al., in prep.

BHR71: the latest news

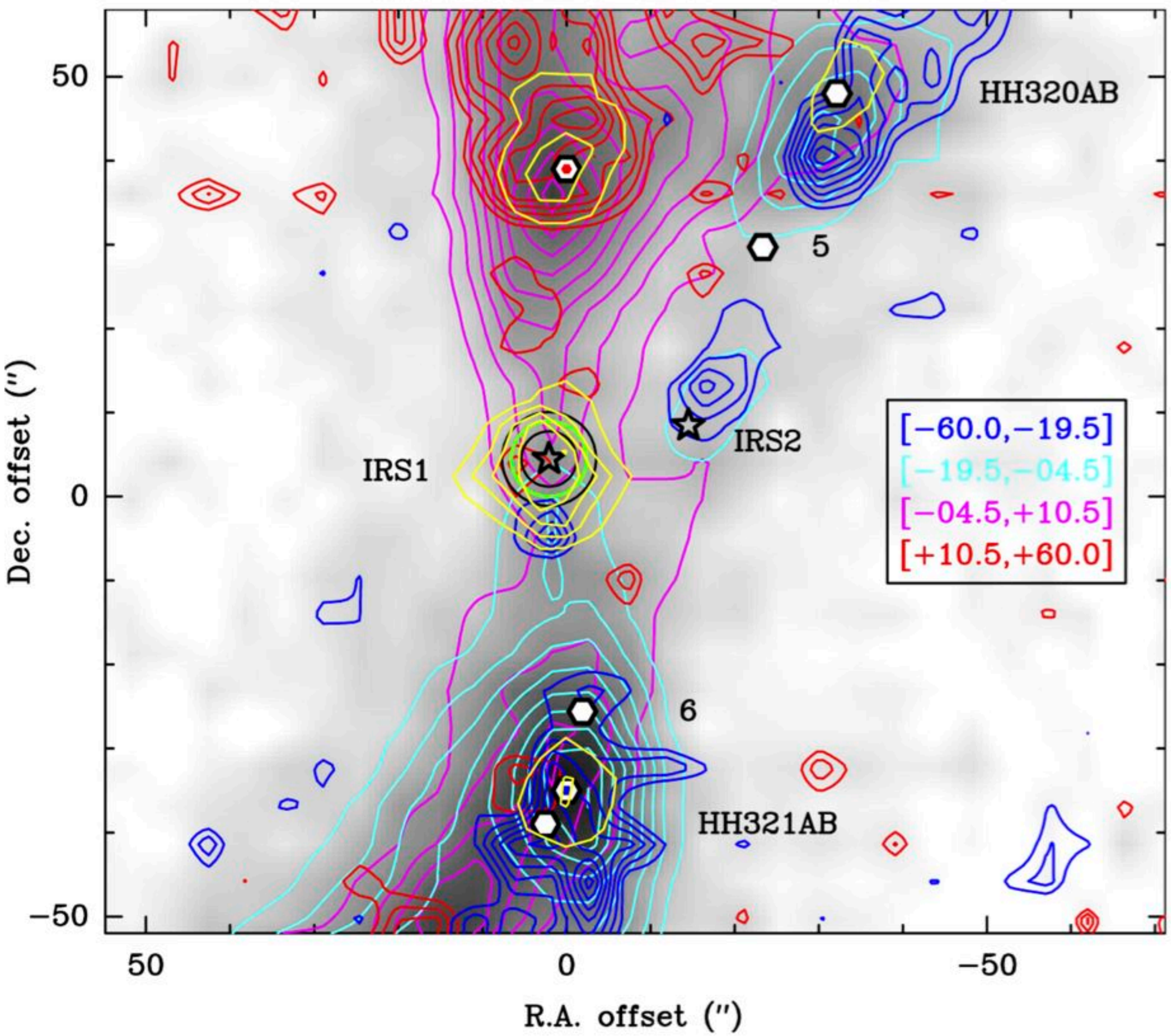

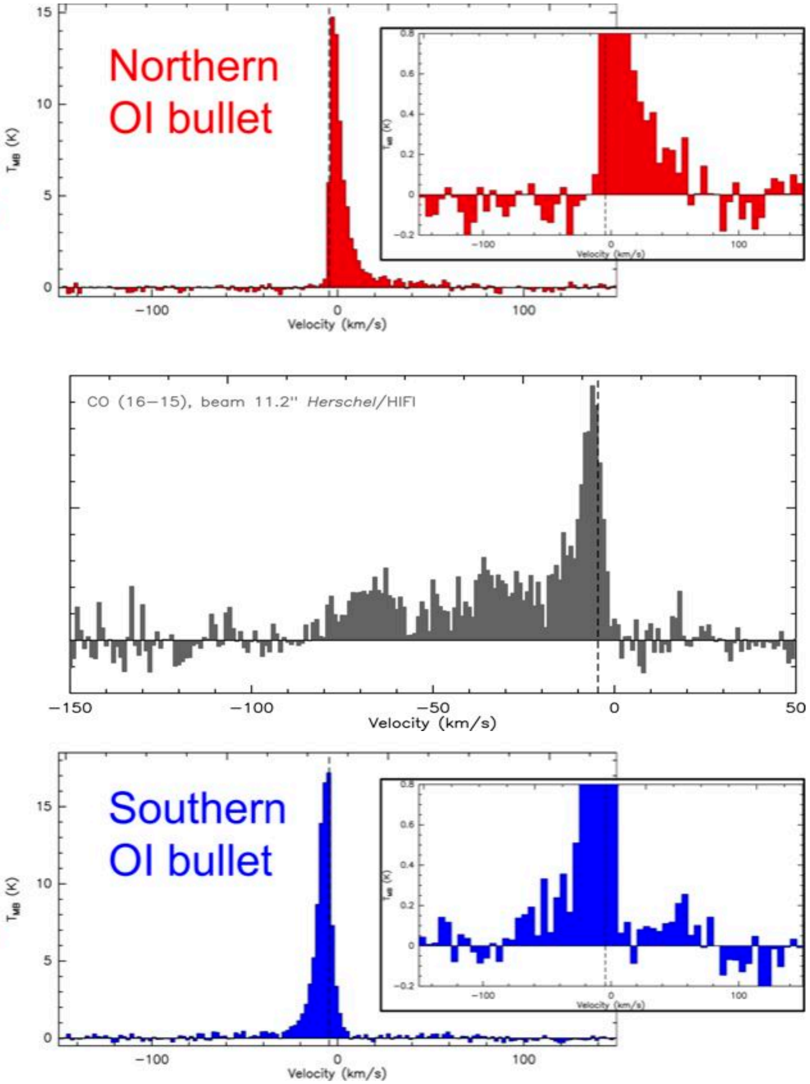

Gusdorf et al., in prep.

BHR71: the latest news

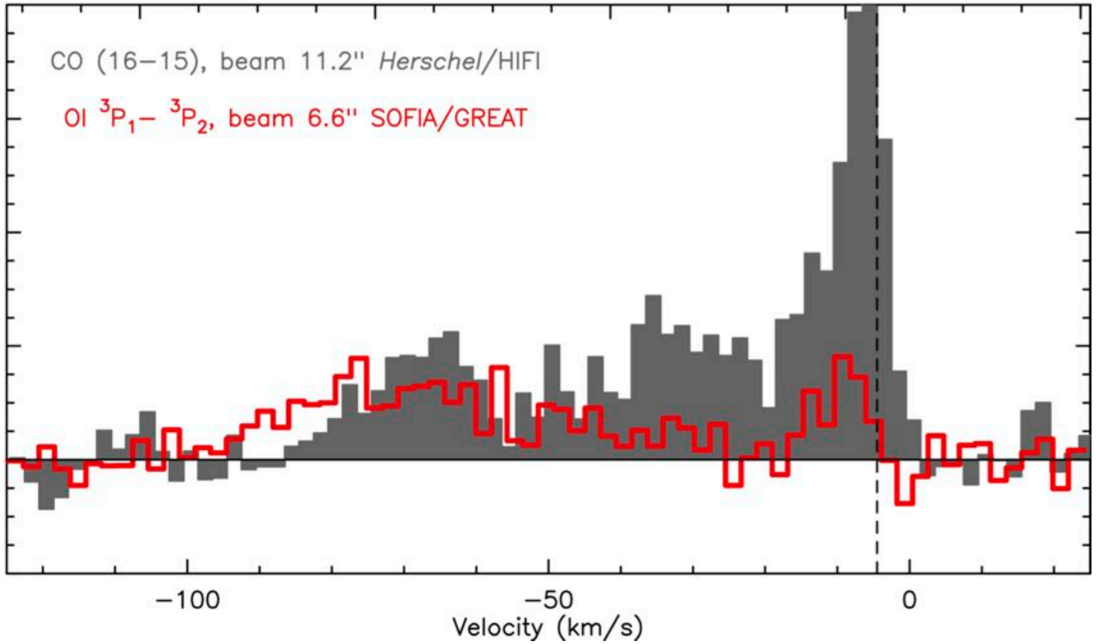

Gusdorf et al., in prep.

BHR71: the latest news

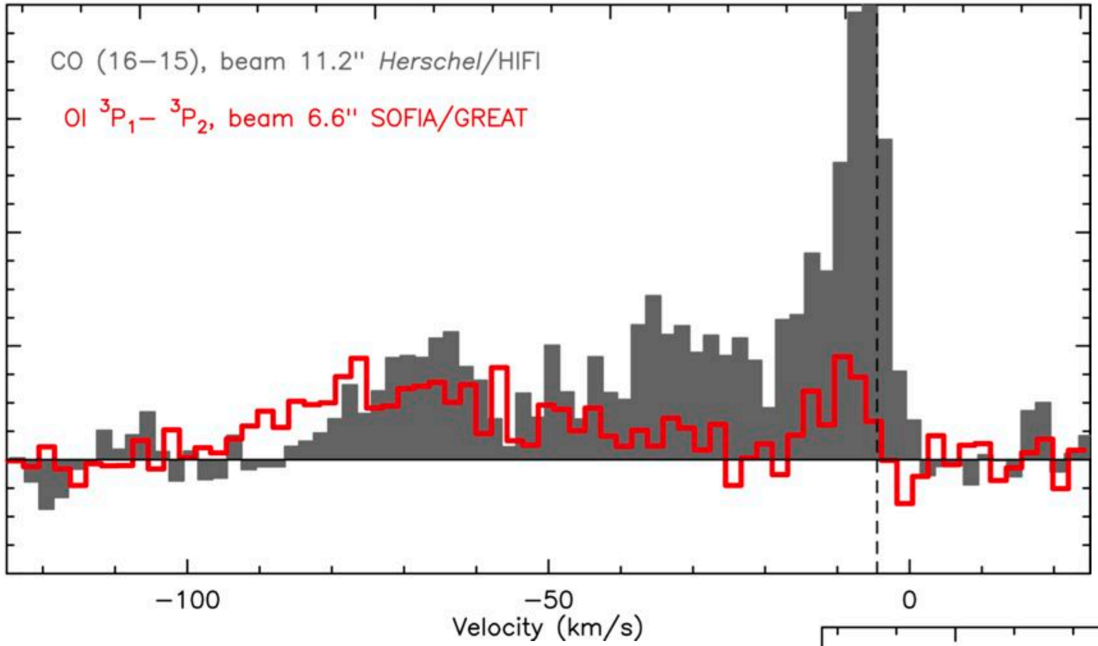

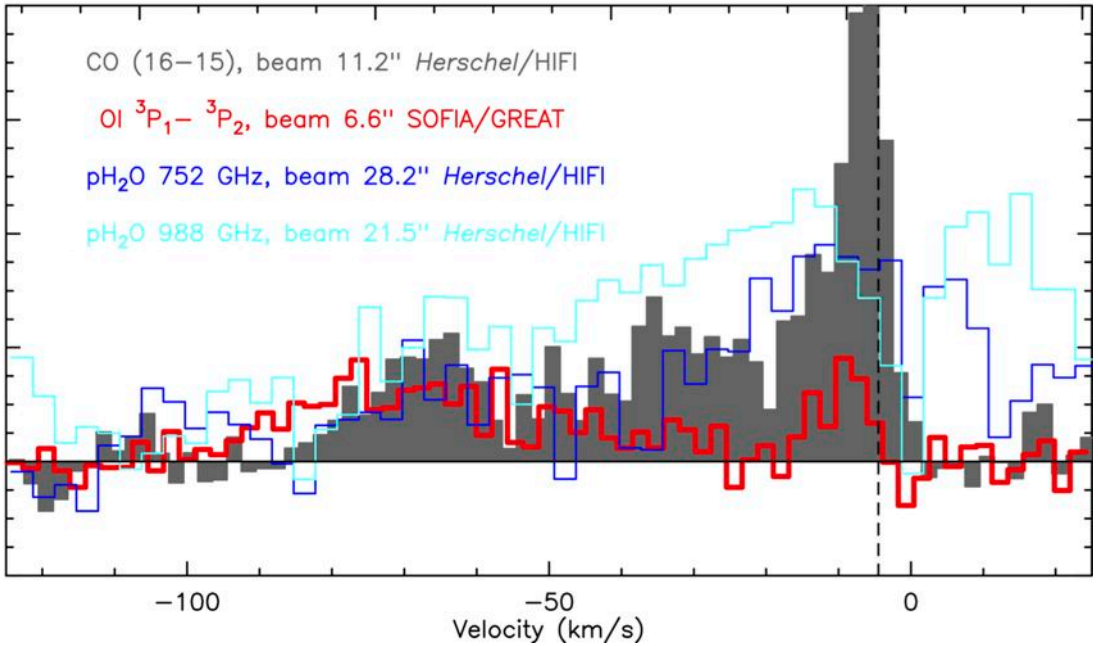

Gusdorf et al., in prep.

…To higher-mass star formation

Intermediate-mass star formation: Cepheus E

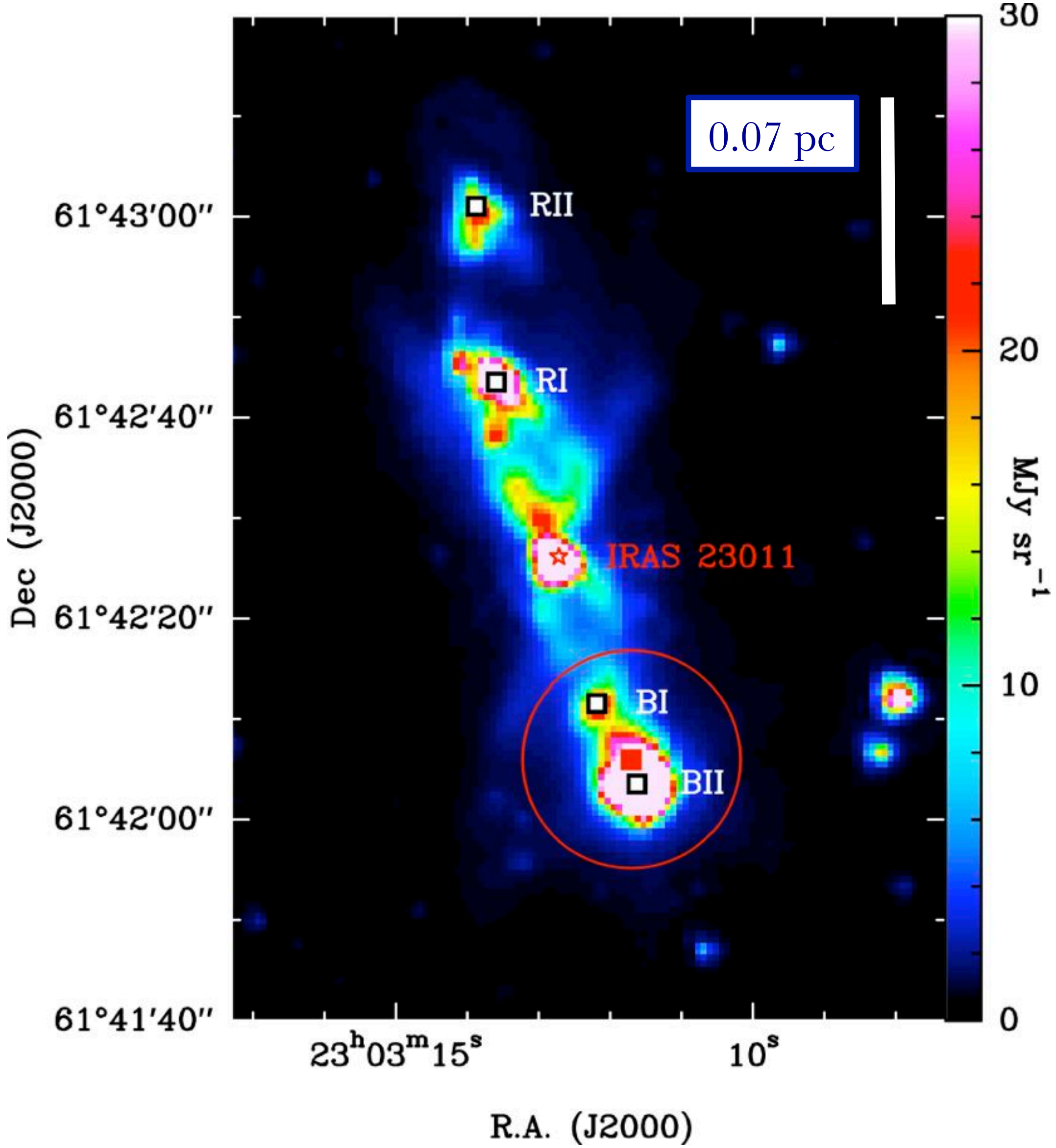

The Cep E outflow at 4.5 μm by *Spitzer*/IRAC

Intermediate-mass star formation: Cepheus E

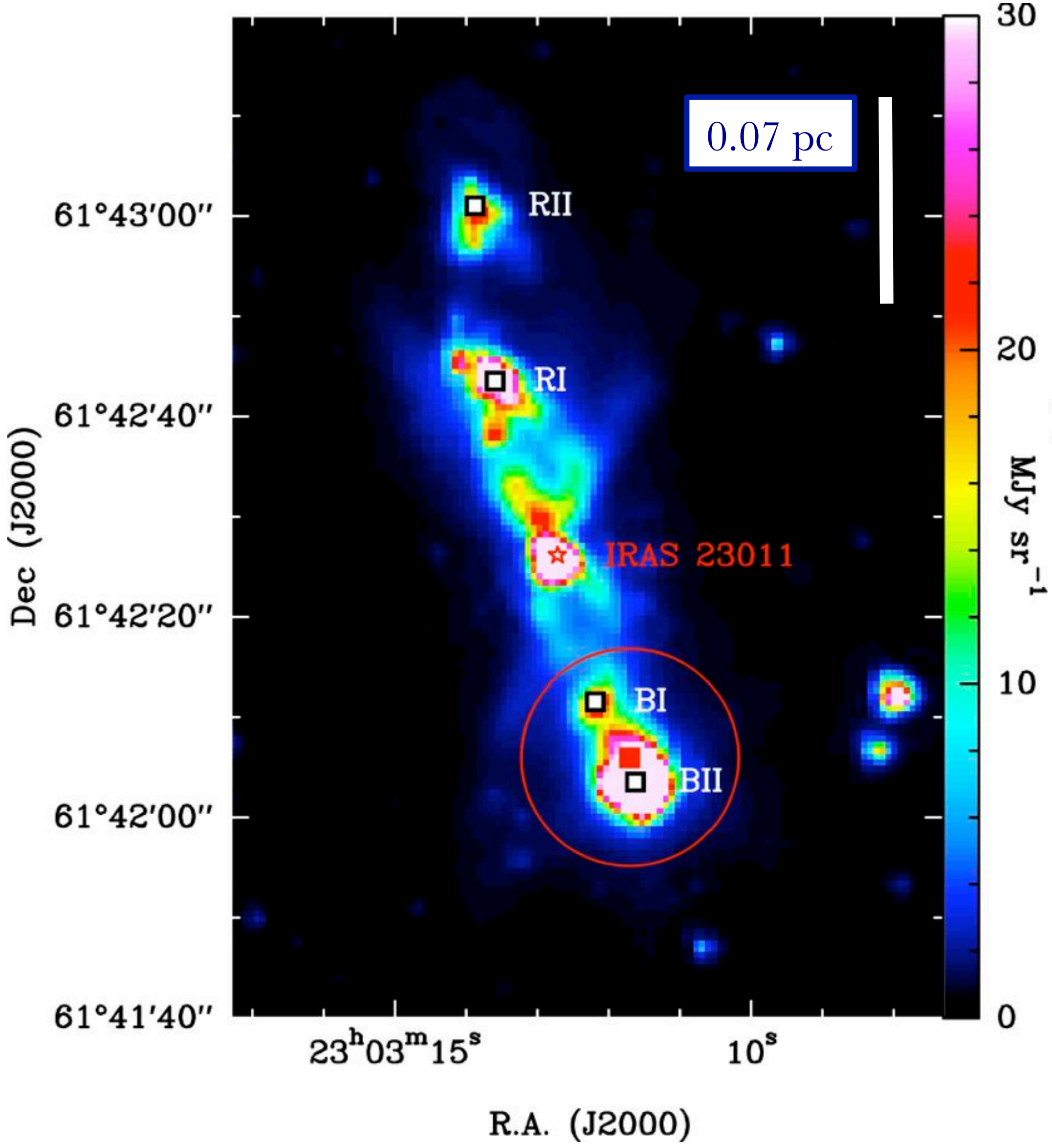

The Cep E outflow at 4.5 μm by *Spitzer*/IRAC

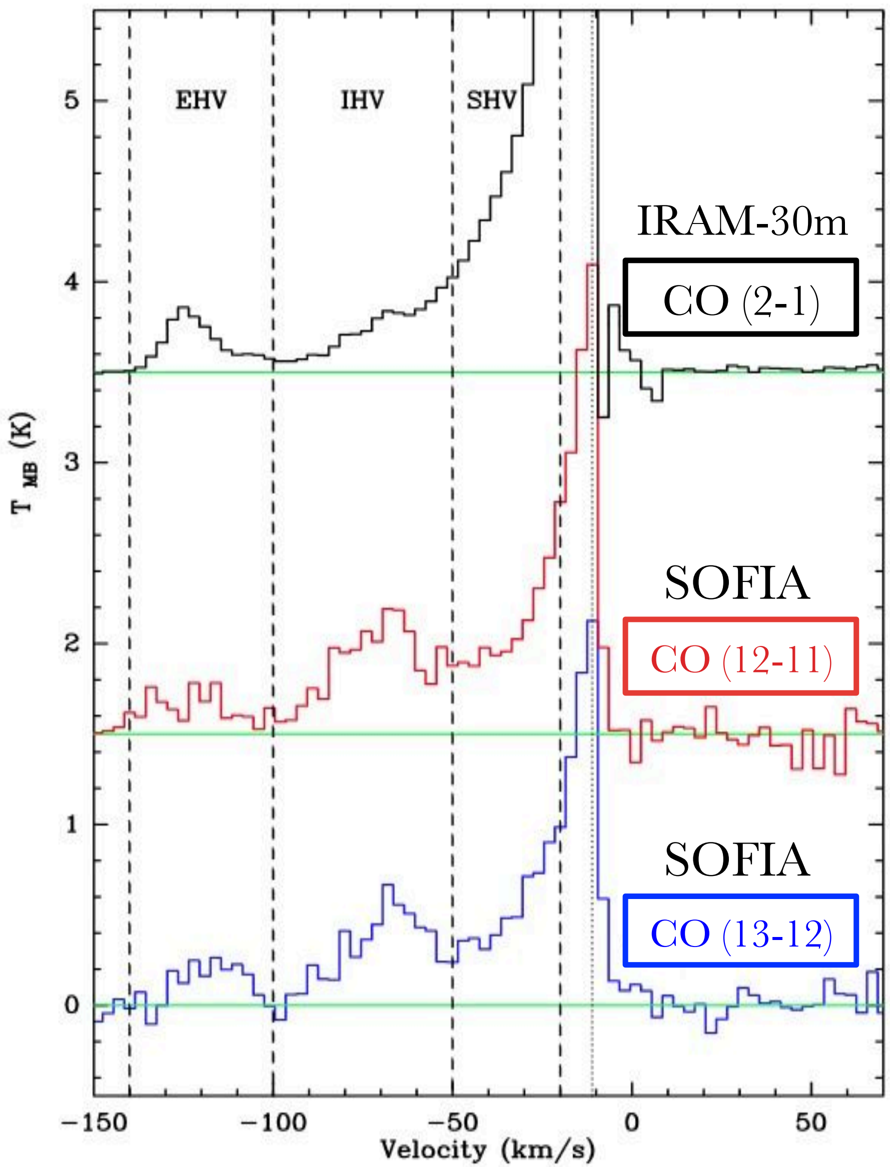

Gomez-Ruiz et al. 2012

Intermediate-mass star formation: Cepheus E

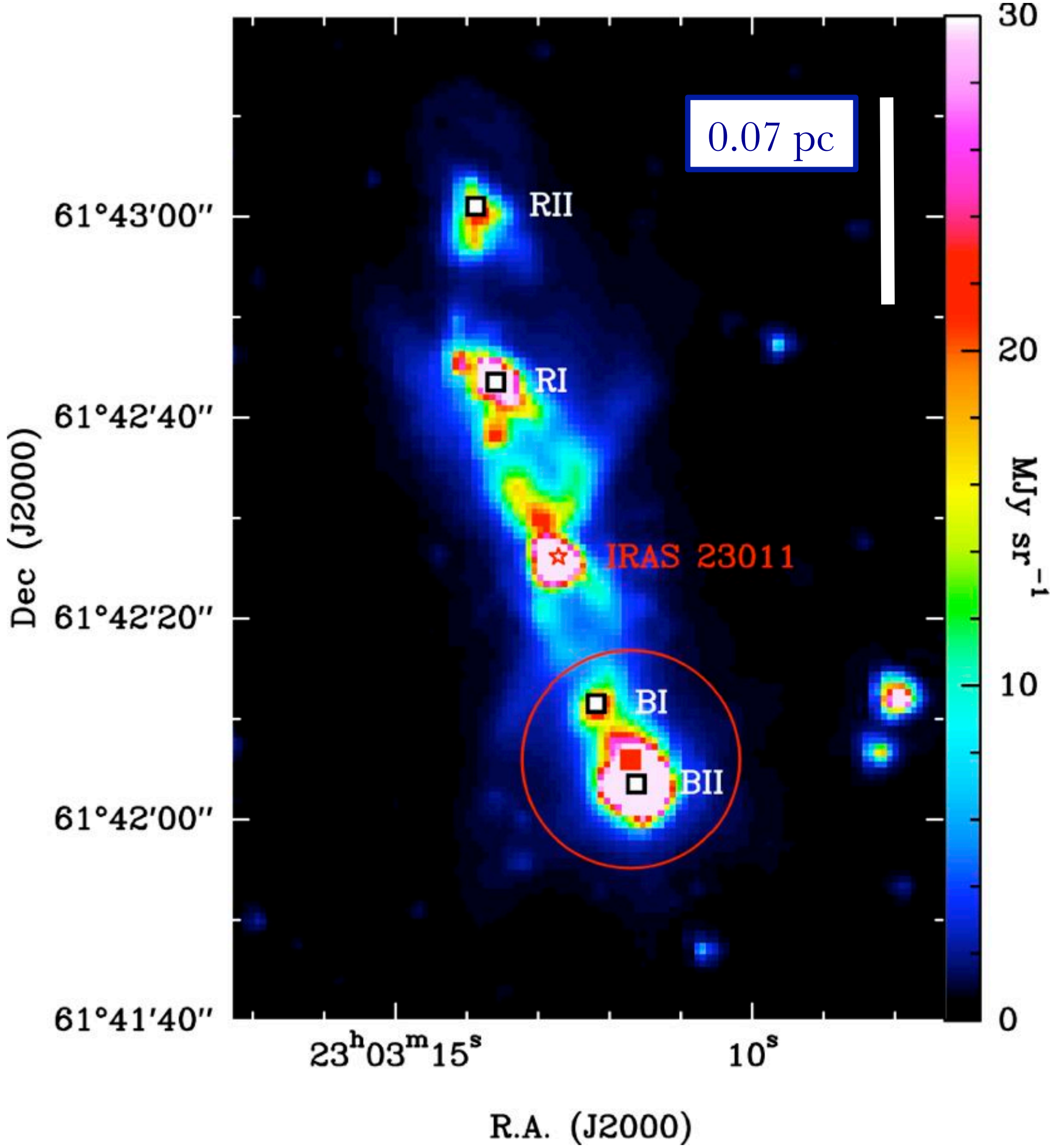

The Cep E outflow at 4.5 μm by *Spitzer*/IRAC

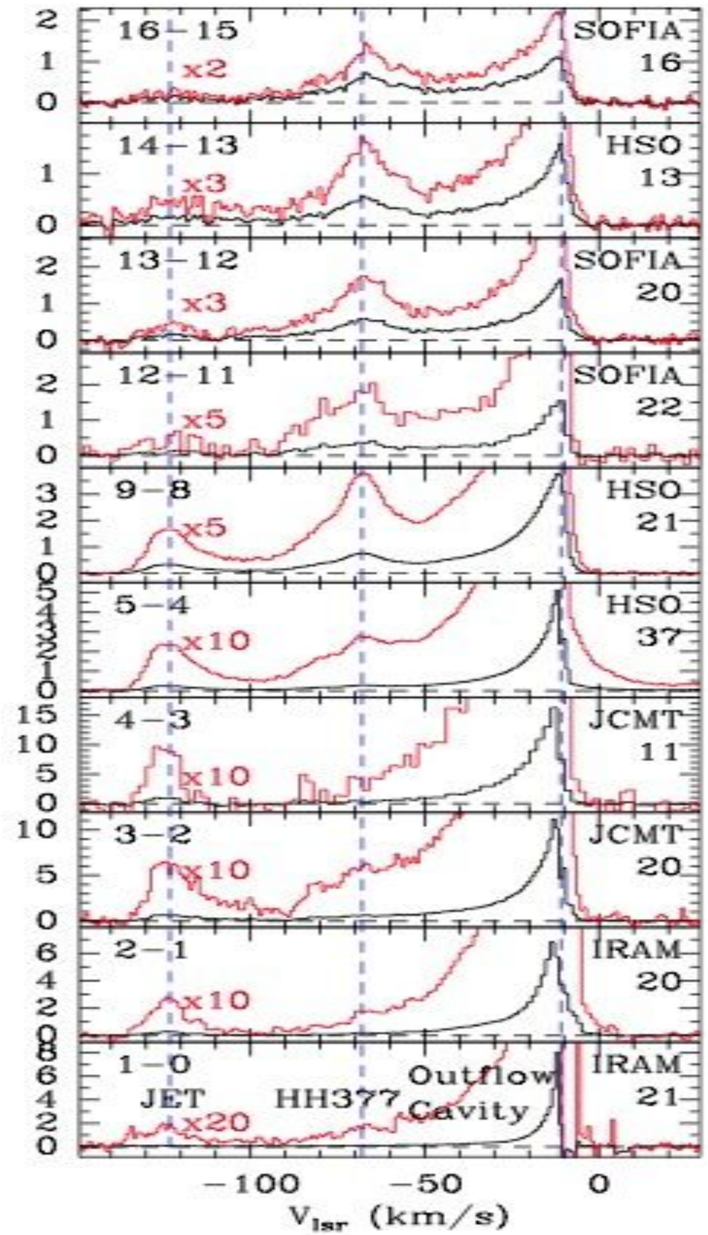

Lefloch et al. 2015

Intermediate-mass star formation: Cepheus E

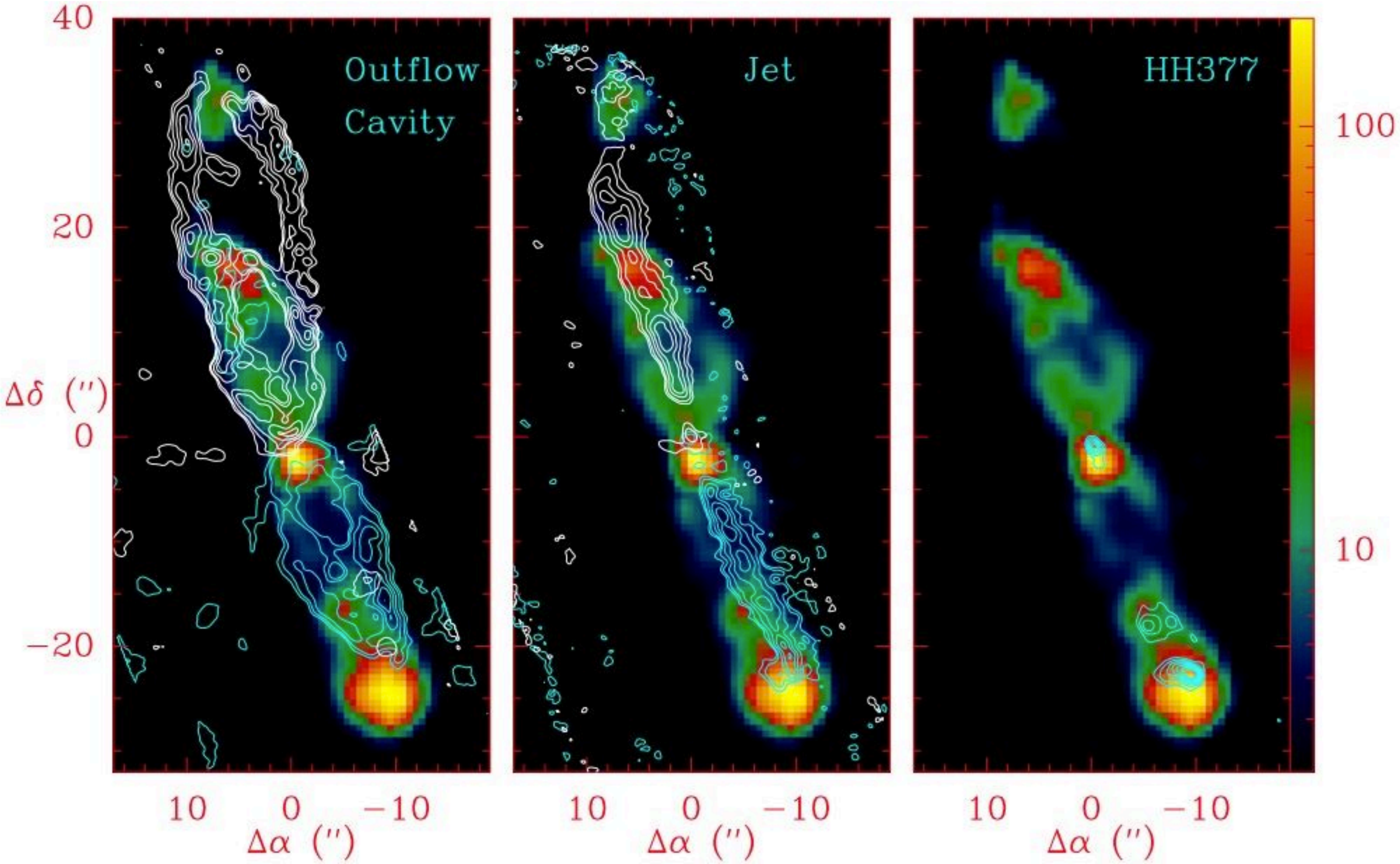

The Cep E outflow in CO (2-1) by the PdBI

Lefloch et al. 2015

Intermediate-mass star formation: Cepheus E

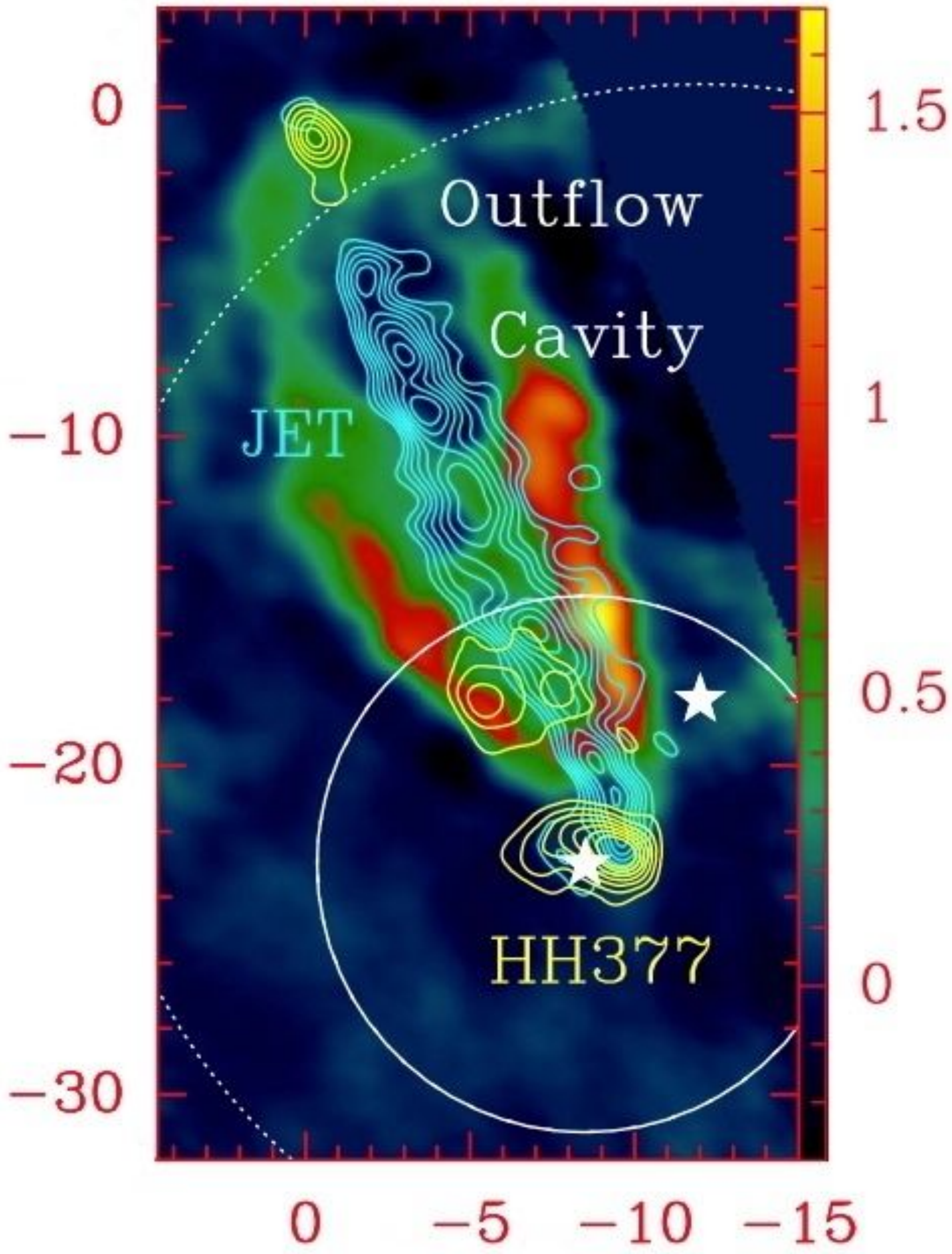

- Jet, cavity, HH 377:

LVG analysis of CO emission

=> (N, T_{kin}) estimates

- Southern lobe:
  - jet mass: 0.02 $M_\odot$, 1.7 $M_\odot$km/s
  - outflow cavity mass: 0.32 $M_\odot$, 2.8 $M_\odot$km/s

=> molecular jet driven bowshock

- (Non-irradiated) shock models of the jet hot component

=> perspectives: chemistry (SO, SiO, HCO^+, IRAM-30m and PdBI, Lefloch et al. in prep, I, II, later H_2O)

Massive star formation: G5.89-0.39

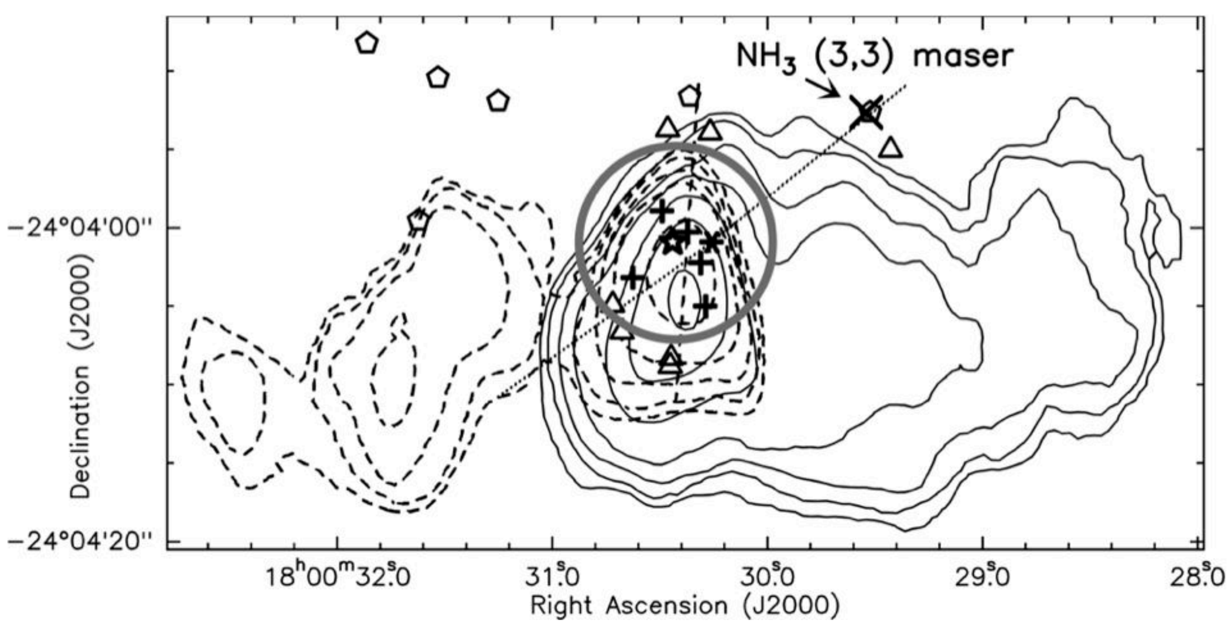

Hunter et al. 2008

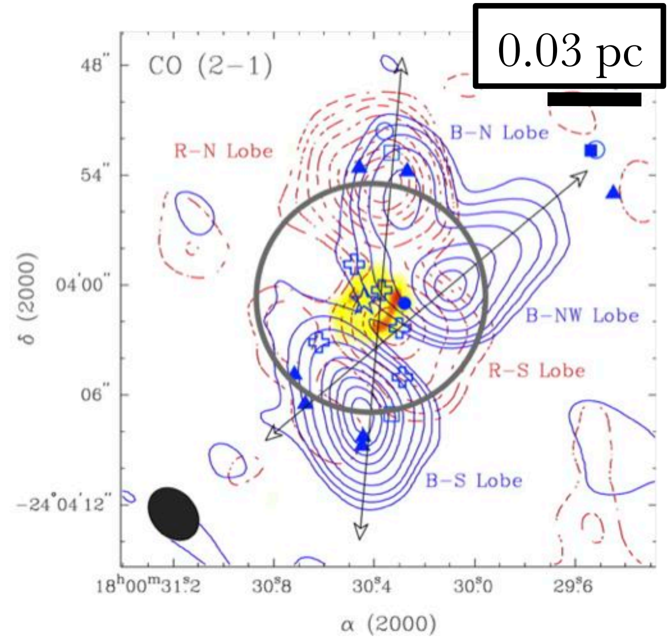

Su et al. 2012

- "The Harvey & Forveille 1988 outflow":
  - one massive O-type (imaged) star (Feld's star);
  - one UC HII region surrounded by a PDR-like cocoon, 5 continuum sources;
  - one Brγ outflow, 3 molecular outflows (seen in H_2, CO, SiO and HCO^+);
  - a collection of OH, H_2O, CH_3OH, and NH_3 maser spots

Massive star formation: G5.89-0.39

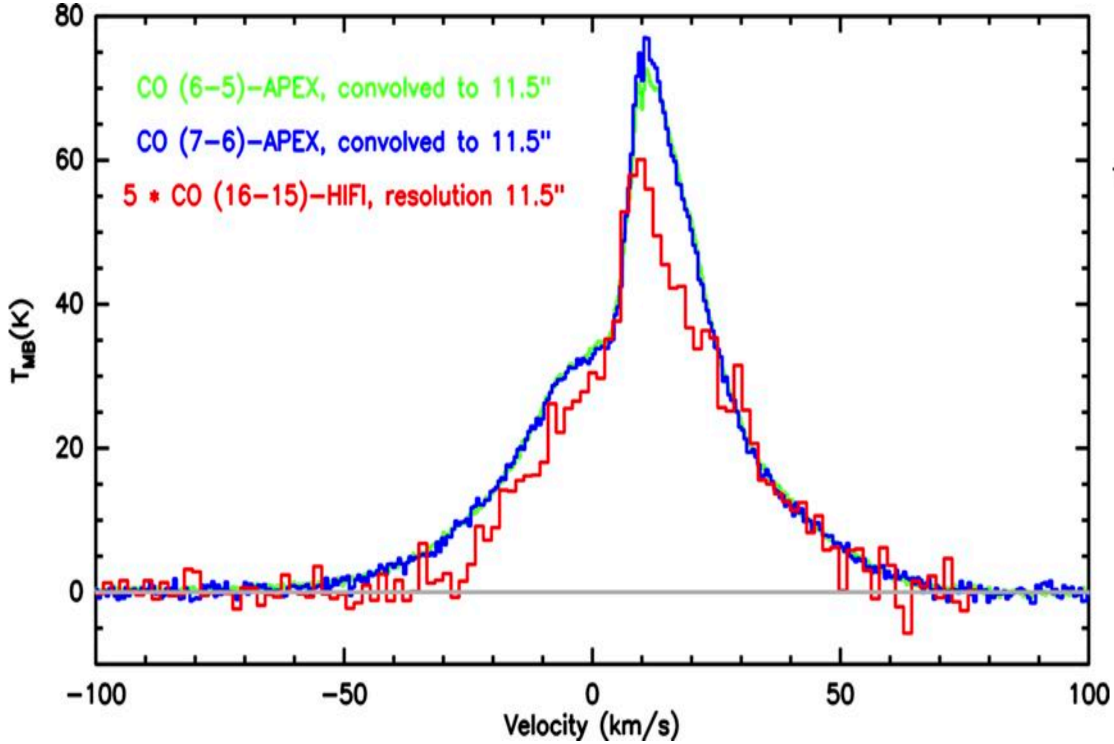

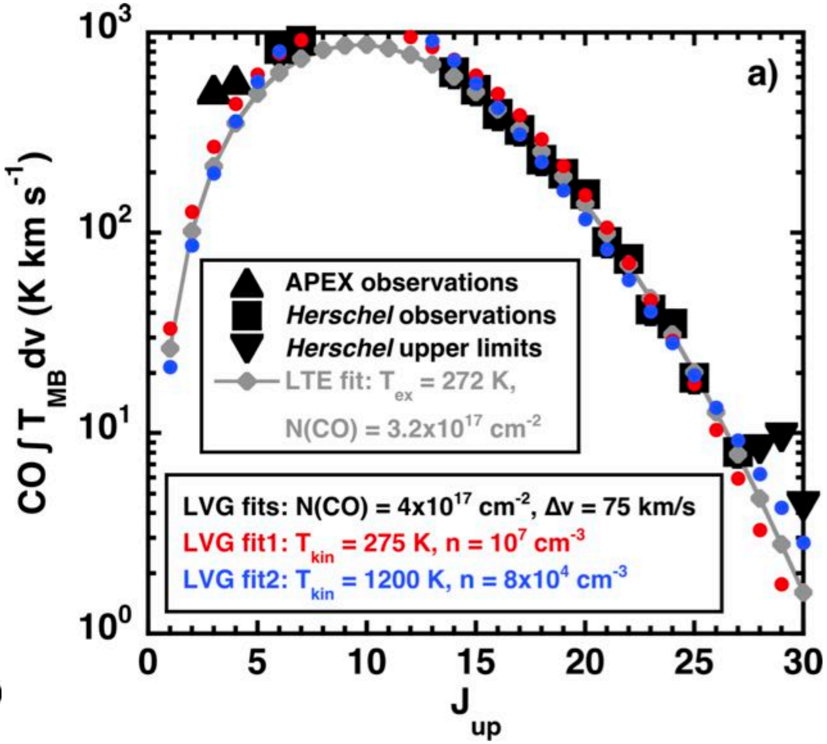

- APEX and *Herschel* (HIFI and PACS) observations of ^{12}CO and ^{13}CO

- Analysis of CO emission:
  - warm component (275 K, 10^7 cm^{-3}) or (1200 K, 10^5 cm^{-3}); N~$3{\cdot}10^{17}$ cm^{-2}
  - colder component thanks to APEX observations of ^{13}CO (3-2), (6-5):

(75 K, $6{\cdot}10^{18}$ cm^{-2})

Gusdorf et al., accepted by A&A

Massive star formation: G5.89-0.39

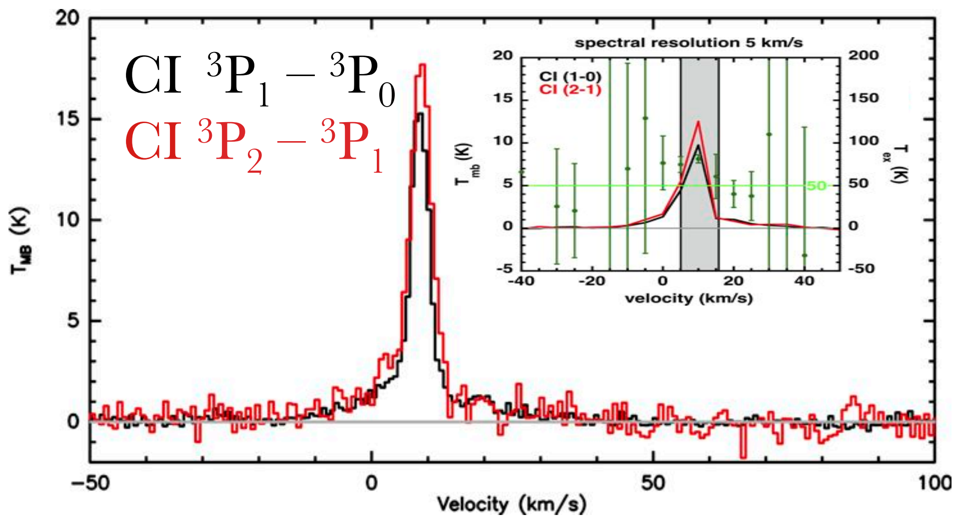

- CI optically thin and in LTE conditions

- T_{ex} ~ 70 +/- 20 K,

$N_{blue} \sim N_{red} \sim 3 \cdot 10^{17}$ cm^{-2}

=> associated to CO cold component

Also observed: SiO, CH^+…

Massive star formation: G5.89-0.39

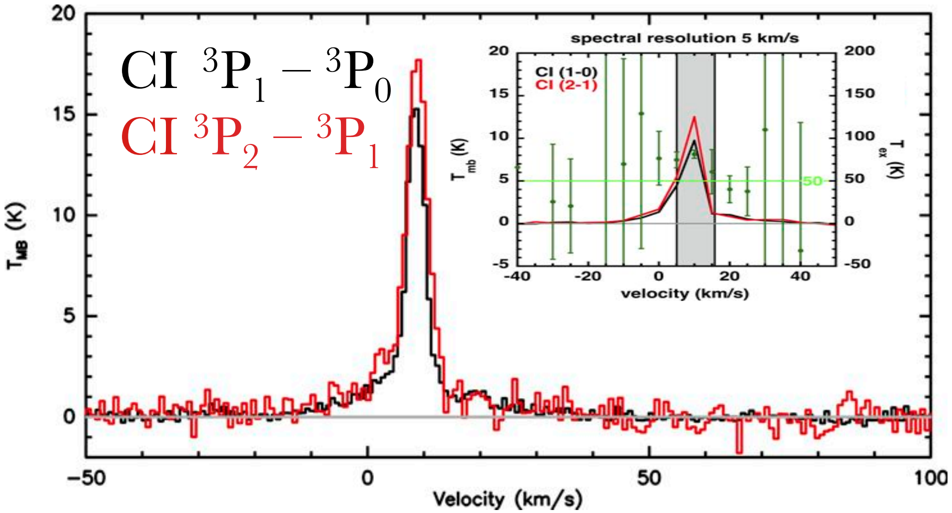

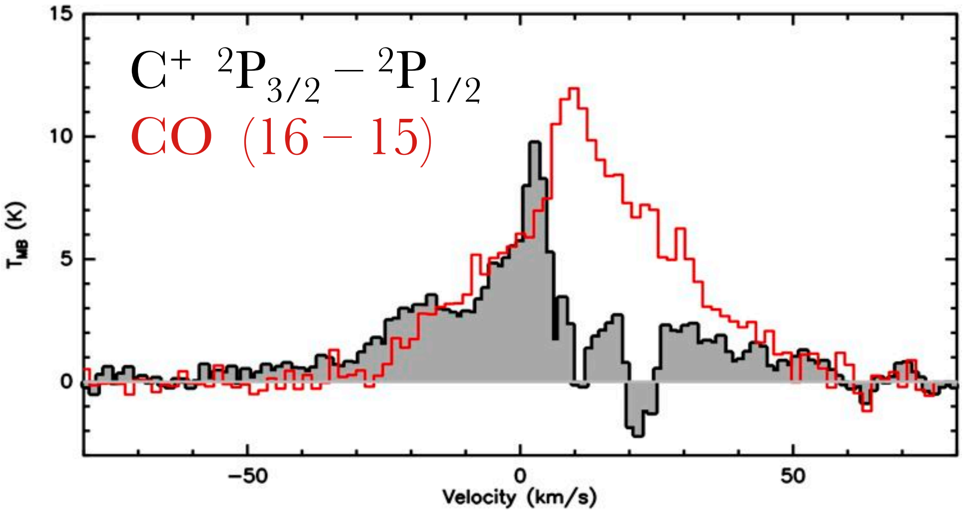

- CI optically thin and in LTE conditions
- T_{ex} ~ 70 +/- 20 K,

$N_{blue} \sim N_{red} \sim 3{\cdot}10^{17}$ cm^{-2}

=> associated to CO cold component

- CII LTE assumption
- similarity of profile with CO (16-15)

=> associated to CO warm component

T_{ex} ~ 250 K,

$N_{blue} \sim 5{\cdot}10^{17}$ cm^{-2} > N (CO)

Also observed: SiO, CH^+…

Gusdorf et al., accepted by A&A

Massive star formation: G5.89-0.39

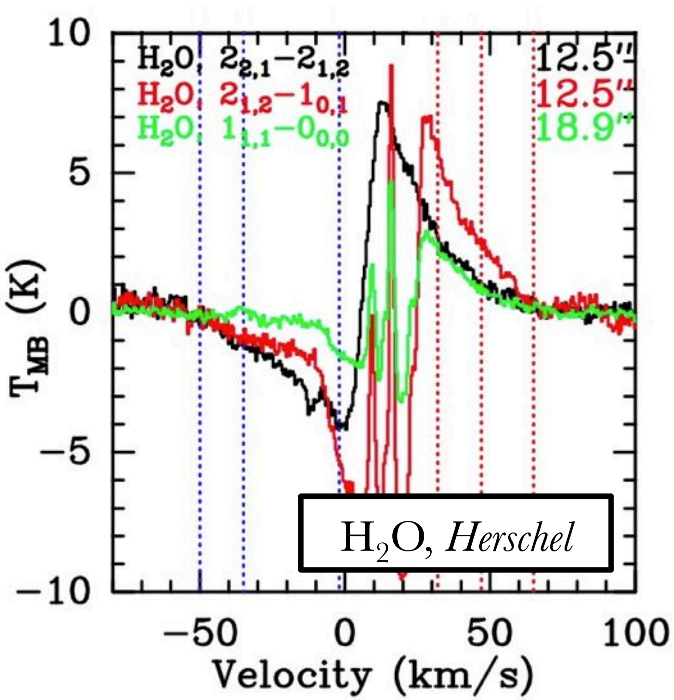

Leurini et al., in press

Massive star formation: G5.89-0.39

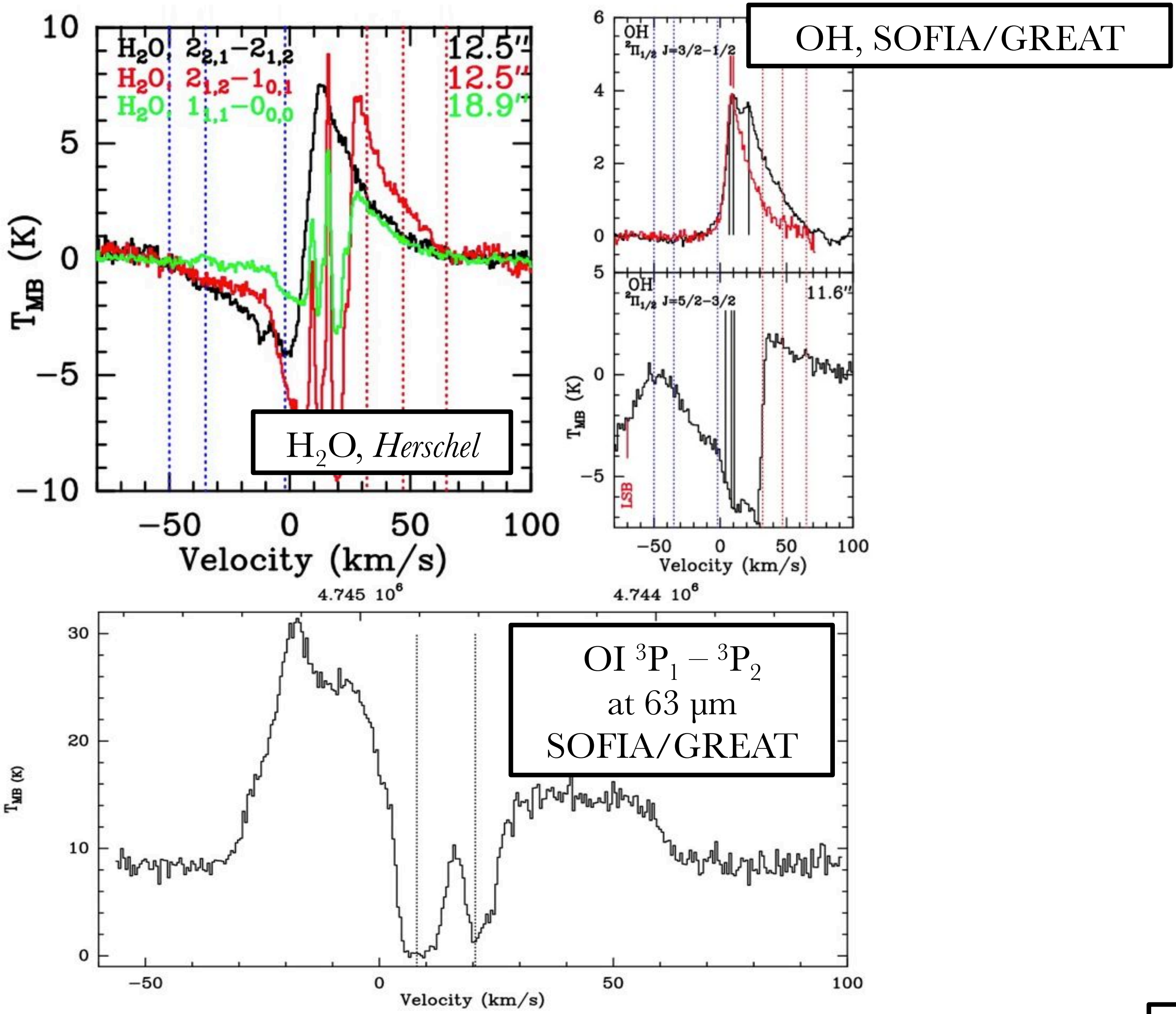

Leurini et al., in press

Massive star formation: G5.89-0.39

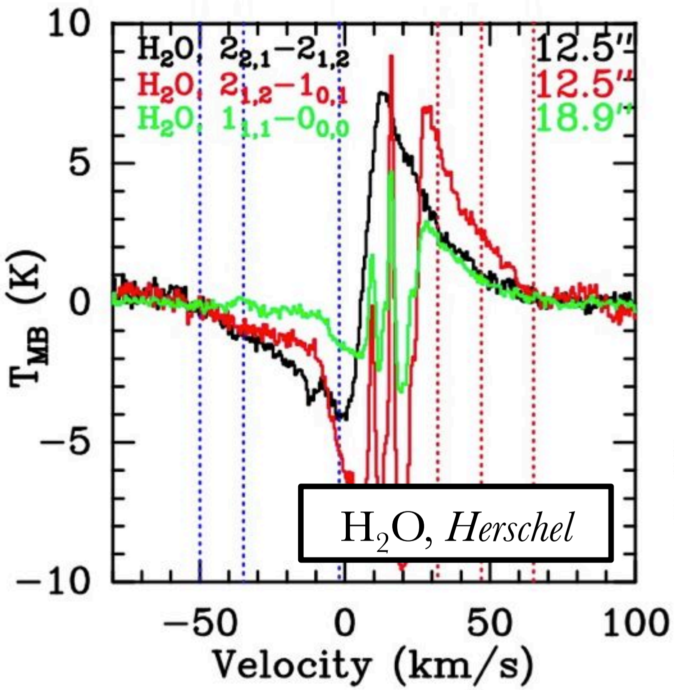

H_2O, *Herschel*

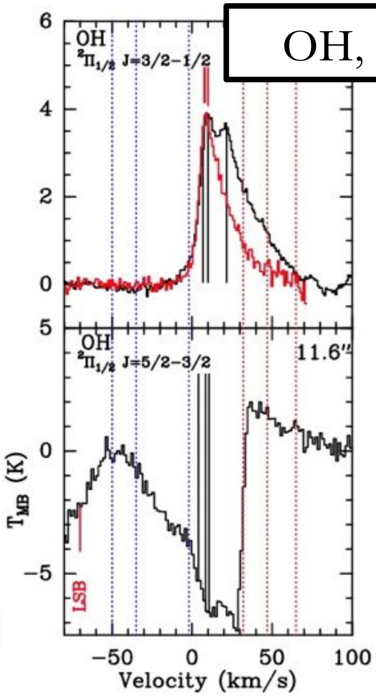

OH, SOFIA/GREAT

Species	$N_{X_{Tex}}$ (cm^{-2})	$X = \frac{N_{X_{Tex}}}{N_{CO}}$	T_{ex} (K)
Blue-shifted wing (Δv = [−50, −2] km s^{-1})			
HF	$(2.7 \pm 0.5) \times 10^{14}$	2×10^{-3}	14
CO[a]	$(1.3 \pm 0.4) \times 10^{17}$		202
CII	$(3.6 \pm 0.8) \times 10^{18}$	28	200
OH	$(3.5 \pm 0.1) \times 10^{14}$	3×10^{-3}	10
o-H_2O (1661 GHz)	$(3.0 \pm 0.1) \times 10^{16}$	2×10^{-1}	30
o-H_2O (1669 GHz)	$(5 \pm 0.3) \times 10^{15}$	4×10^{-2}	10
Red-shifted wing (Δv = [+32, +70] km s^{-1})			
CO[a]	$(5 \pm 2) \times 10^{16}$		208
CII	$(1.2 \pm 0.7) \times 10^{18}$	24	200
OH[b]	3×10^{14}	6×10^{-3}	>100
o-H_2O[b]	3×10^{14}	6×10^{-3}	>100
p-H_2O[b]	2×10^{14}	4×10^{-3}	>100

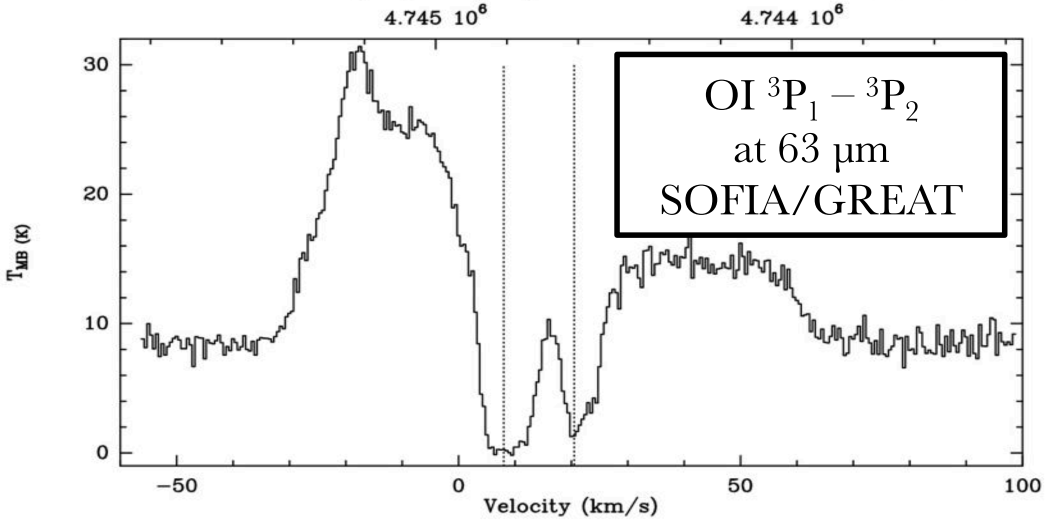

OI $^3P_1 - ^3P_2$
at 63 μm
SOFIA/GREAT

	$[OI]_{63\mu m}$ Blue	$[OI]_{63\mu m}$ Red	CO+[CI]+[CII] Blue	CO+[CI]+[CII] Red
N (10^{21} cm^{-2})	8.3	>7.5	11-22	>(6–11)
M ($M_\odot$)	0.1	>0.1	0.4–0.8	>(0.2–0.4)
Δv_{max} (km s^{-1})	50	58	50	50
t_d (yr)	400	350	760	760
P ($M_\odot$ km s^{-1})	6.1	>6.5	21–41	>(11–21)
F_m (10^{-2} $M_\odot$ km s^{-1} yr^{-1})	2	>2	2.7–5.4	>(1.5–2.7)
E_k (10^{45} erg)	3.1	>3.7	10.3–20.7	>(5.6–10.3)
L_m ($L_\odot$)	63	>89	112–224	>(61–112)

Leurini et al., in press

Massive star formation: Cep A

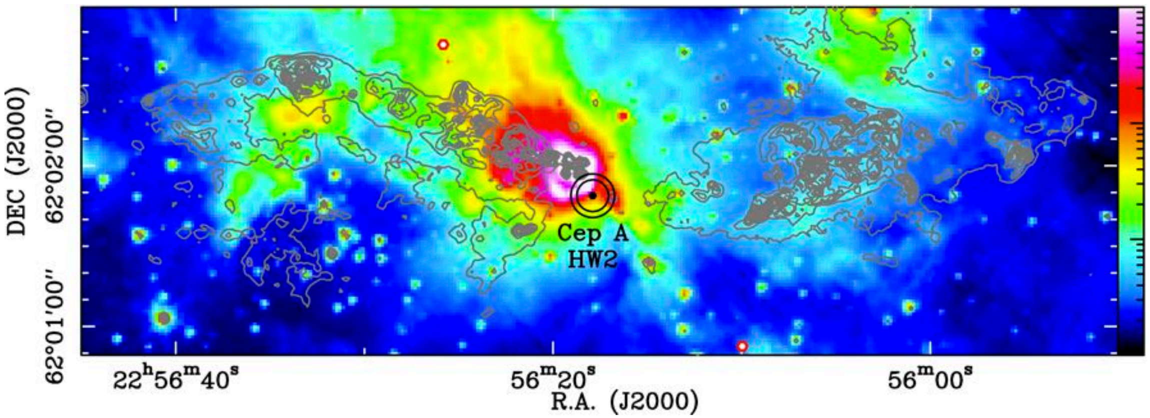

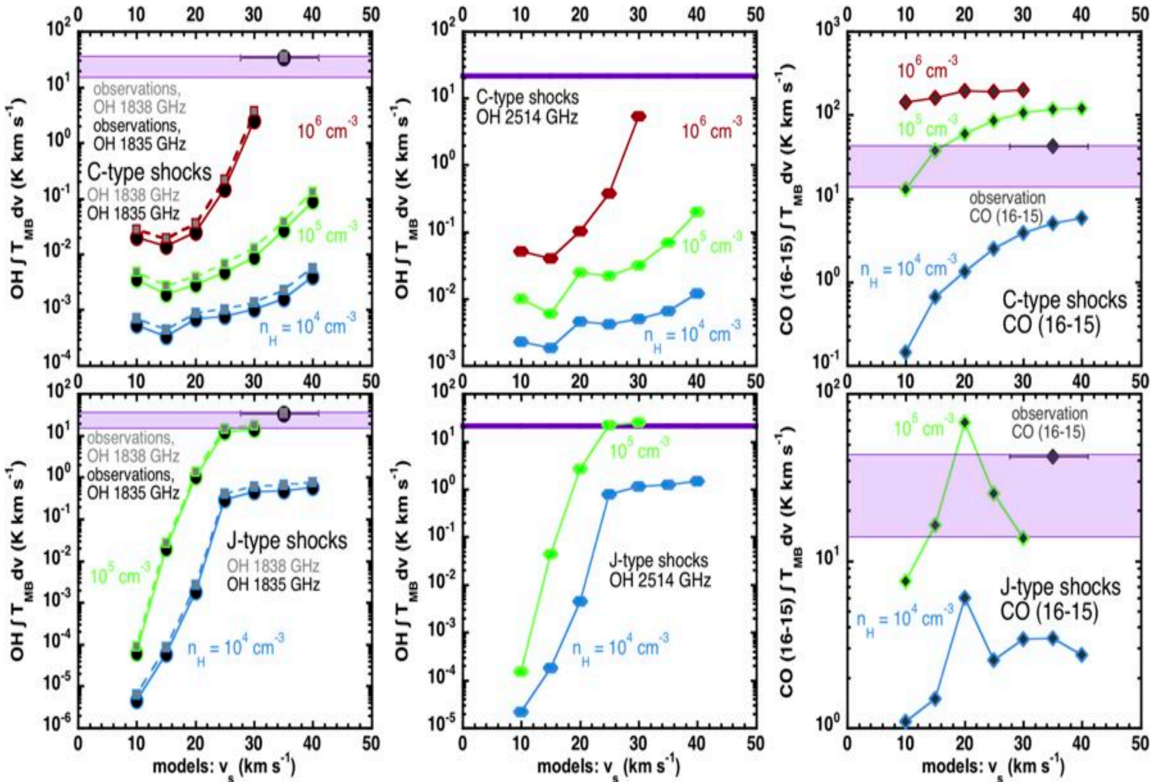

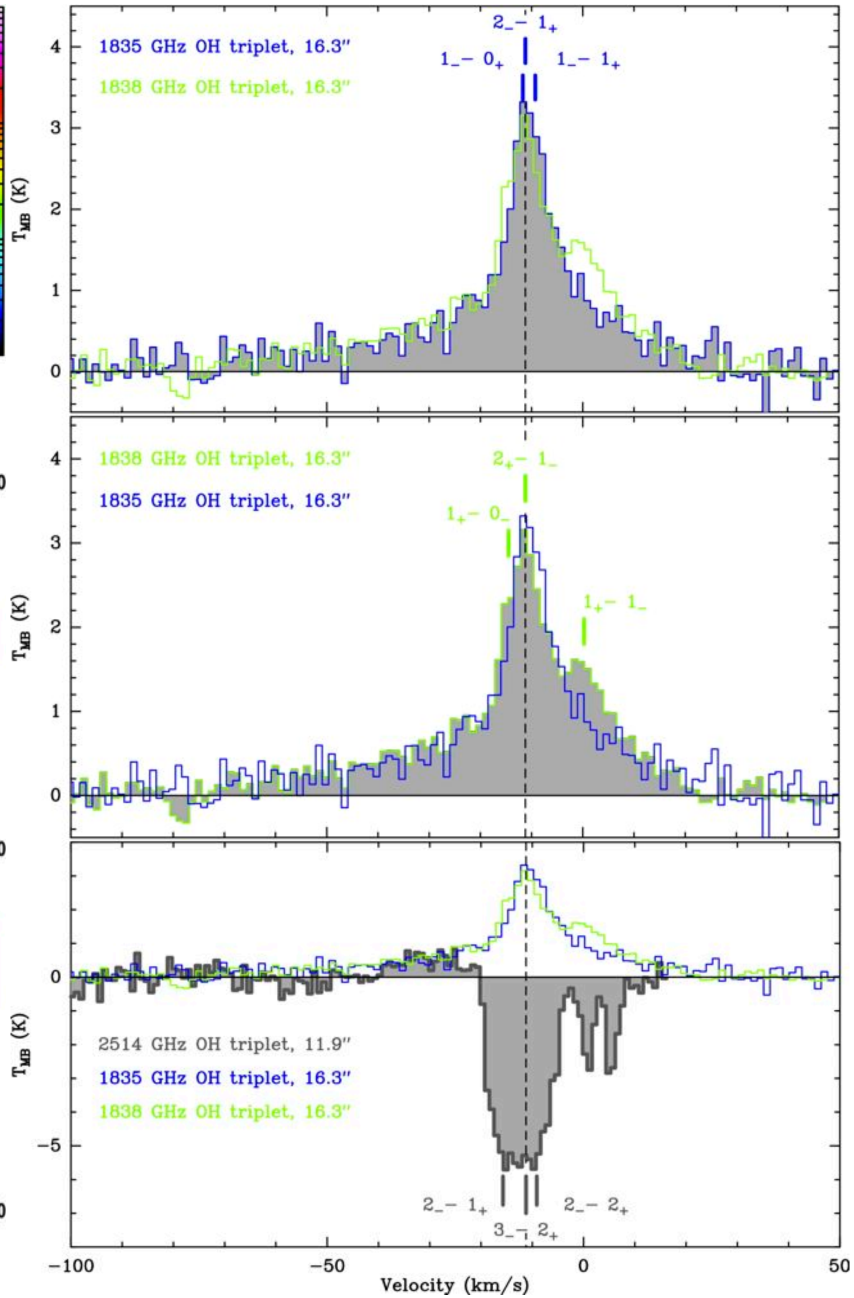

Gusdorf et al. 2015b

Filaments and ridges

Filaments and ridges

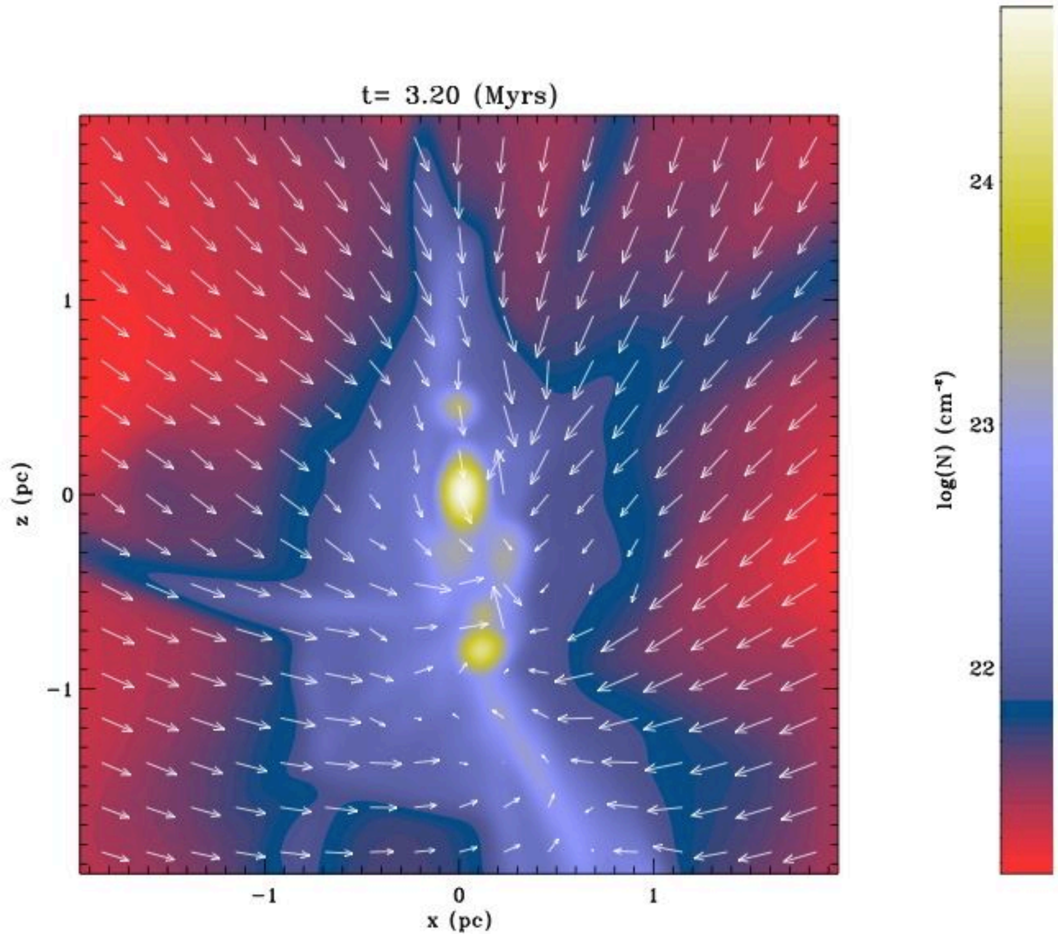

Schneider et al. 2010

Filaments and ridges

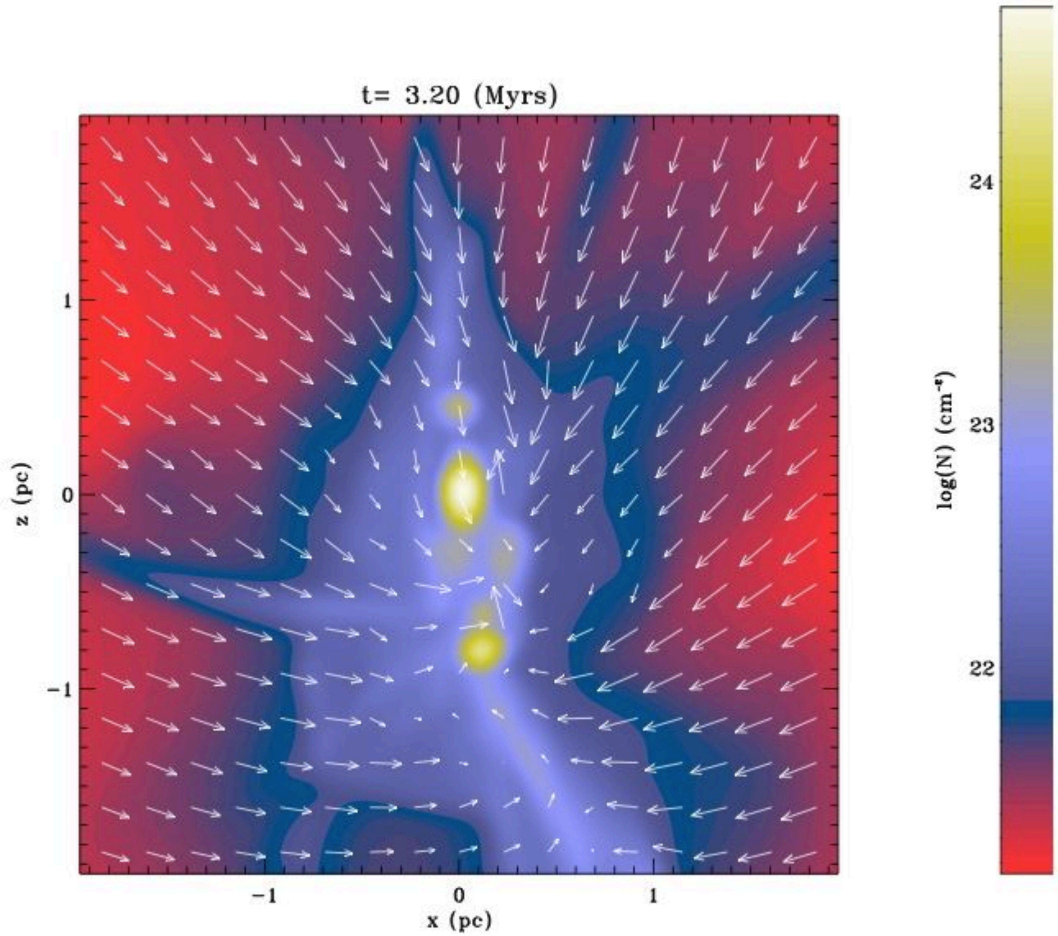

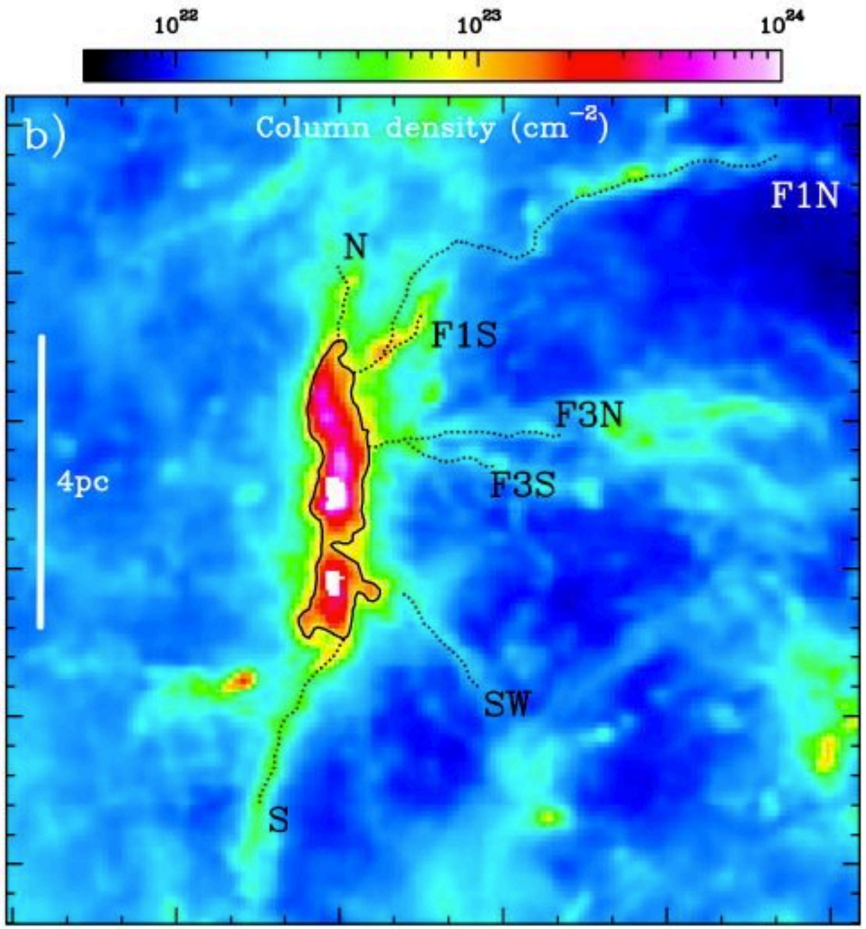

Schneider et al. 2010

Hennemann et al. 2012

The W43-MM1 ridge

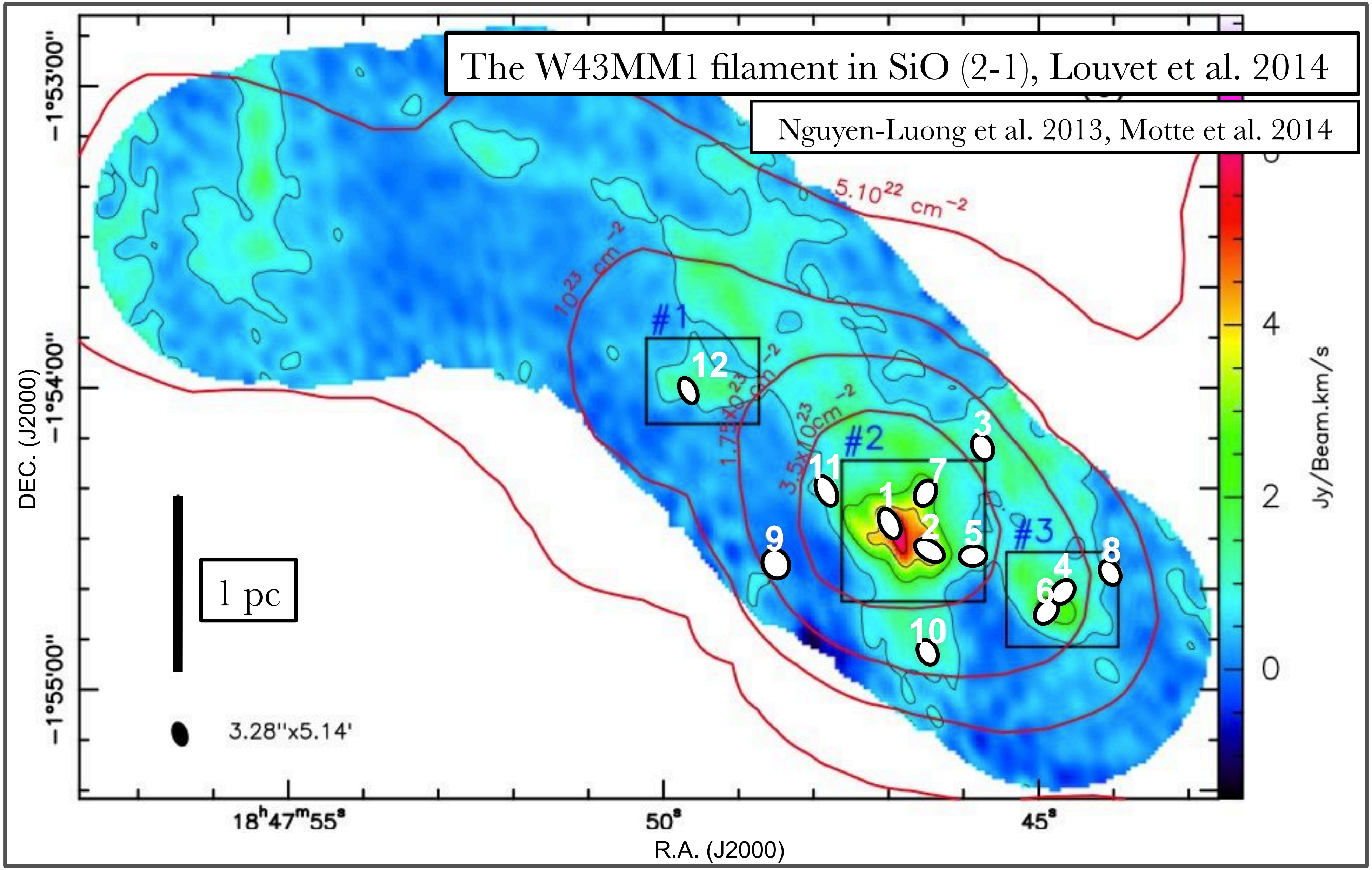

The W43-MM1 ridge

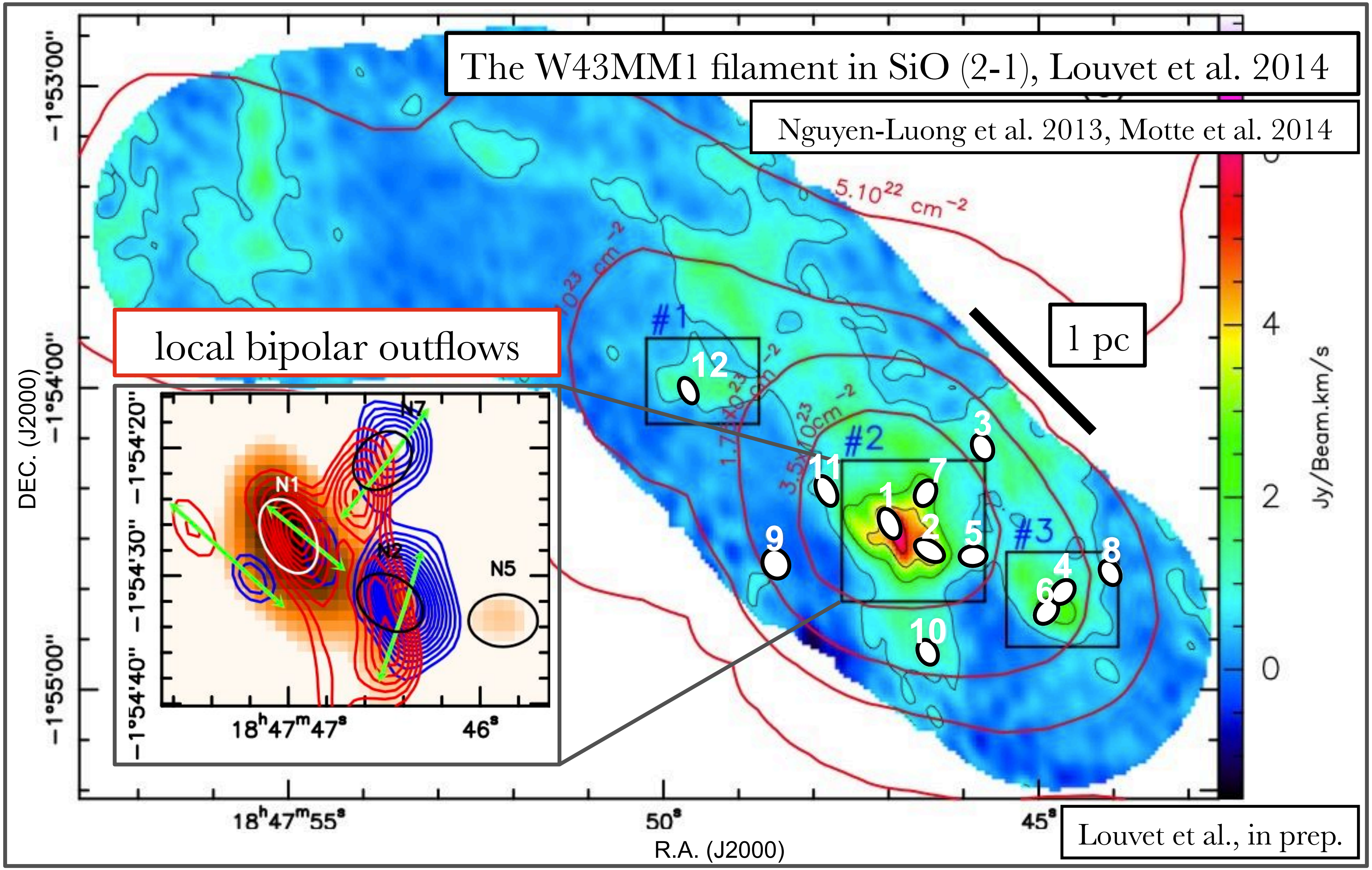

The W43-MM1 ridge

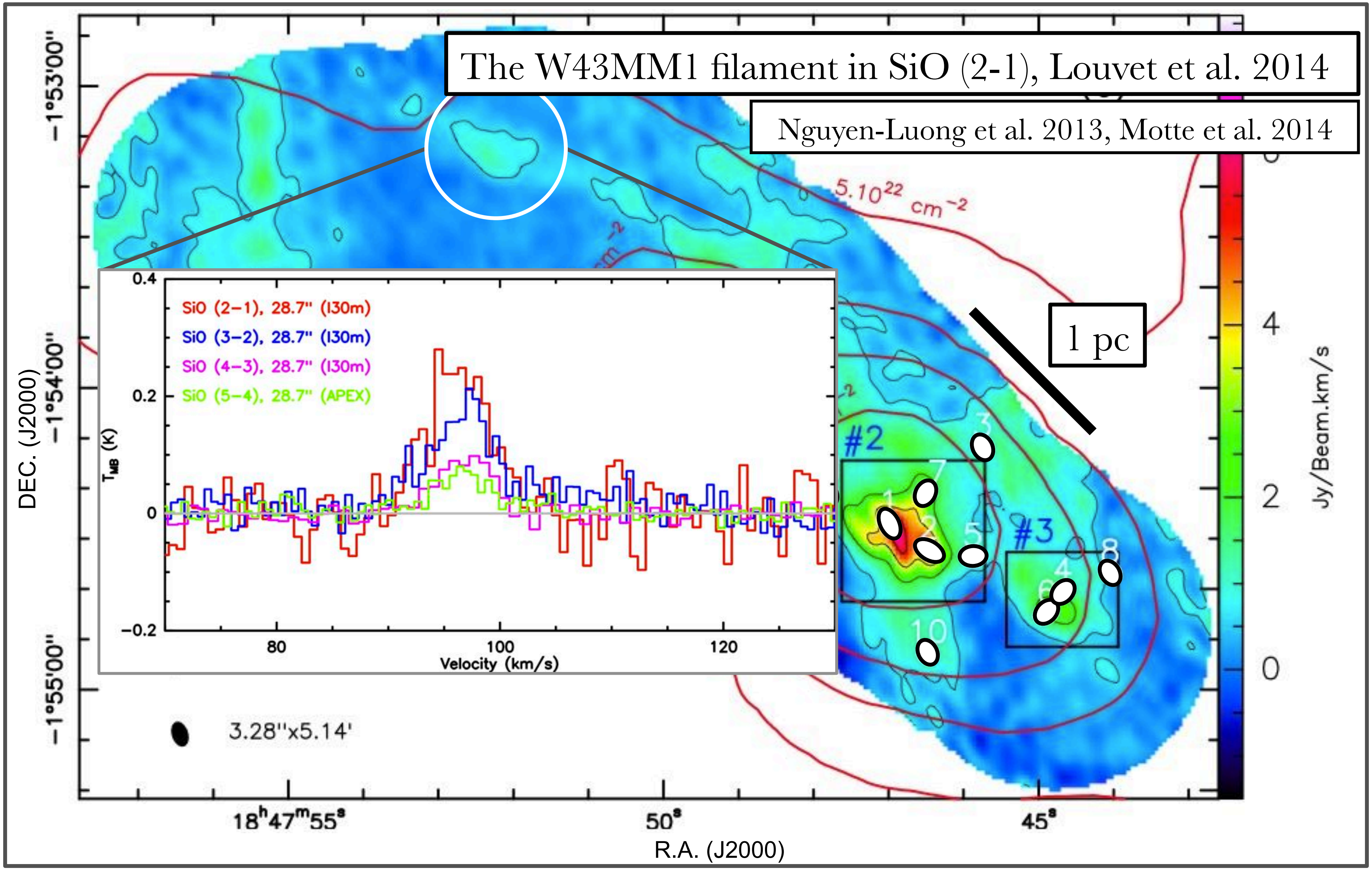

The W43-MM1 ridge

- Models are ready (Louvet et al., in prep.):
  - two scenarios: 10% pre-shock Si in the gas phase (Sig) or in the mantle (Sim)
  - two values of interstellar radiation field tested: $G_0 = 0, 1$

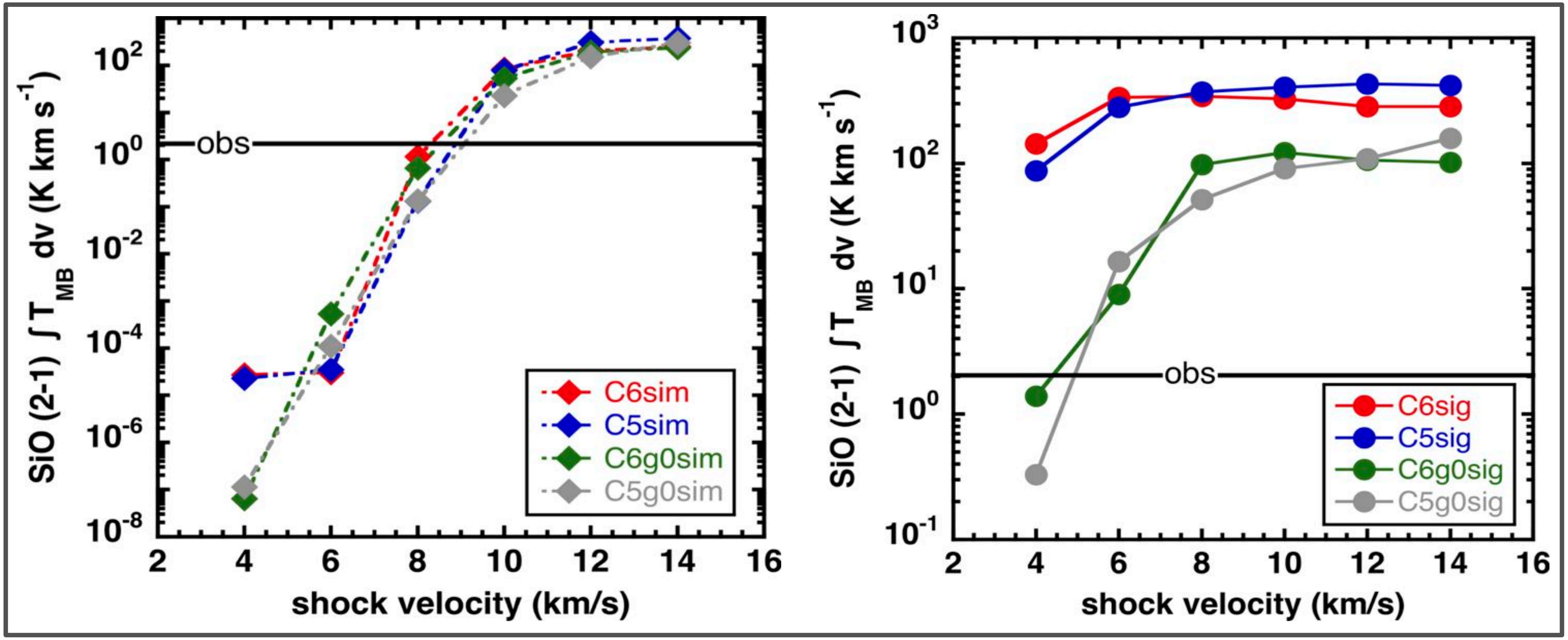

The W43-MM1 ridge

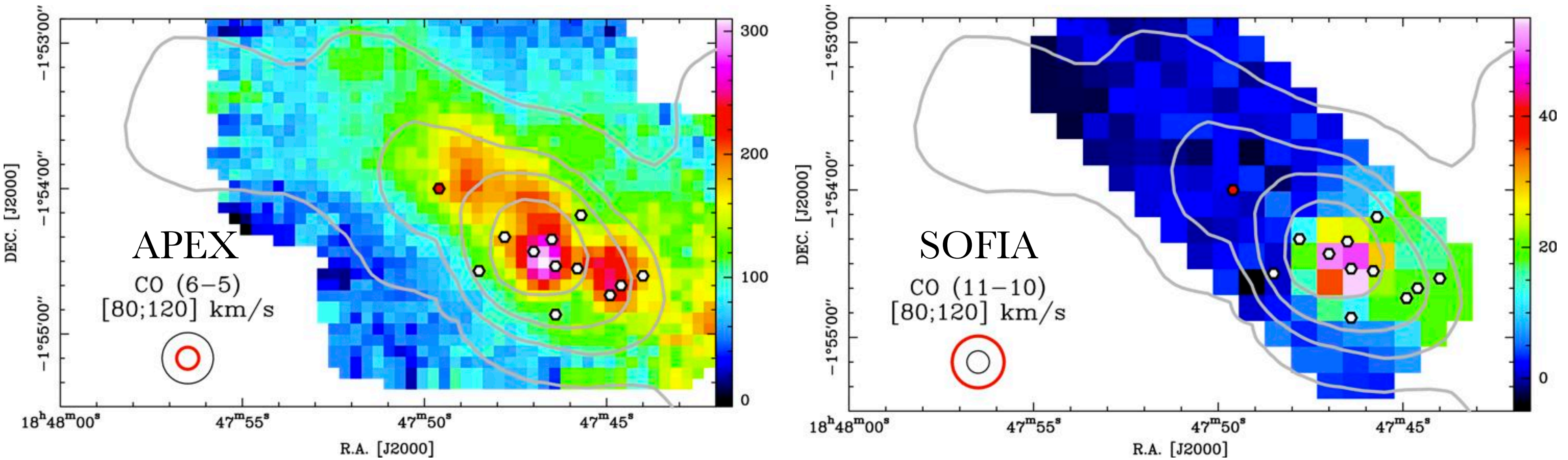

Gusdorf et al., in prep.

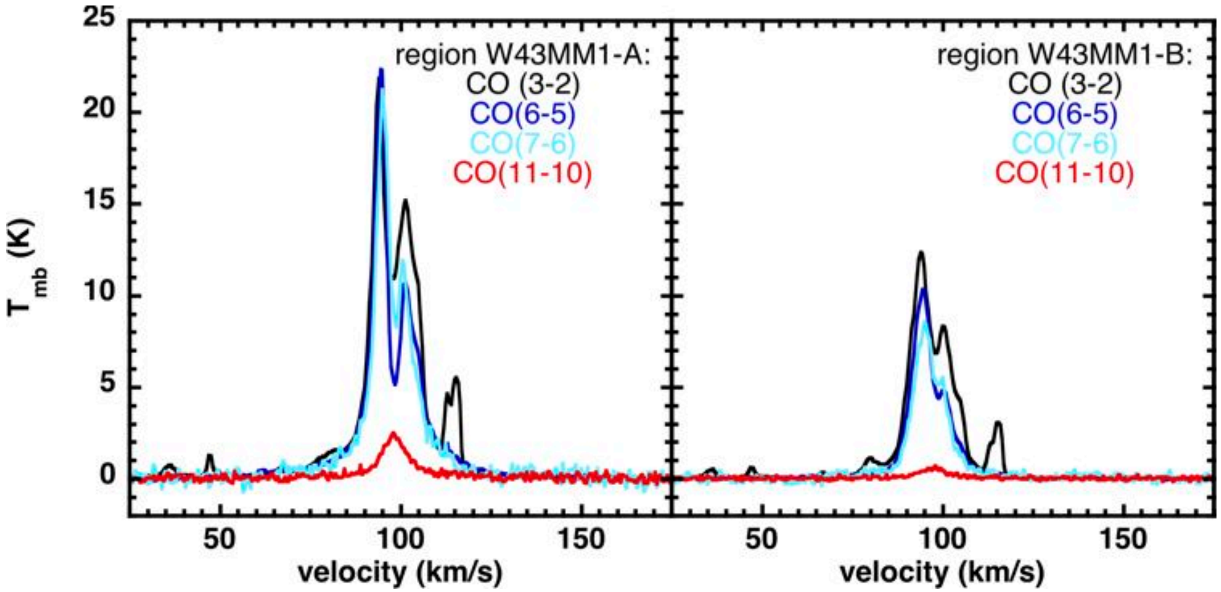

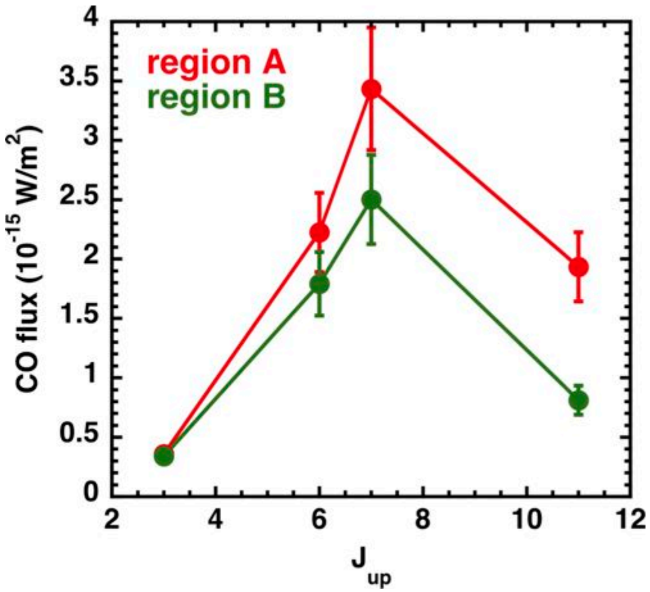

The W43-MM1 ridge

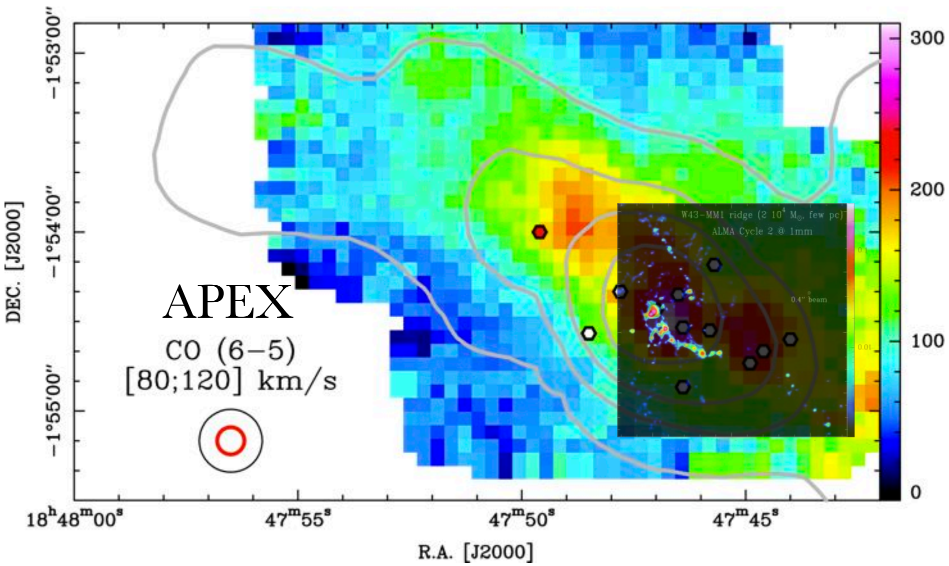

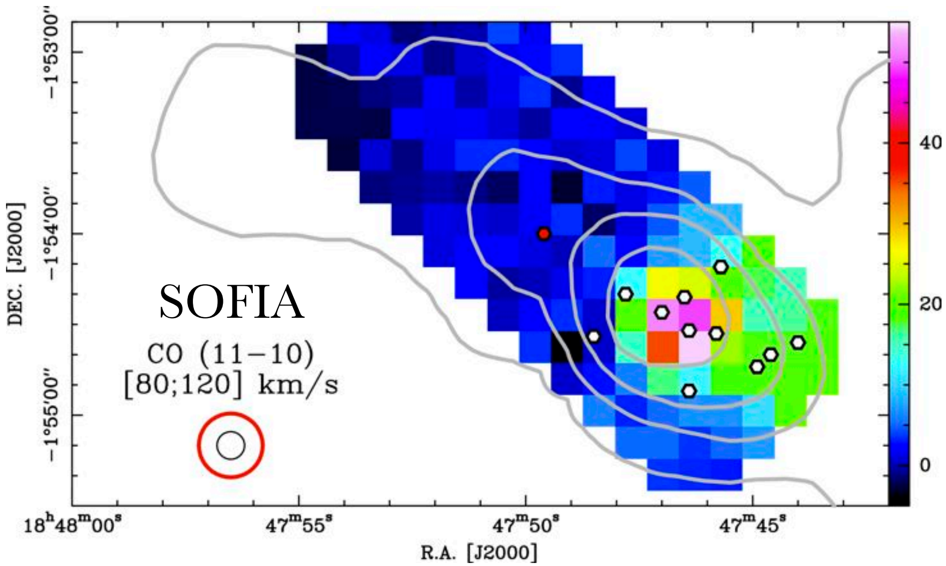

ALMA Cycle 2, 2500 AU, 0.4'', preliminary !! PI : F. Motte

Gusdorf et al., in prep.

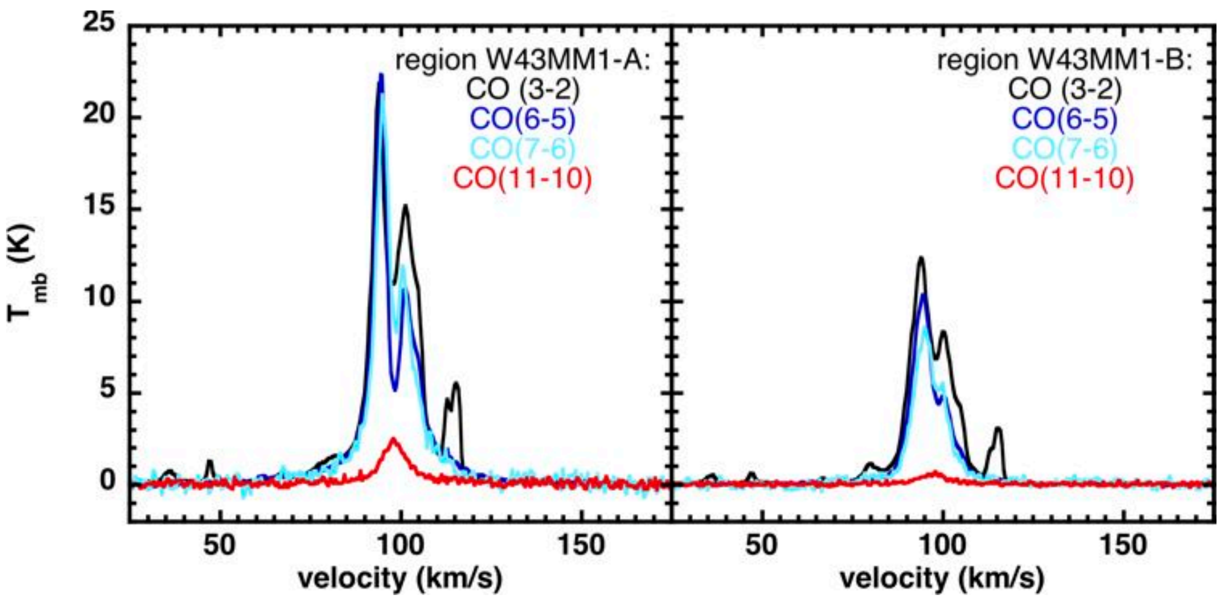

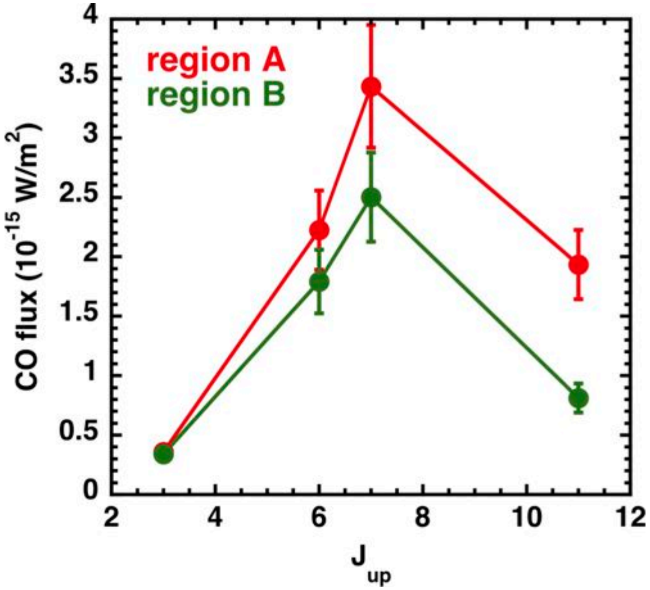

The extra-Galactic perspective

- CO ladders observations from external galaxies

Large scale effects from PDR, XDR, and shock contributions

NGC 253 Hailey-Dunsheath et al. 2008 ; M82 Panuzzo et al. 2010 ; NGC 891 Nikola et al. 2011 ; NGC 6240 Meijerink et al. 2013

- *Herschel*/PACS observations of NGC1068, Hailey-Dunsheath et al. 2012

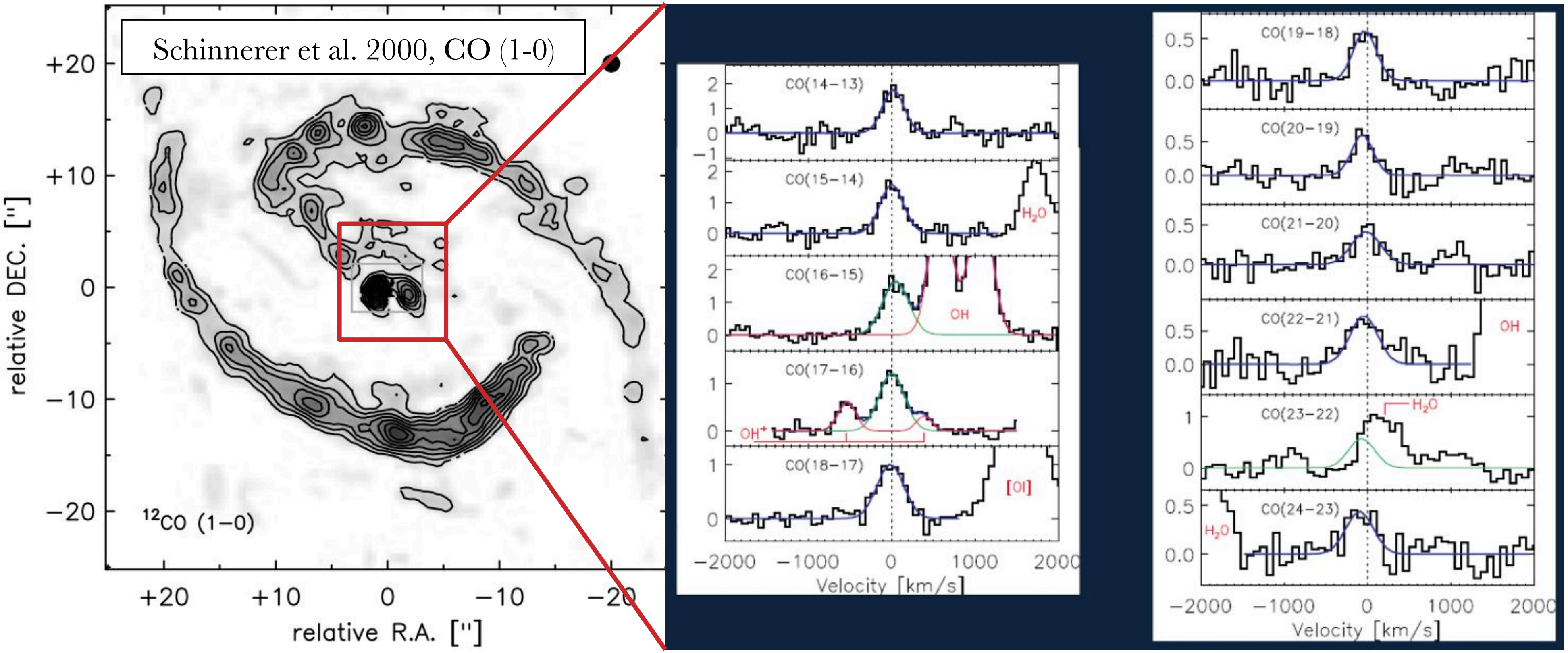

The extra-Galactic perspective

Table 4
Heating Mechanisms

	ME	HE	Full
XDR	$n_{\rm H} = 10^{5.75}$ cm^{-3}	$n_{\rm H} = 10^{5.25}$ cm^{-3}	⋯
	$F_X = 9$ erg cm^{-2} s^{-1}	$F_X = 160$ erg cm^{-2} s^{-1}	⋯
	$A \sim (130\ \rm pc)^2$	$A \sim (21\ \rm pc)^2$	⋯
PDR	⋯	$n_{\rm H} = 10^{6.5}$ cm^{-3}	$n_{\rm H} = 10^{6}$ cm^{-3}
	⋯	$G_0 = 10^{4.75}$	$G_0 = 10^{5}$
	⋯	$L_{\rm FUV} \sim 2 \times 10^{9}\ L_\odot$	$L_{\rm FUV} \sim 10^{10}\ L_\odot$
Shock	C-shock	C-shock	⋯
	$n_0 = 2 \times 10^{5}$ cm^{-3}	$n_0 = 10^{6}$ cm^{-3}	⋯
	$v = 20$ km s^{-1}	$v = 40$ km s^{-1}	⋯
	$A \sim (150\ \rm pc)^2$	$A \sim (16\ \rm pc)^2$	⋯

Notes. Details for the models used in Figure 9. XDR and PDR models are from Meijerink et al. (2007), ME C-shock model is from Flower & Pineau Des Forêts (2010), and HE C-shock model is from Kaufman & Neufeld (1996).

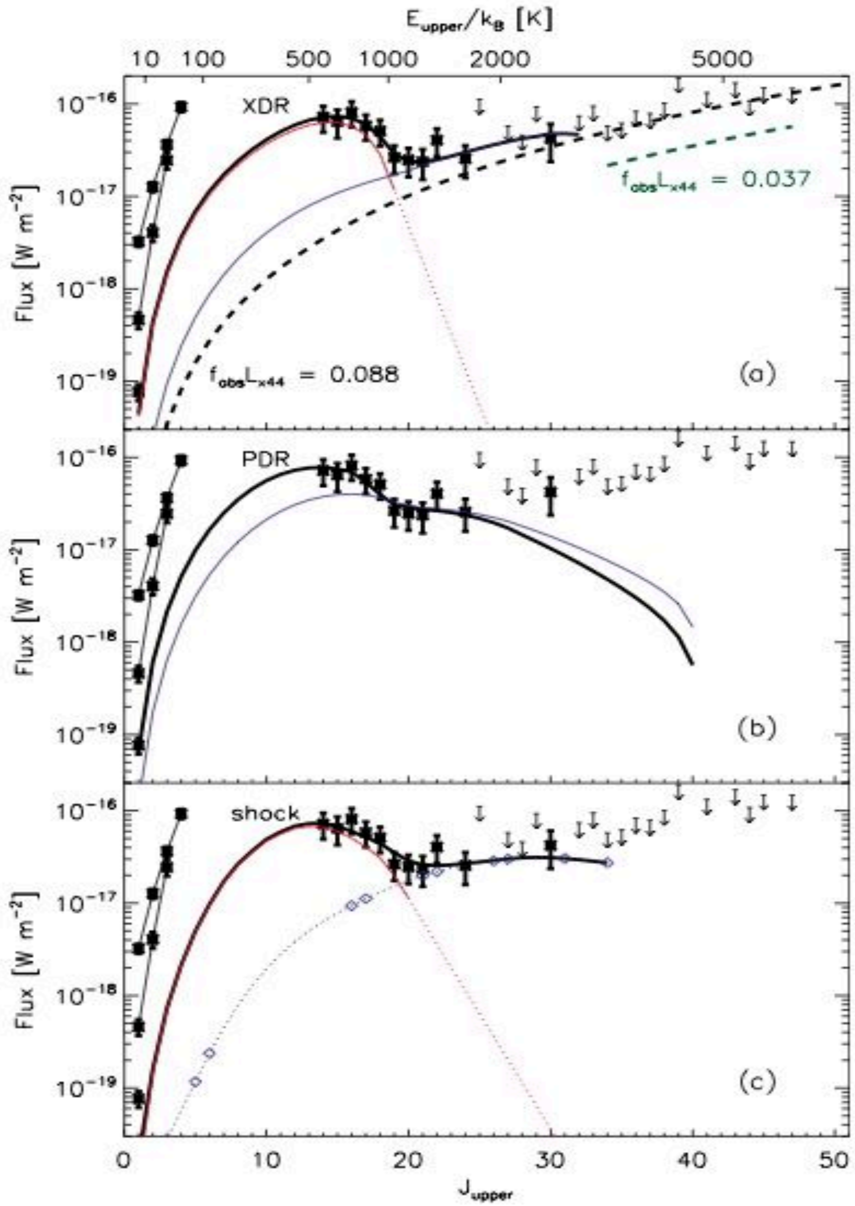

The extra-Galactic perspective

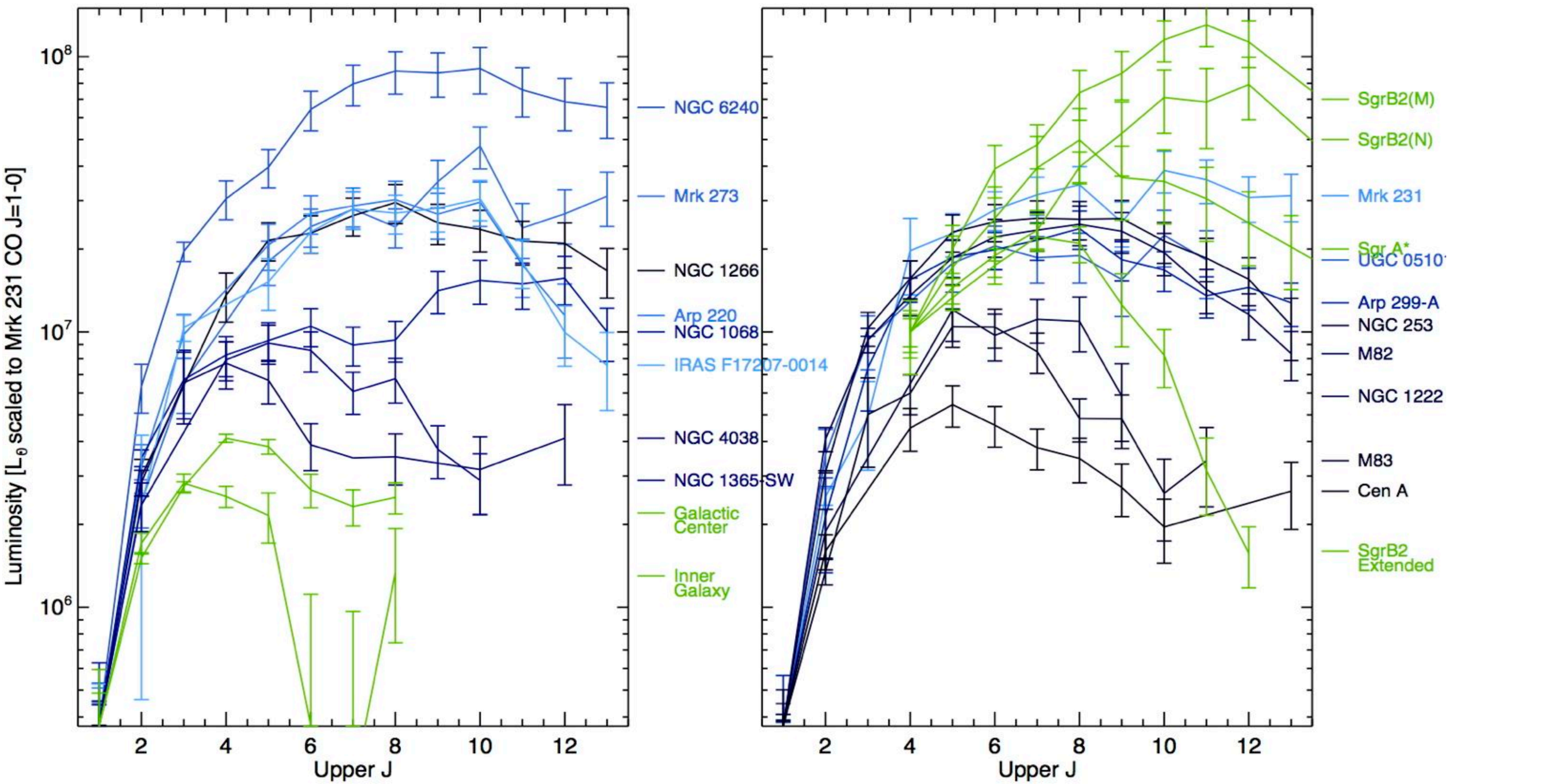

Kamenetzky et al. 2014

Supernova remnants

W28

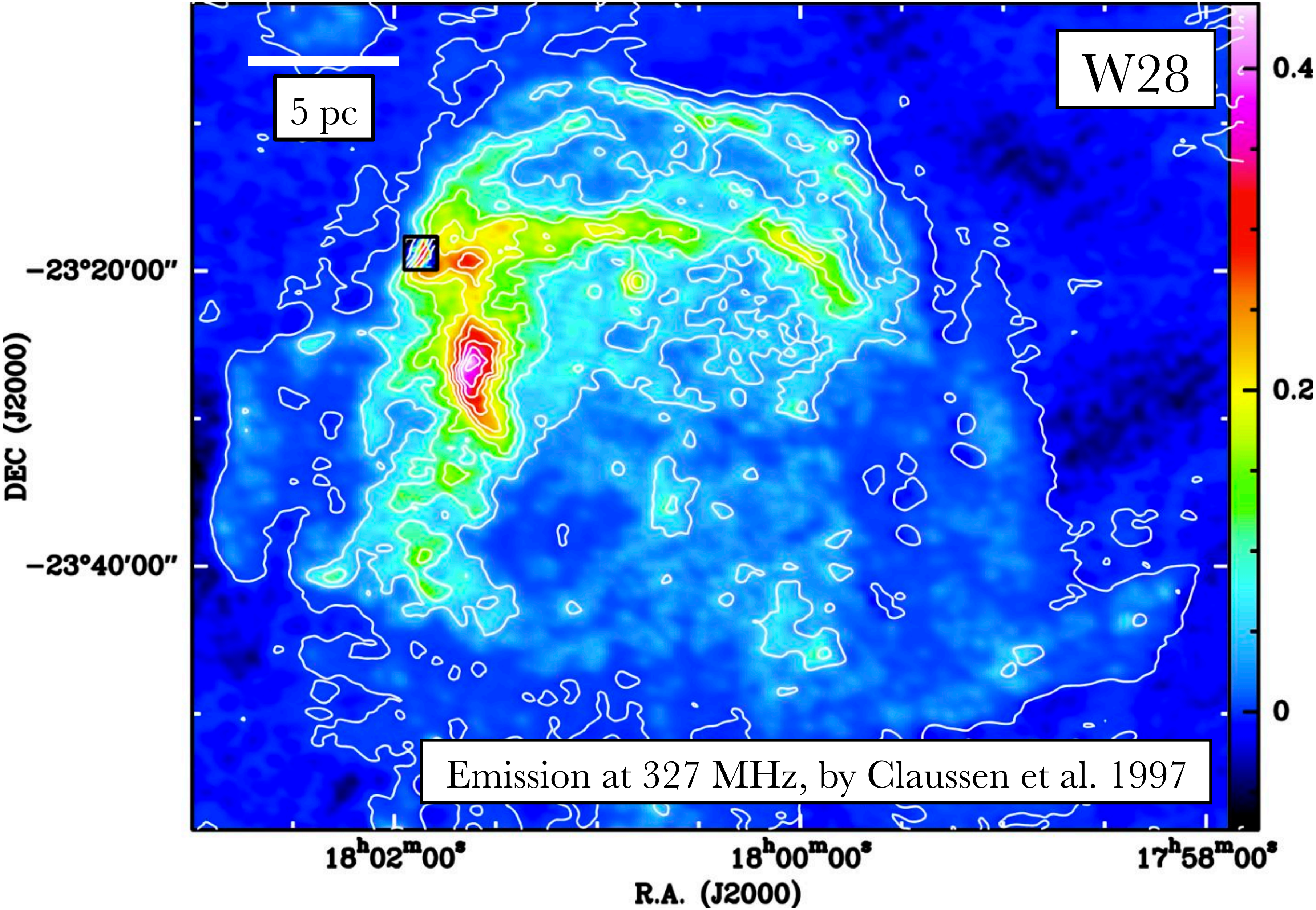

5 pc
W28
0.4
0.2
0
−23°20′00″
−23°40′00″
DEC (J2000)
18h02m00s
18h00m00s
17h58m00s
R.A. (J2000)
Emission at 327 MHz, by Claussen et al. 1997

W28

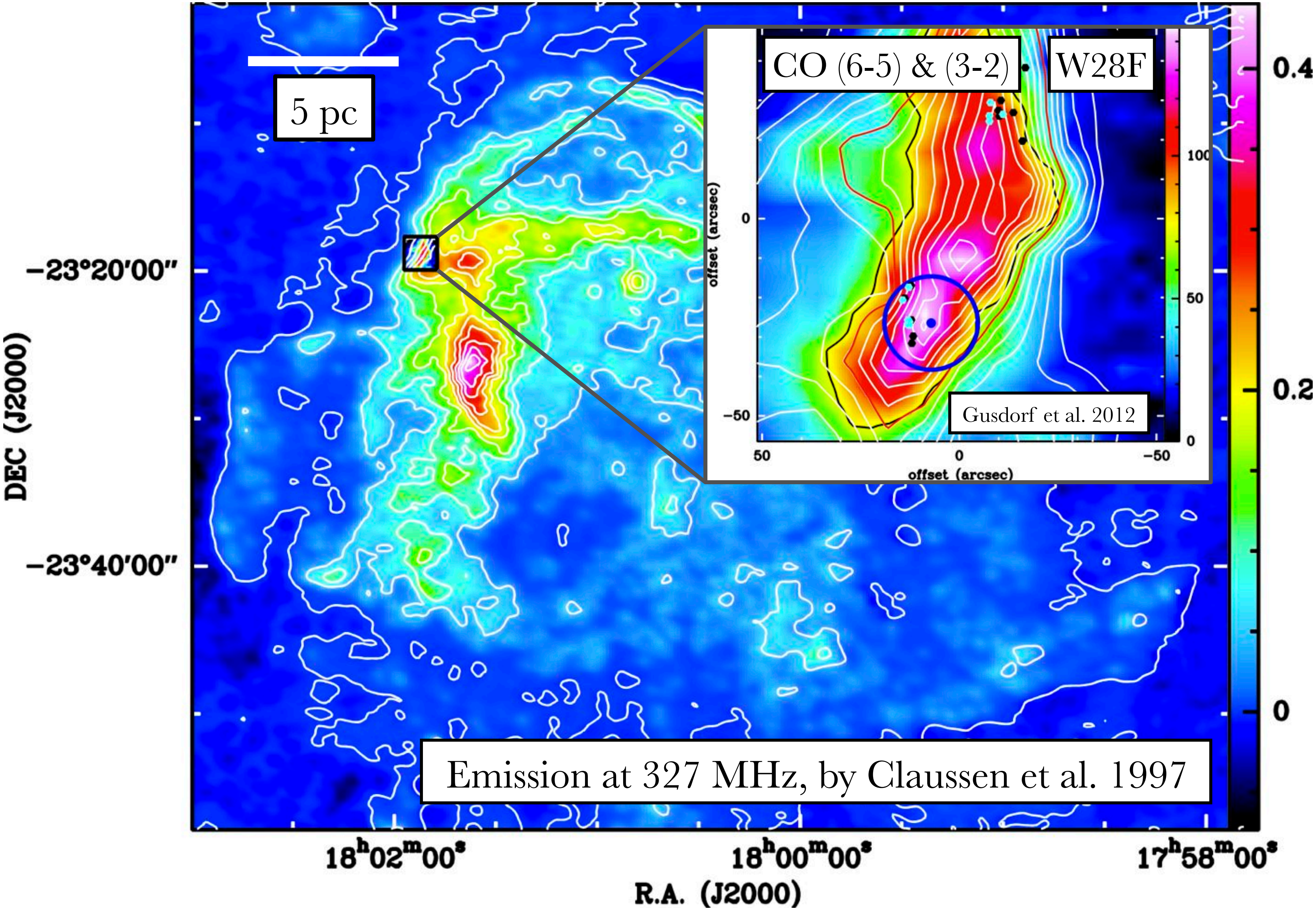
5 pc
CO (6-5) & (3-2)
W28F
Gusdorf et al. 2012
offset (arcsec)
offset (arcsec)
−23°20′00″
−23°40′00″
DEC (J2000)
18h02m00s
18h00m00s
17h58m00s
R.A. (J2000)
0.4
0.2
0
100
50
Emission at 327 MHz, by Claussen et al. 1997

W28

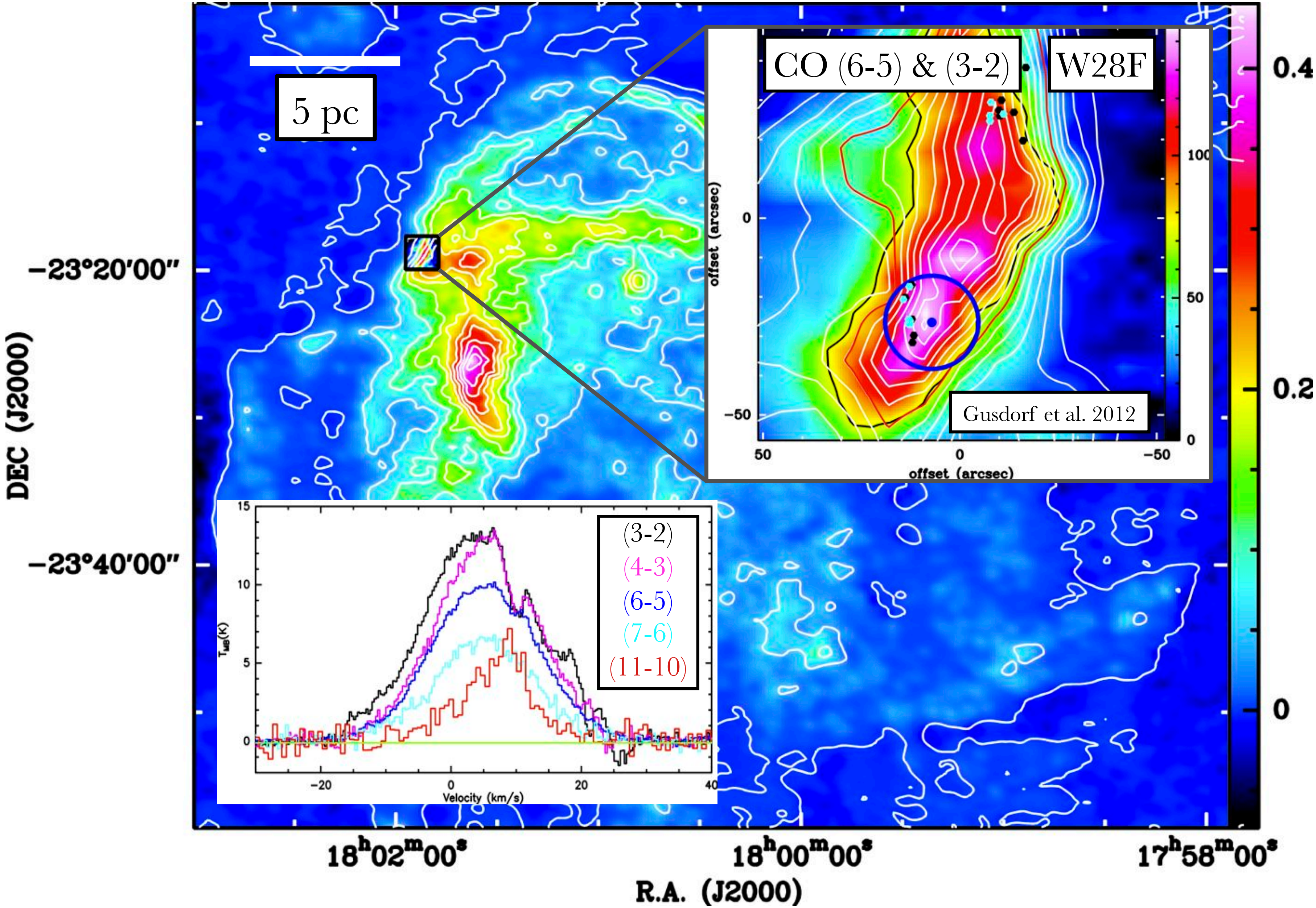
5 pc
CO (6-5) & (3-2)
W28F
Gusdorf et al. 2012
offset (arcsec)
offset (arcsec)
(3-2)
(4-3)
(6-5)
(7-6)
(11-10)
Velocity (km/s)
T_{MB}(K)
−23°20′00″
−23°40′00″
DEC (J2000)
18h02m00s
18h00m00s
17h58m00s
R.A. (J2000)
0.4
0.2
0

W28

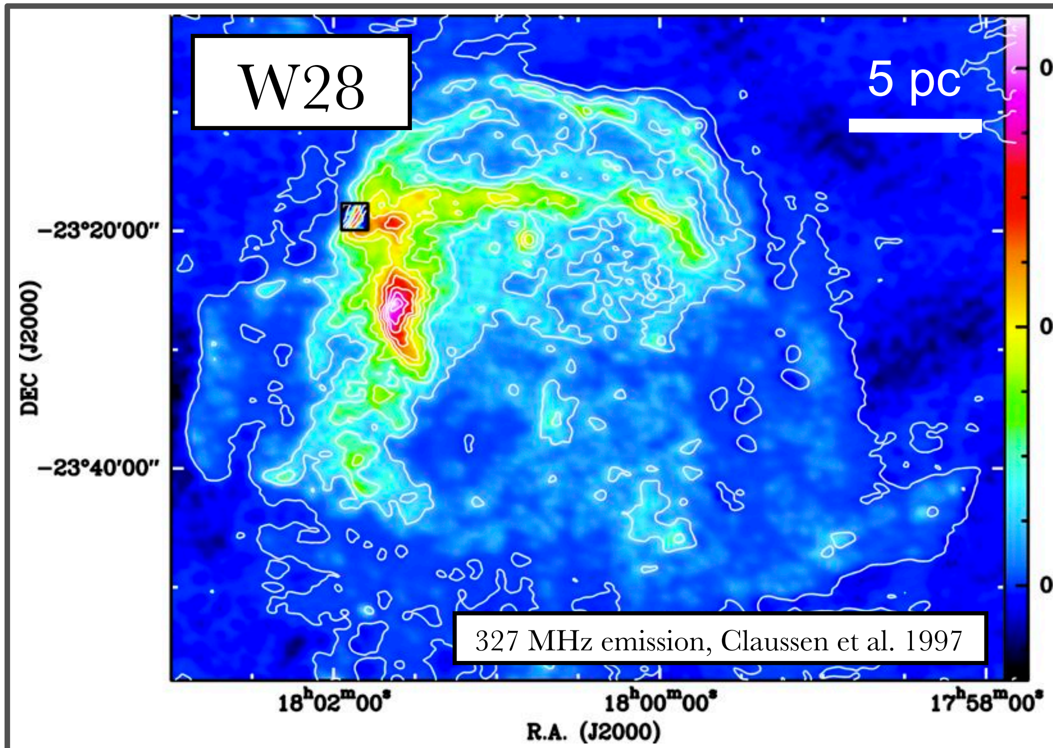

W28
5 pc
327 MHz emission, Claussen et al. 1997
−23°20'00"
−23°40'00"
DEC (J2000)
18h02m00s
18h00m00s
17h58m00s
R.A. (J2000)
0.4
0.2
0

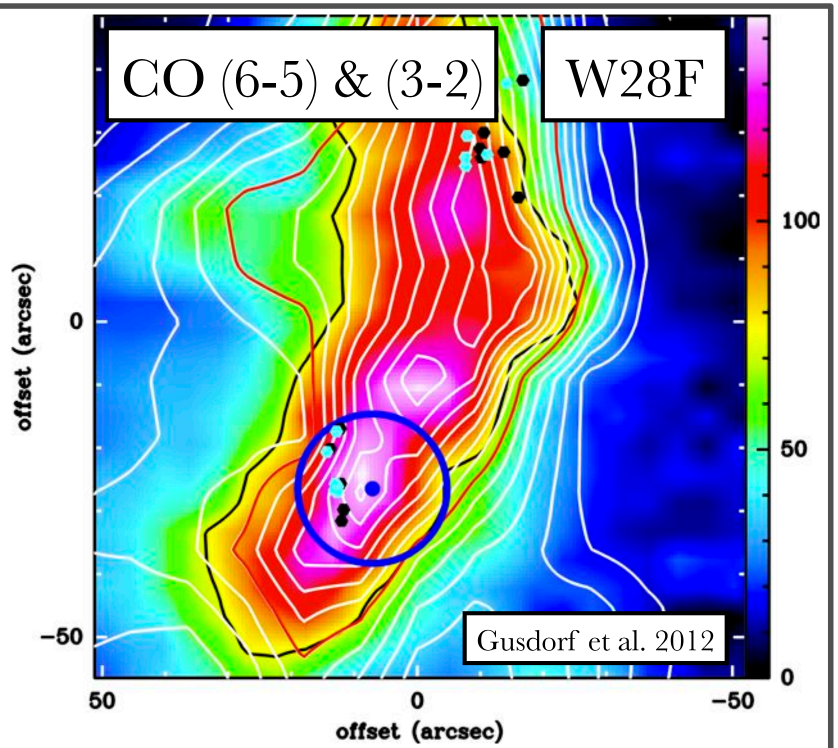

CO (6-5) & (3-2)
W28F
Gusdorf et al. 2012
offset (arcsec)
offset (arcsec)
0
−50
50
0
−50
100
50
0

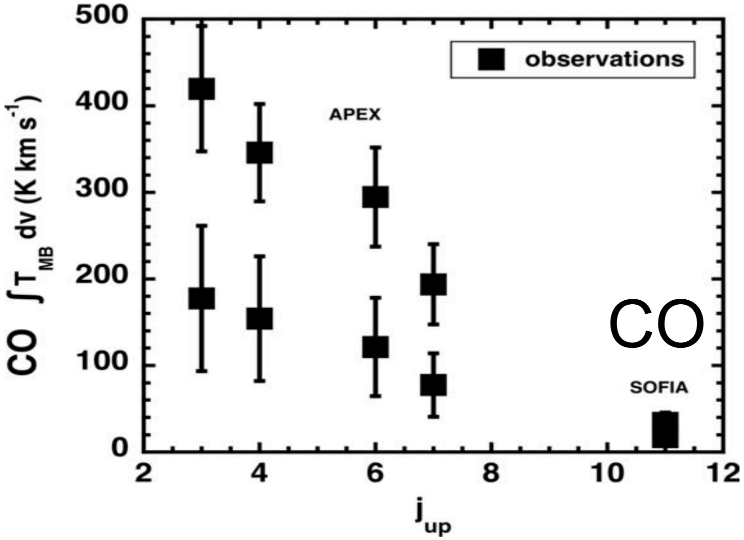

observations
APEX
SOFIA
CO
CO ∫T_MB dv (K km s-1)
j_up
500
400
300
200
100
0
2
4
6
8
10
12

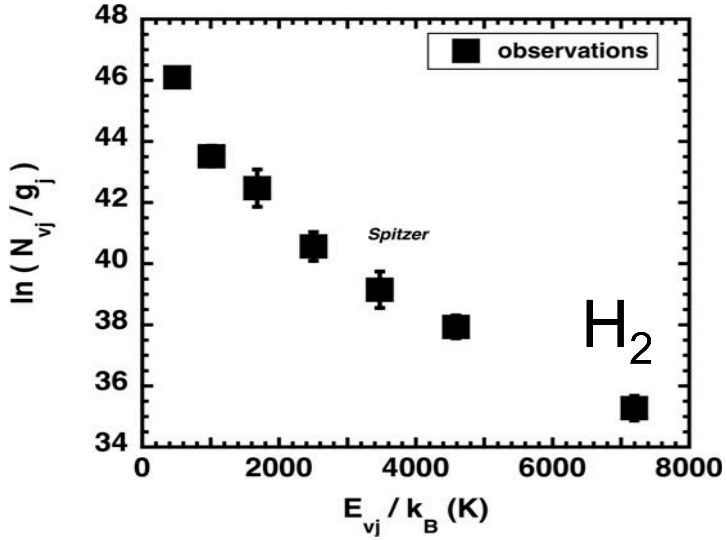

observations
Spitzer
H2
ln (N_vj / g_j)
E_vj / k_B (K)
48
46
44
42
40
38
36
34
0
2000
4000
6000
8000

W28

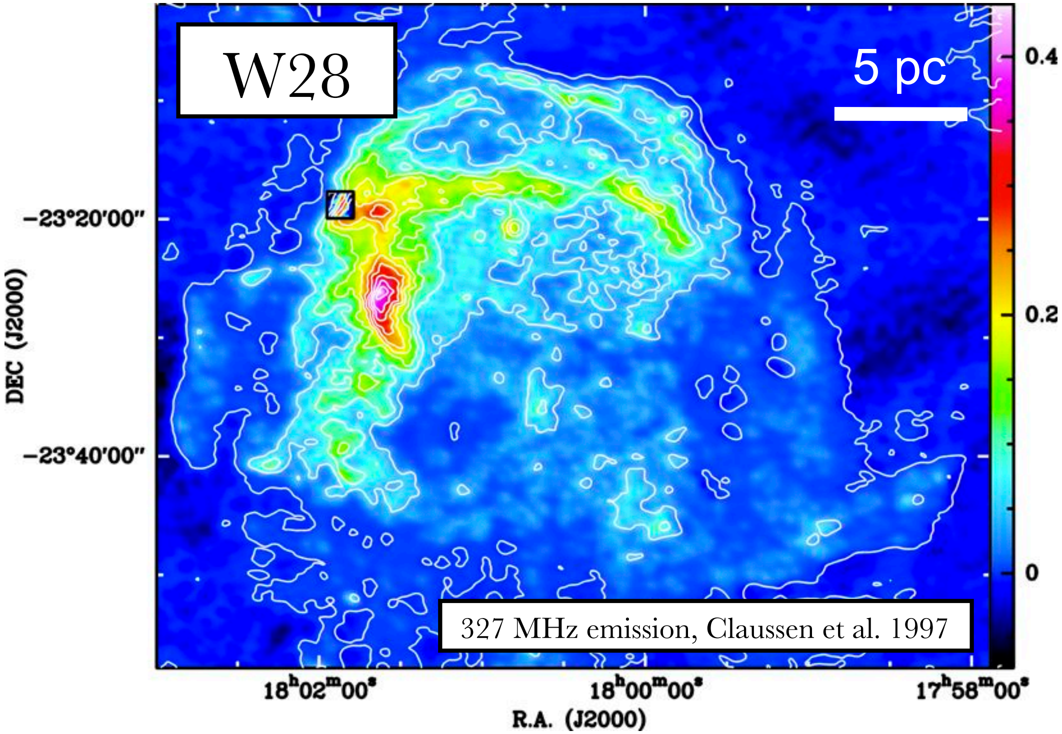
W28
5 pc
327 MHz emission, Claussen et al. 1997
DEC (J2000)
R.A. (J2000)

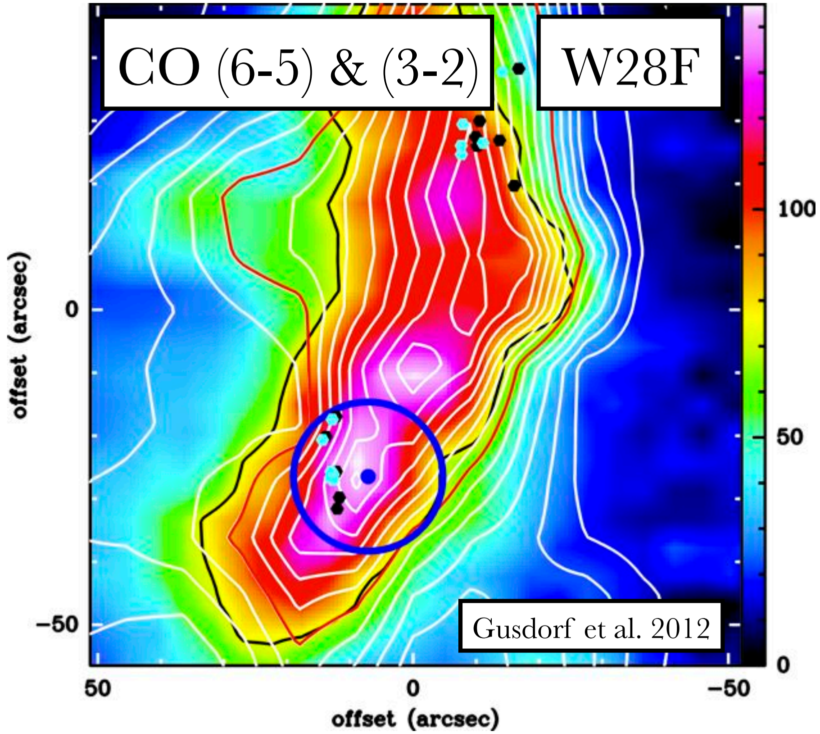
CO (6-5) & (3-2)
W28F
Gusdorf et al. 2012
offset (arcsec)

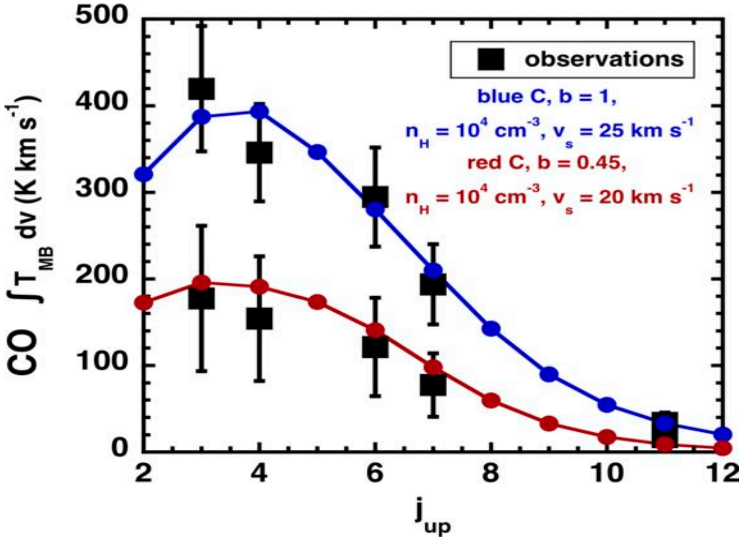
observations
blue C, b = 1,
n_H = 10^4 cm^-3, v_s = 25 km s^-1
red C, b = 0.45,
n_H = 10^4 cm^-3, v_s = 20 km s^-1
CO ∫T_MB dv (K km s^-1)
j_up

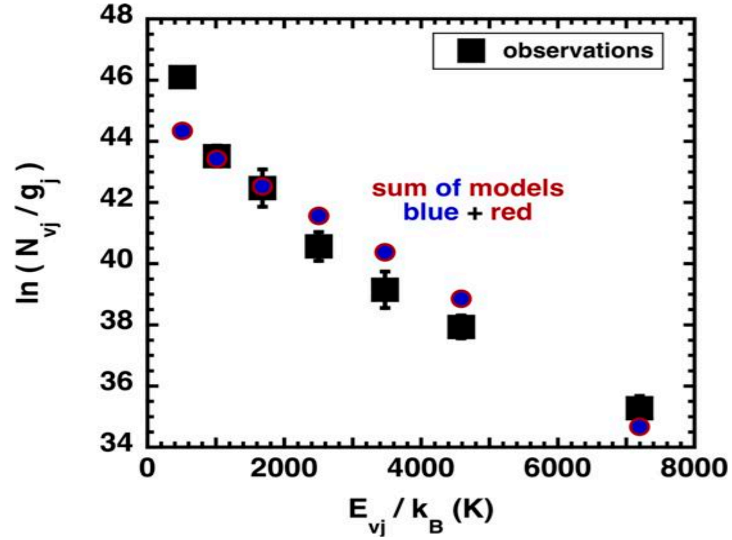
observations
sum of models
blue + red
ln (N_vj / g_j)
E_vj / k_B (K)

W28

- 2 C-shocks, $n_H = 10^4$ cm^{-3}, v_s = 20-25 km/s, B = 45-100 μG constrain:
  - the momentum injected by the shock :
  - 140 – 420 $M_\odot$ km s^{-1} per position
  - the energy injected by the shock:

  6 – 18 10^{45} erg per position

IC 443

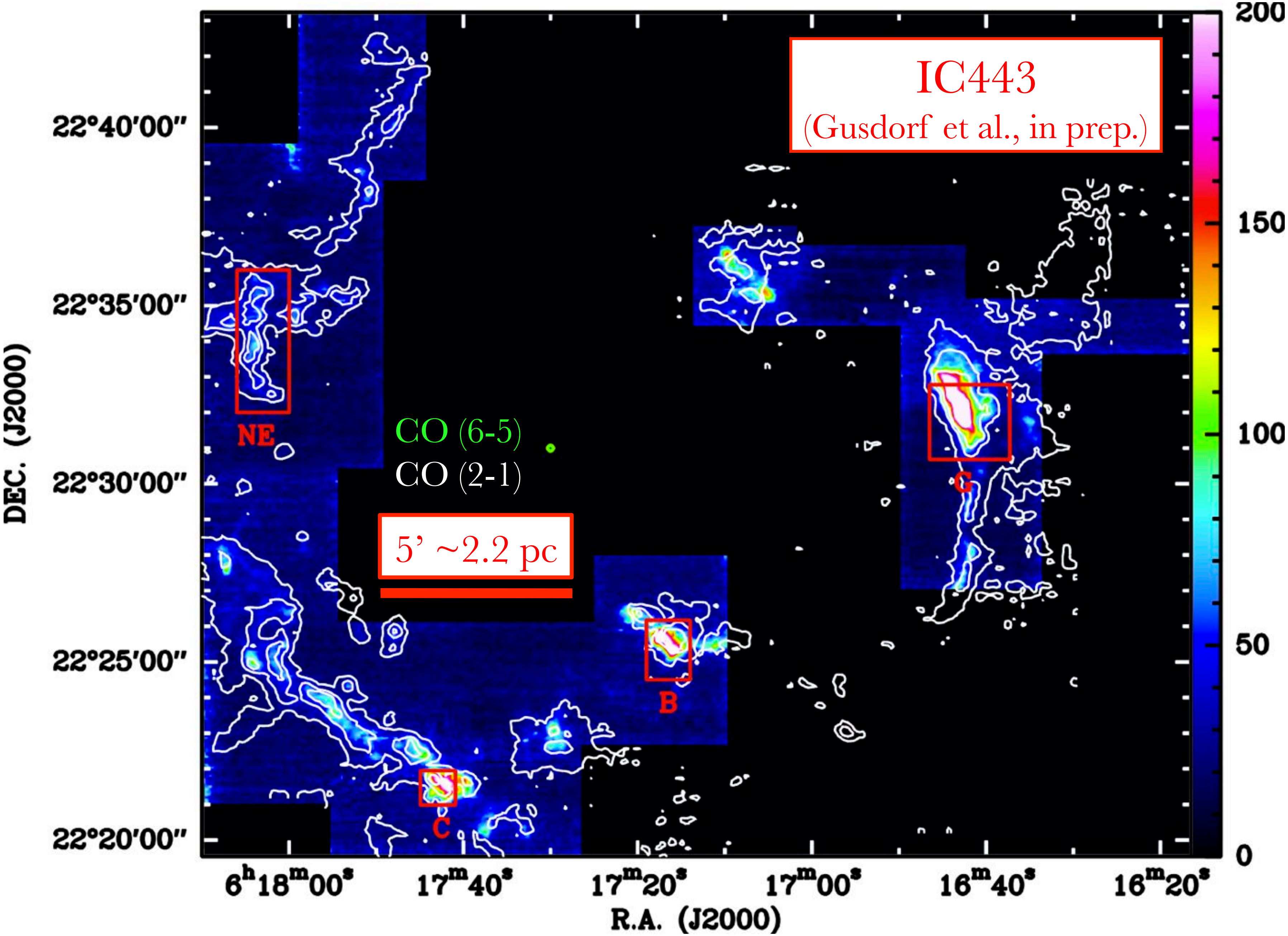
IC443
(Gusdorf et al., in prep.)
CO (6-5)
CO (2-1)
5' ~2.2 pc
NE
G
B
C
22°40'00"
22°35'00"
22°30'00"
22°25'00"
22°20'00"
DEC. (J2000)
6h18m00s
17m40s
17m20s
17m00s
16m40s
16m20s
R.A. (J2000)
200
150
100
50
0

IC 443

- IC443 : CO (6-5) + H_2 0-0 S(5)

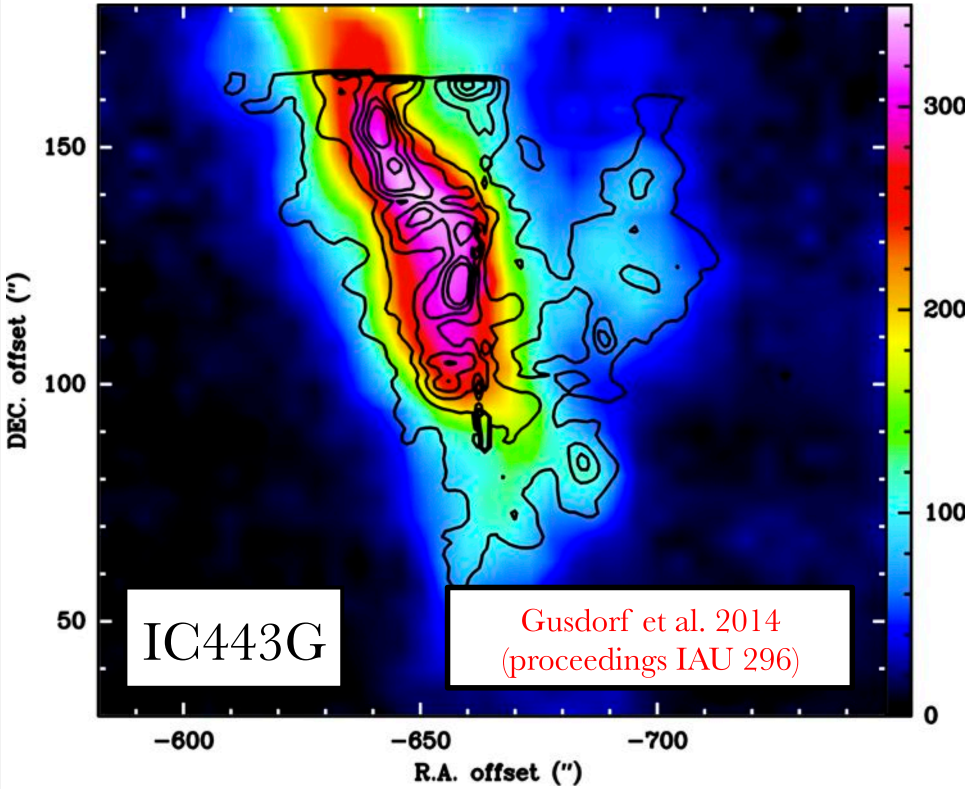

IC 443

- IC443 : CO (6-5) + H_2 0-0 S(5) + YSOs

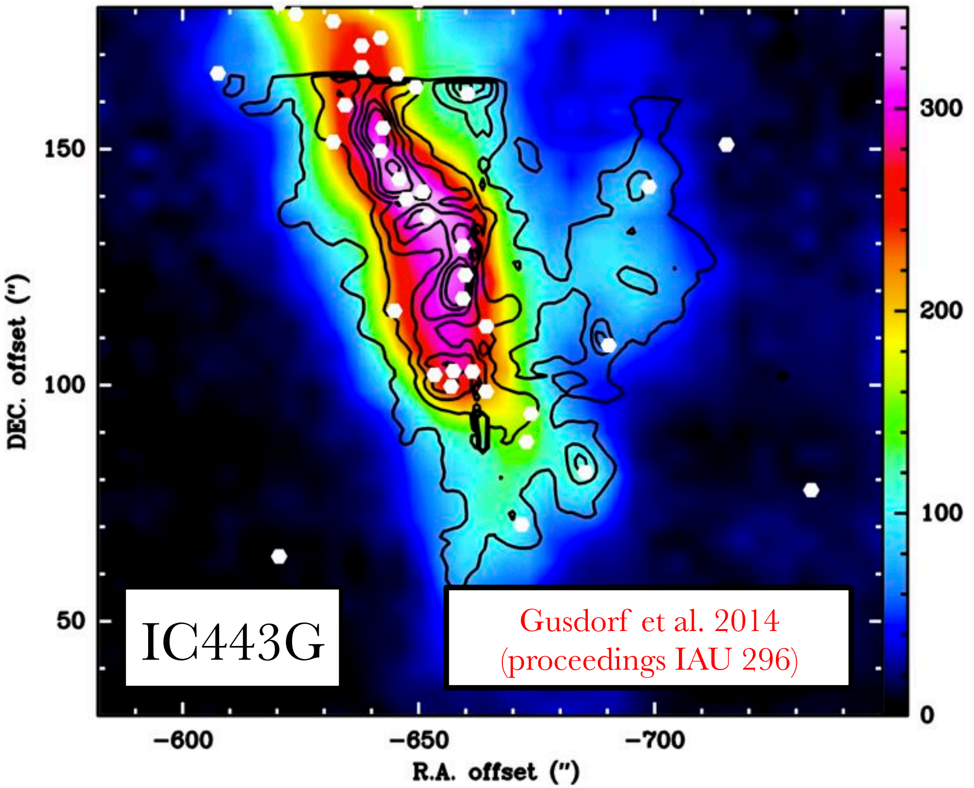

IC 443

- IC443 : CO (6-5) + H_2 0-0 S(5) + YSOs + molecular cloud CO (1-0)

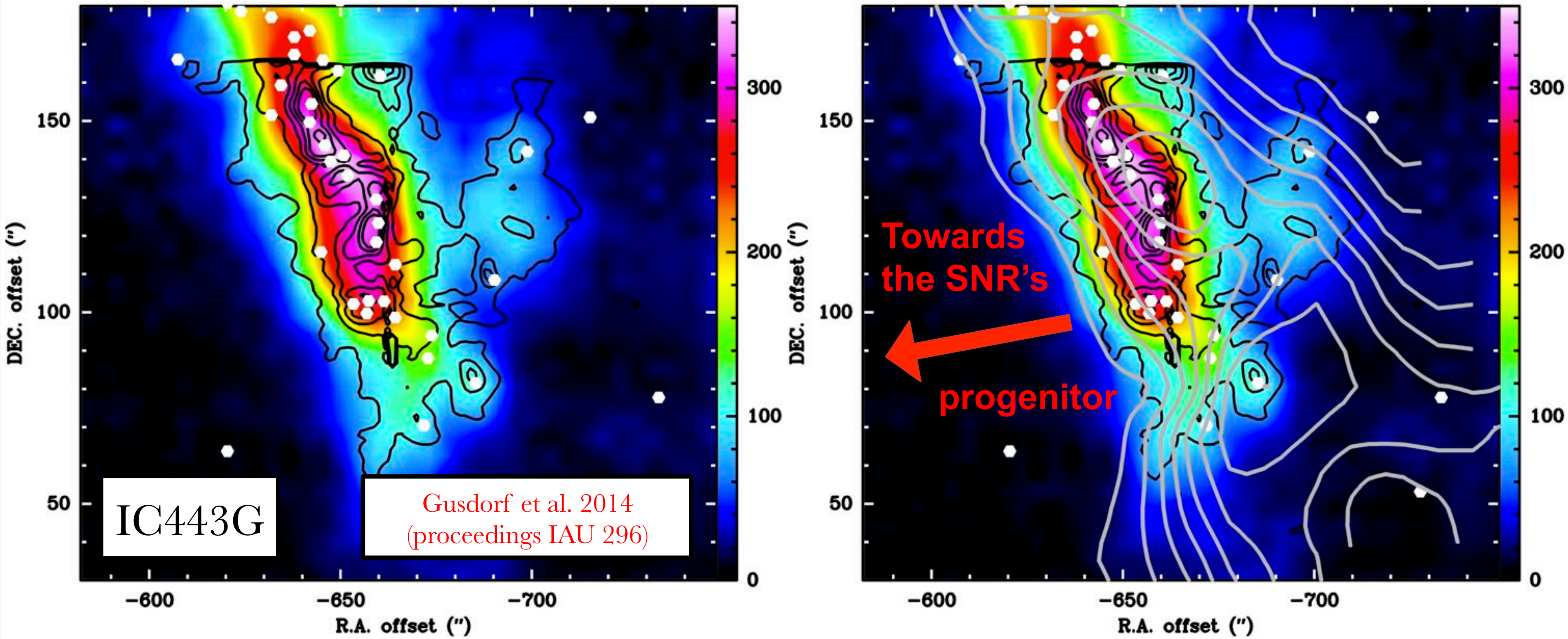

IC 443

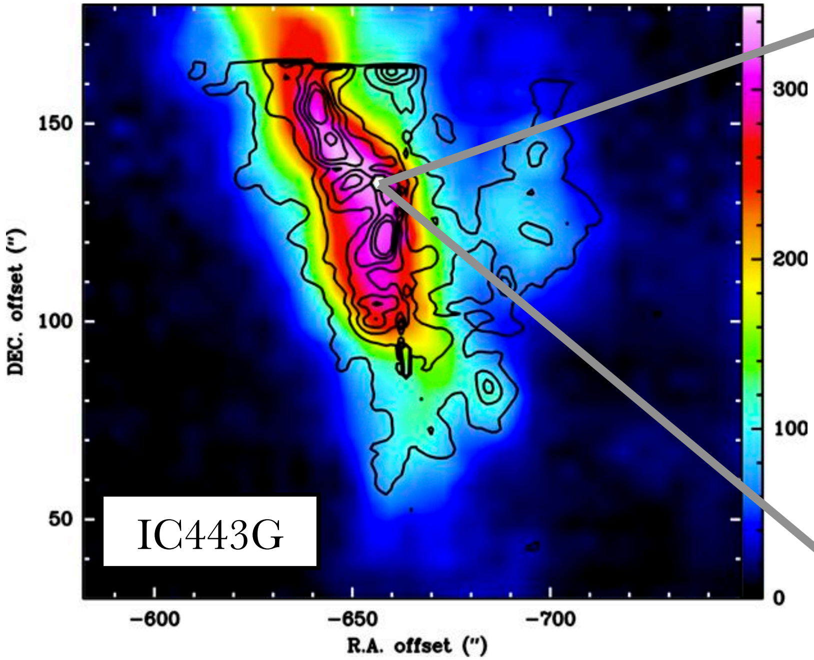

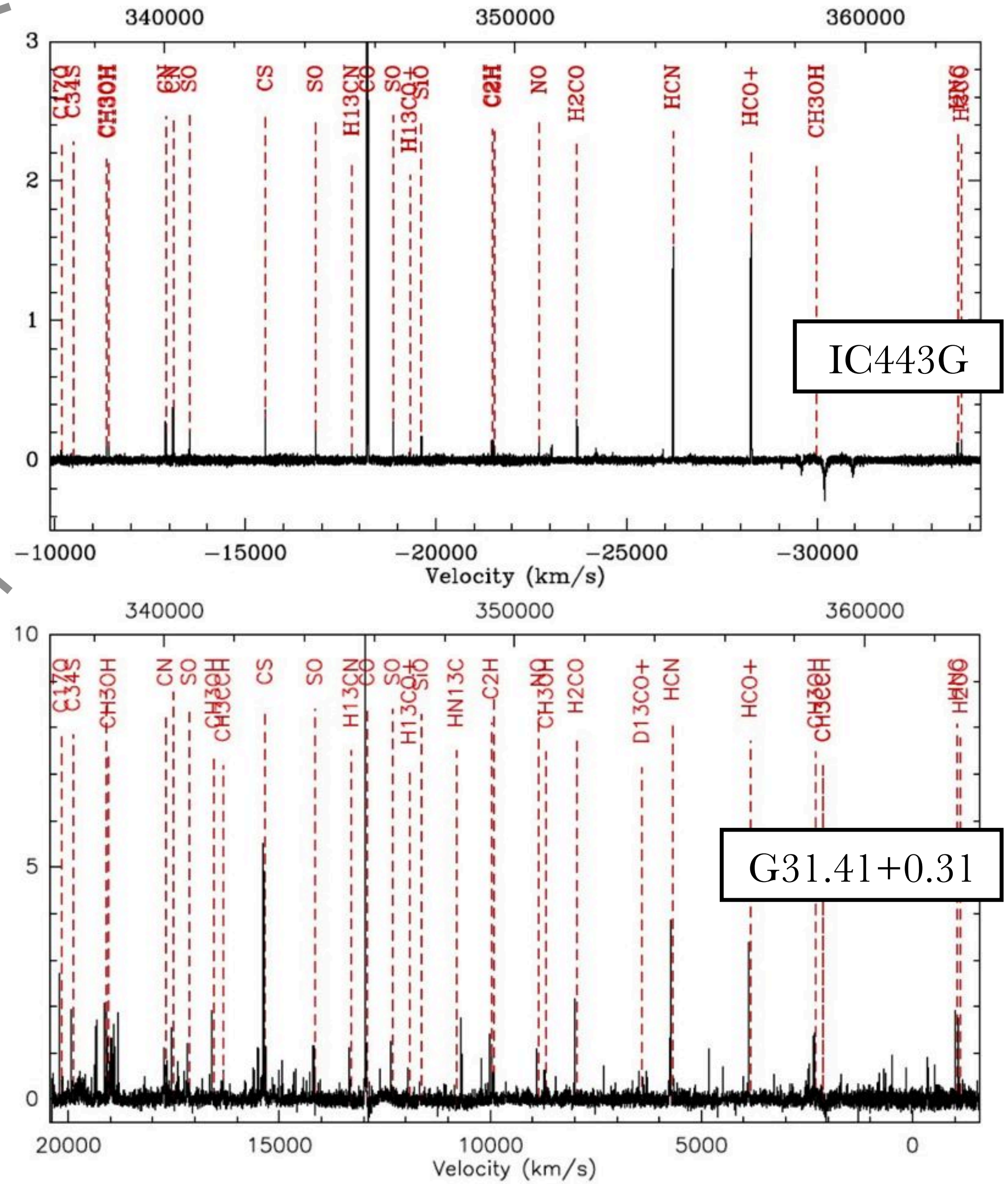

- Riquelme et al., in prep. :
  - Spectral survey IC443G
  - compared to hot core G31.41+0.31
  - X-, γ- rays, and cosmic rays

IC 443

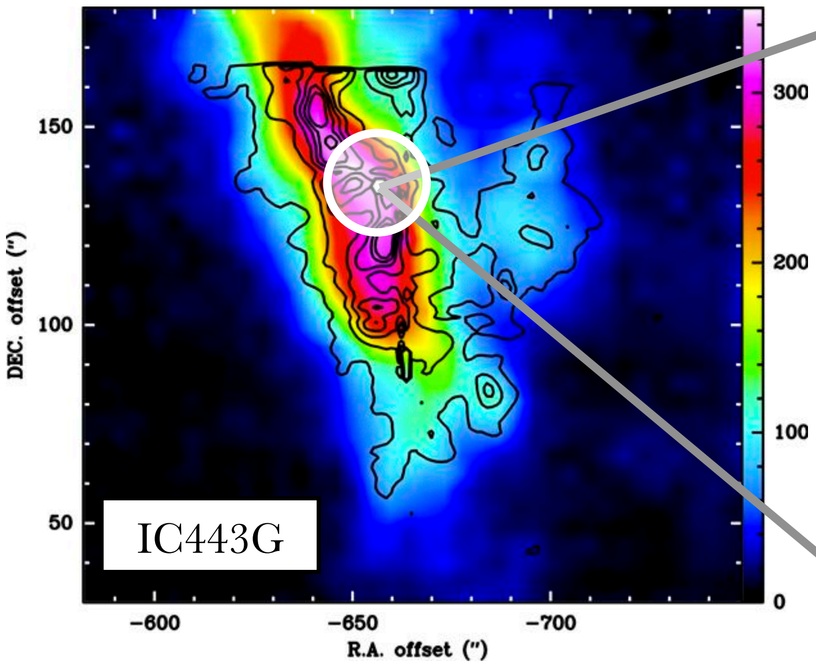

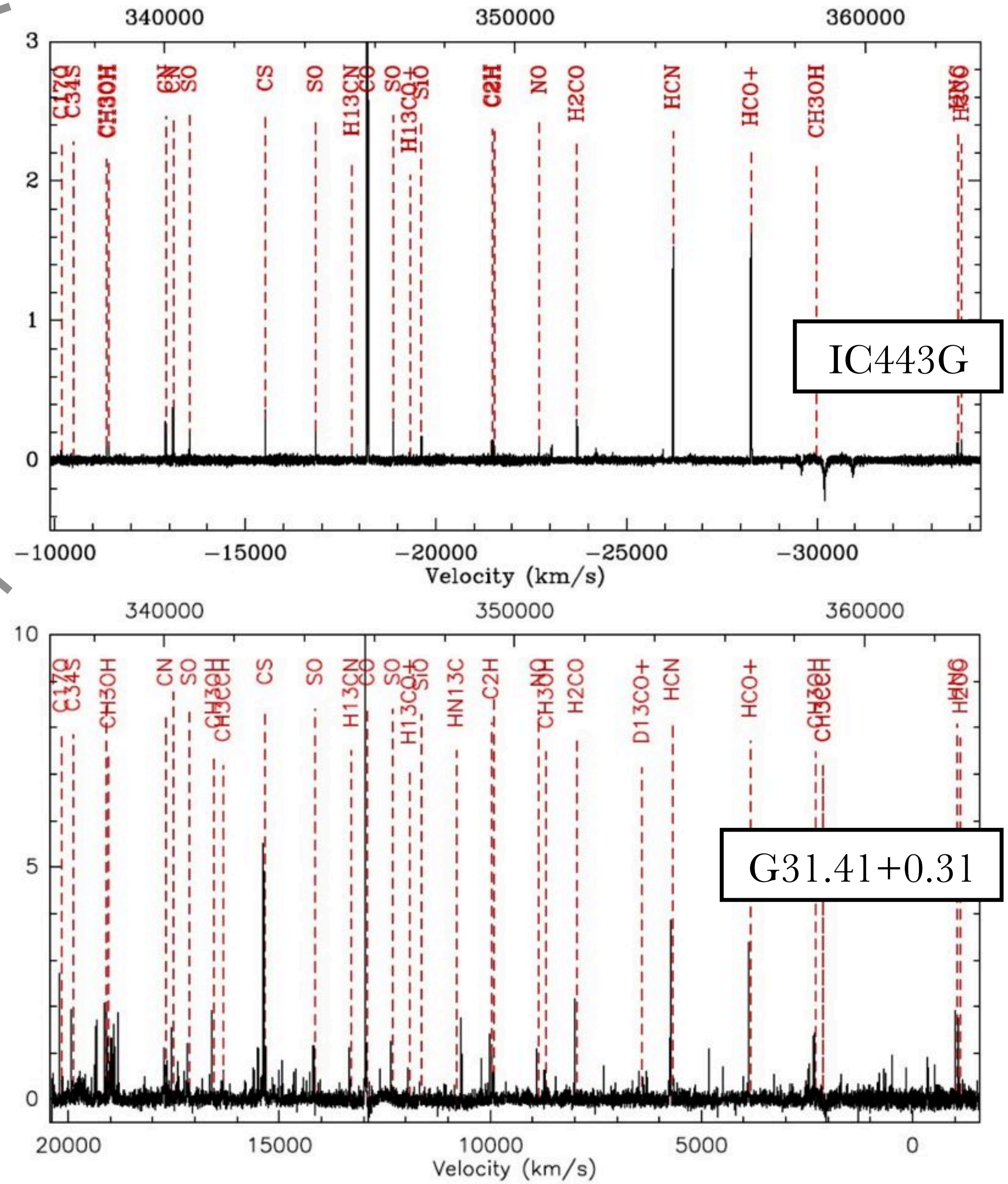

- Riquelme et al., in prep. :
  - Spectral survey IC443G
  - compared to hot core G31.41+0.31
  - X-, γ- rays, and cosmic rays

IC 443

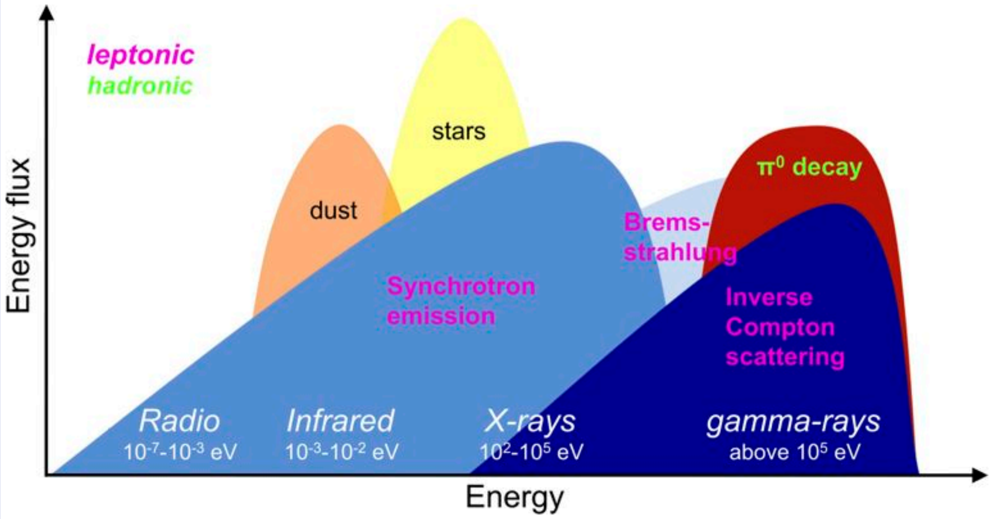

- protons – MIS :
  - π^0 decomposition ➡ γ
- leptons – MIS :
  - Bremsstrahlung ➡ γ
  - Inverse Compton ➡ γ
  - Synchrotron ➡ γ

IC 443

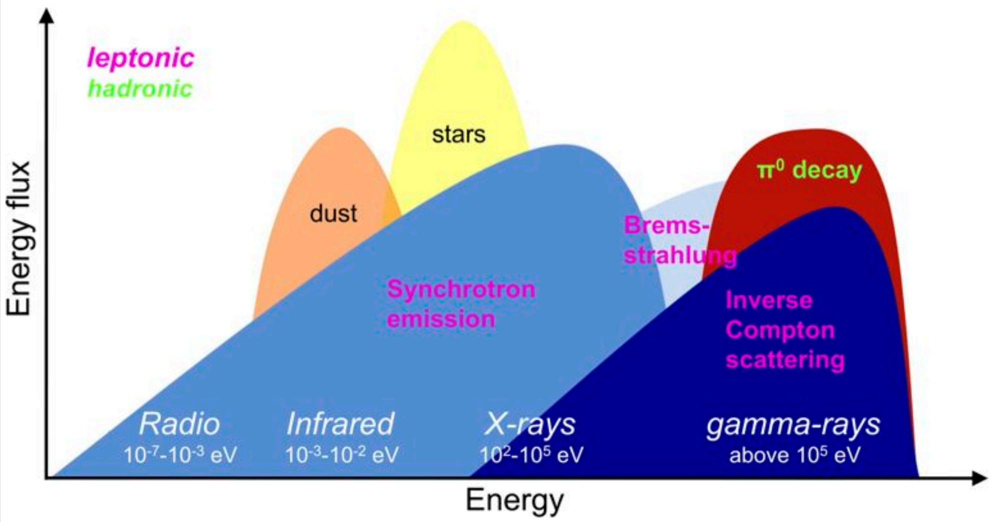

- protons – MIS :
  - π^0 decomposition ➡ γ
- leptons – MIS :
  - Bremsstrahlung ➡ γ
  - Inverse Compton ➡ γ
  - Synchrotron ➡ γ

- Contribution to RCs studies

through ISM studies:

W28F, 3C391

(Gusdorf et al. 2012, Neufeld et al. 2014)

W44E&F (Anderl, Gusdorf & Güsten 2014)

G349.7+0.2 (Rho et al., in press)

Meyer et al, 2015

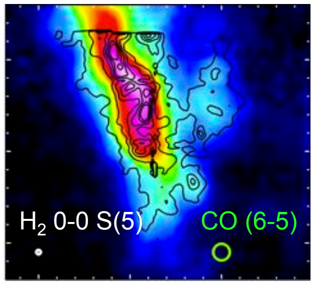

IC 443

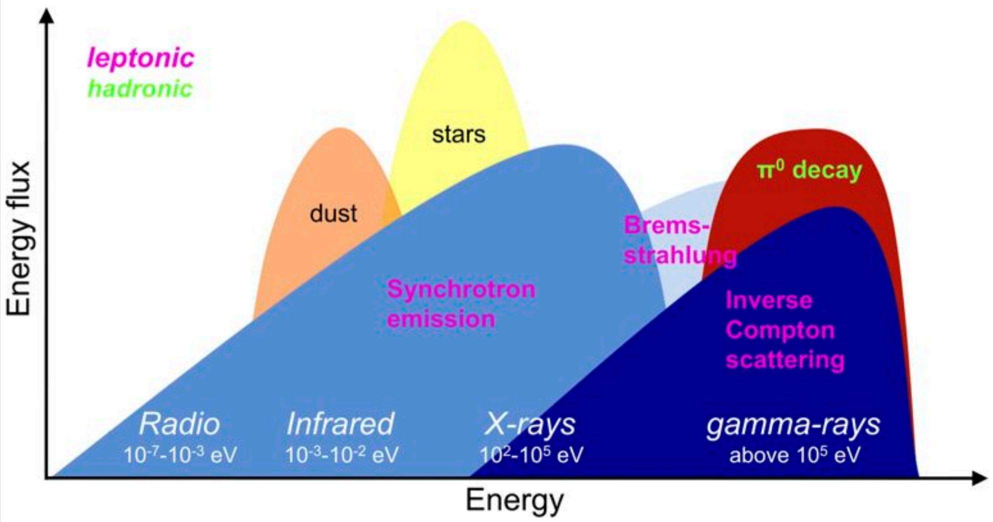

- protons – MIS :
  - π^0 decomposition ➡ γ
- leptons – MIS :
  - Bremsstrahlung ➡ γ
  - Inverse Compton ➡ γ
  - Synchrotron ➡ γ

- Contribution to RCs studies

through ISM studies:

W28F, 3C391

(Gusdorf et al. 2012, Neufeld et al. 2014)

W44E&F (Anderl, Gusdorf & Güsten 2014)

G349.7+0.2 (Rho et al., in press)

Meyer et al, 2015

HESS

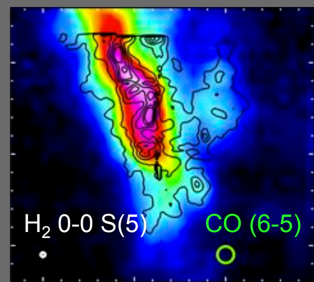

IC 443

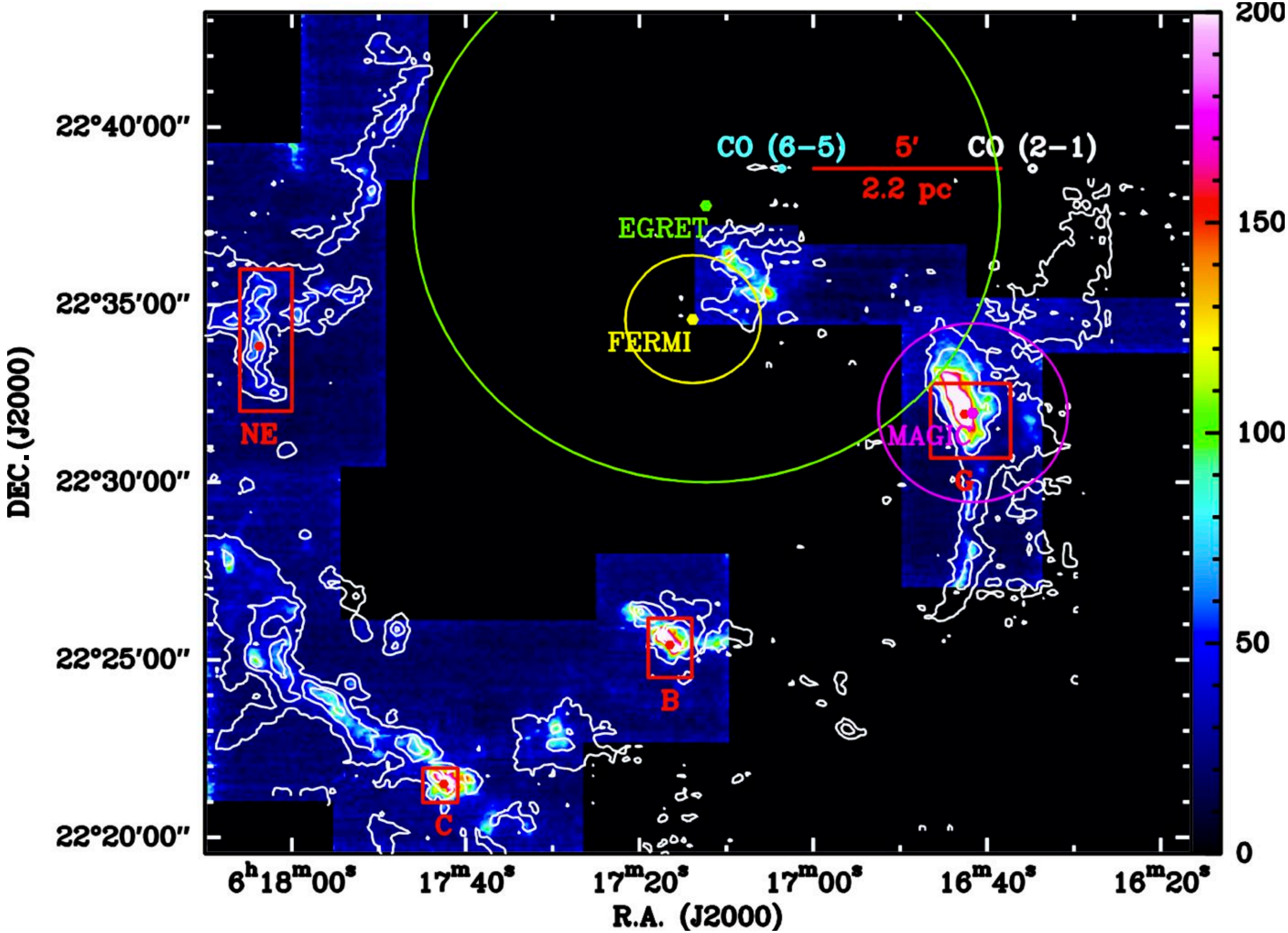

CO (6–5)
5′
2.2 pc
CO (2–1)
EGRET
FERMI
MAGIC
NE
G
B
C
22°40′00″
22°35′00″
22°30′00″
22°25′00″
22°20′00″
DEC. (J2000)
6h18m00s
17m40s
17m20s
17m00s
16m40s
16m20s
R.A. (J2000)
200
150
100
50
0

IC 443

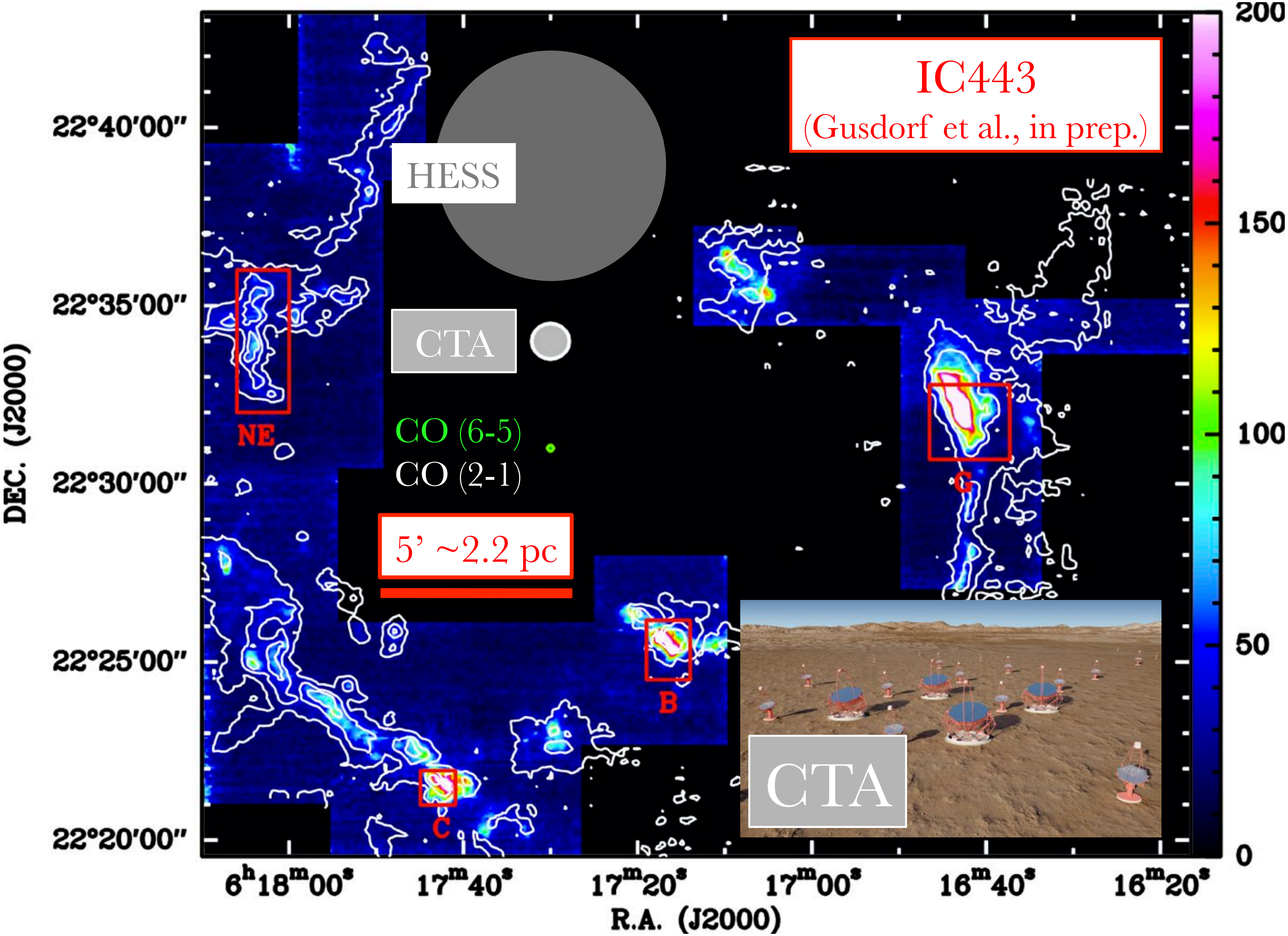

IC443
(Gusdorf et al., in prep.)
HESS
CTA
CO (6-5)
CO (2-1)
5' ~2.2 pc
NE
G
B
C
CTA
22°40'00"
22°35'00"
22°30'00"
22°25'00"
22°20'00"
DEC. (J2000)
6h18m00s
17m40s
17m20s
17m00s
16m40s
16m20s
R.A. (J2000)
200
150
100
50
0

IC 443

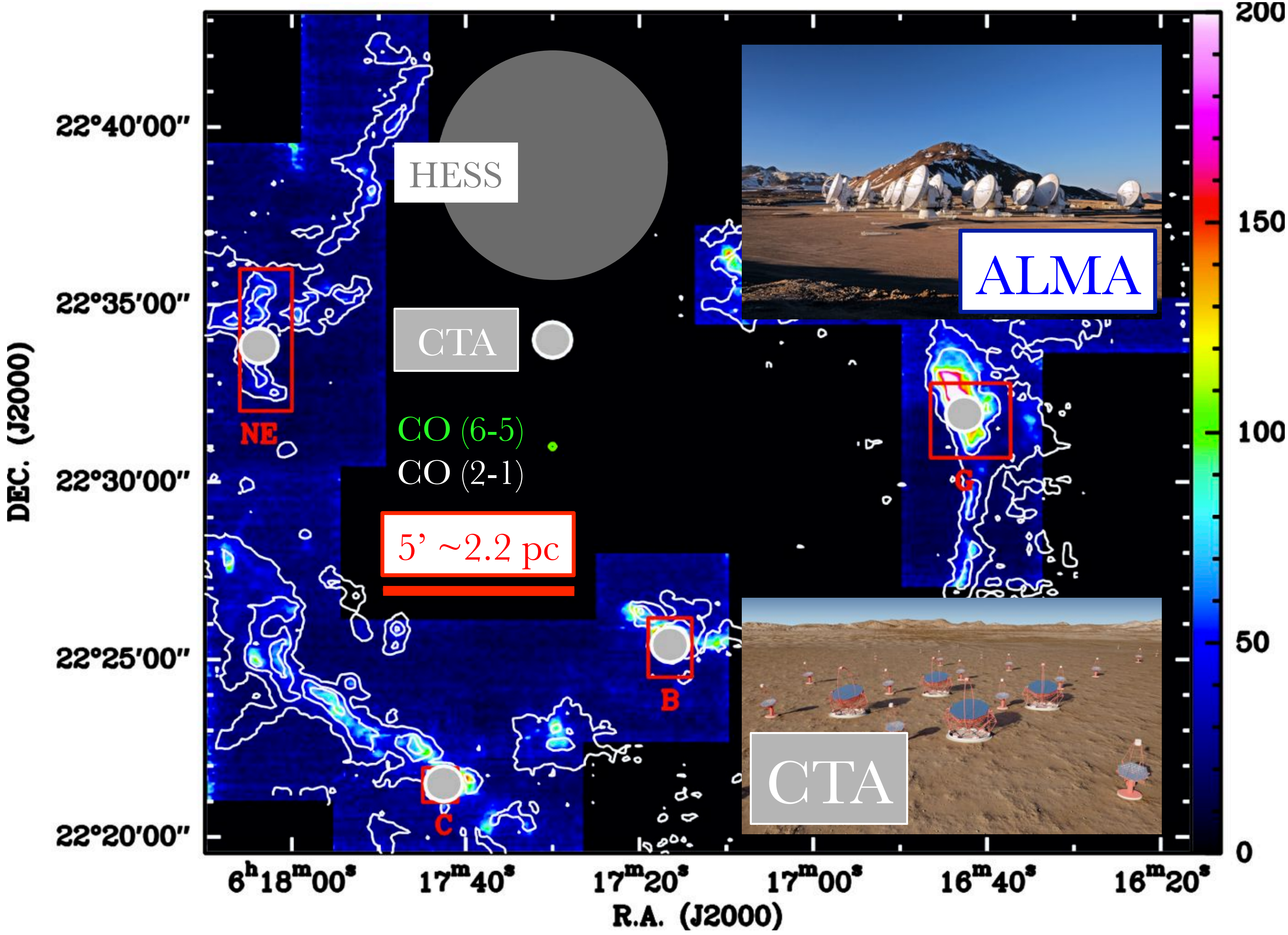
HESS
CTA
CO (6-5)
CO (2-1)
5' ~2.2 pc
NE
G
B
C
ALMA
CTA
22°40'00"
22°35'00"
22°30'00"
22°25'00"
22°20'00"
DEC. (J2000)
6h18m00s
17m40s
17m20s
17m00s
16m40s
16m20s
R.A. (J2000)
200
150
100
50
0

Perspectives

Perspectives

- Importance of studying various environments

All objectives are intricated

- Extend shock studies:
  - whole objects
  - 2-, 3-D geometry (line profiles fitting)
  - processes (UV field influence, X-rays, γ-rays, cosmic rays)
  - chemistry (SiO, H_2O, tracers, COMs: spectral surveys)
  - methods ('big data')

- Extend the context
  - link with extra-Galactic
  - link with CRs

Thanks for your attention !